NOTICE

The quality of this microform is heavily dependent upon the quality of the original thesis submitted for microfilming. Every effort has been made to ensure the highest quality of reproduction possible.

If pages are missing, contact the university which granted the degree.

Some pages may have indistinct print especially if the original pages were typed with a poor typewriter ribbon or if the university sent us an inferior photocopy.

Reproduction in full or in part of this microform is governed by the Canadian Copyright Act, R.S.C. 1970, c. C-30, and subsequent amendments.

AVIS

La qualité de cette microforme dépend grandement de la qualité de la thèse soumise au microfilmage. Nous avons tout fait pour assurer une qualité supérieure de reproduction.

S'il manque des pages, veuillez communiquer avec l'université qui a conféré le grade.

La qualité d'impression de certaines pages peut laisser à désirer, surtout si les pages originales ont été dactylographiées à l'aide d'un ruban usé ou si l'université nous a fait parvenir une photocopie de qualité inférieure.

La reproduction, même partielle, de cette microforme est soumise à la Loi canadienne sur le droit d'auteur, SRC 1970, c. C-30, et ses amendements subséquents.

Studies on Enzyme Intermediates of Yeast Cytochrome c Peroxidase

Ted Fox

A Thesis

in

The Department

of

Chemistry and Biochemistry

Presented in Partial Fulfillment of the Requirements
for the Degree of Doctor of Philosophy at
Concordia University
Montréal, Quebec, Canada

ISBN 0-315-64676-4

ABSTRACT

Study of Enzyme Intermediates in Yeast Cytochrome c Peroxidase

Ted Fox, Ph.D.
Concordia University, 1991.

Cytochrome c Peroxidase (CCP) possesses a Fe^{4+}=O heme and a stable protein radical during catalysis, commonly called compound I. Covalent attachment of a second redox centre, pentaammineruthenium (a_5Ru) to surface histidine (His) residues of CCP was possible by a simple substitution reaction. Cation-exchange chromatography was used to purify at least six distinct species, two of which contain one surface-bound a_5Ru centre per CCP molecule. The a_5Ru is attached to His-60 in one derivative and most likely to one of the remaining surface His residues (6 or 96) in the second derivative. Investigation of the electron transfer reactivity of Fe^{4+}=O by flash photolysis shows that reduction of the Fe^{4+}=O centre is surprisingly slow considering the reduction potential of ~ 1 V for this reaction. This slow intramolecular electron transfer may be attributed to a high reorganization energy associated with reduction of Fe^{4+} to Fe^{3+} and/or to the lack of an efficient pathway for electron transfer between the two redox sites. The latter is not surprising since the attached a_5Ru centre is far from the cyt c binding site and what is thought to be the biologically relevant electron transfer pathway.

The steady-state tryptophan (Trp) fluorescence properties of native CCP are typical of a hemoprotein in which heme quenches much of the fluorescence. CCP is one of a growing number of enzymes that contains a stable protein radical during

catalysis and the first to utilize Trp as the primary radical site. Consequently, unfolding of the protein in 8 M urea relieves ~ 50% of the heme quenching and allowed us to probe the protein radical site of CCP (purportedly Trp-191). Unfolded compound I has a 13% lower fluorescence intensity, presumably because the radical site (Trp-191) is no longer fluorescent. Treating CCP with excess H_2O_2 causes both a loss in enzymatic activity and in the observed fluorescence of unfolded protein which further decreased over a 24-hour period, probably because of the destruction of fluorescent residues. However, > 10% enzymatic activity is retained 24 h after CCP has been oxidized by a 10-fold excess of H_2O_2.

"Sustain the faith that persistent scientific effort eventually solves most problems, often in a suprisingly novel way"

Arthur Kornberg

(From his autobiography "For the love of Enzymes-The Odyssey of a Biochemist")

ACKNOWLEDGEMENTS

I would like to thank my supervisor, Ann English, for her guidance and support during the last few years, and for introducing me to the wonderful world of peroxidases.

I would also like to thank the other members of my committee, Dr.'s M.J.Kornblatt and P.H.Bird for their helpful suggestions during the project. Thanks to Bruce Hill for his help when he was at Concordia.

Thanks to Jim Hazzard and Gordon Tollin for their help when I was in Arizona. Thanks to Steve Edwards and Tom Poulos for doing the x-ray structure work, and to Bernie Gibbs for amino acid analysis.

Thanks to the departmental secretaries, especially Barbara Harris and more recently Pat Stewart, for cutting through the miles of red tape no graduate student can overcome.

Thanks to my friends for assuring me that I was not completely losing my mind and for all those unrepeatable camping and fishing trips we had. Thanks especially to Paul Taz for the support he gives graduate and project students, and for providing the gang with the "goof-off lounge" for moments of relaxation.

Thanks to my parents for always being there and supporting the decisions I've made. This degree would not have been possible without their love and support.

Finally, thanks to my fiancée, Sheryl, for her love, support and for being patient and understanding at times when I couldn't spend enough time with her.

To Mum, Dad, Rommel and Kate

TABLE OF CONTENTS

1.0	INTRODUCTION	1
	1.1 REFERENCES	14
2.0	PREPARATION AND PURIFICATION OF a_3Ru(His)CCP DERIVATIVES	19
	2.1 INTRODUCTION	19
	2.2 EXPERIMENTAL SECTION	28
	2.2.1 Materials	28
	2.2.2 Methods	29
	2.3 RESULTS	34
	2.4 DISCUSSION	58
	2.5 REFERENCES	62
3.0	ELECTRON TRANSFER KINETICS OF a_3Ru(His)CCP DERIVATIVES	65
	3.1 INTRODUCTION	65
	3.2 EXPERIMENTAL SECTION	69
	3.2.1 Materials	69
	3.2.2 Methods	70
	3.3 RESULTS	72
	3.4 DISCUSSION	90
	3.5 REFERENCES	95
4.0	FLUORESCENCE PROPERTIES OF CCP, COMPOUND I AND a_3Ru(His)CCP DERIVATIVES	100
	4.1 INTRODUCTION	100
	4.2 EXPERIMENTAL SECTION	105
	4.2.1 Materials	105
	4.2.2 Methods	105
	4.3 RESULTS	108
	4.4 DISCUSSION	131
	4.5 REFERENCES	137
5.0	SUMMARY	140
6.0	SUGGESTIONS FOR FURTHER STUDY	143
7.0	APPENDIX	144

LIST OF FIGURES

Figure 1.1:	Structure of Protoporphyrin IX	2
Figure 1.2:	Proposed mechanism for heterolytic cleavage of hydrogen peroxide in the active site of CCP	3
Figure 2.1:	(a) Location of His residues in CCP and their distances from the iron centre from the x-ray structure at 1.7 Å resolution; (b) Computer graphics display of the C_α backbone of CCP showing the location of the heme and the three surface His residues	22
Figure 2.2:	Computer graphics generated space filling models of CCP highlighting in red (a) His-60 and (b) His-6.	24
Figure 2.3:	Anion-exchange chromatography of native CCP and a_5Ru-modified CCP.	36
Figure 2.4:	Cation-exchange chromatography of the CCP species from the a_5Ru reaction mixture	37
Figure 2.5:	FPLC cation-exchange chromatography of the same sample as Figure 2.4.	38
Figure 2.6:	(a) FPLC cation-exchange rechromatography of band 4 in Figure 2.5. (b) Rechromatography of peak 4a in (a) above.	39
Figure 2.7:	(a) FPLC cation-exchange rechromatography of band 5 in Figure 2.5. (b) Rechromatography of peak 5b in (a) above.	41
Figure 2.8:	Absorption spectra of a_5Ru(His) at pH 7 and at pH 11.	46
Figure 2.9:	Absorption spectra of native CCP (pH 7.0) and the cyanide complex of CCP (pH 11).	47
Figure 2.10:	Difference spectra of the CCP-CN species of peaks (a) 4a' and (b) 5b' minus CCP-CN.	48
Figure 2.11:	A 2 Å density difference map [a_5Ru(His-60)CCP - native CCP] showing the attachment of a_5Ru at His-60.	50

Figure 2.12: Absorbance decrease at 424 nm due to the decay of compounds of CCP, peak 4a' and peak 5b'. Semilog plot of the ratio of the absorbance change at time, t ($\Delta A_t = A_t - A_\infty$) to the total absorbance change ($\Delta A_0 = A_0 - A_\infty$) vs. time. 51

Figure 2.13: Observed absorbance change at 240 nm following the mixing of DEPC with free His and a_5RuHis. 53

Figure 2.14: Observed absorbance change at 240 nm following the mixing of DEPC with 10 μM (a) native CCP and peak 4a' and (b) native CCP and peak 5b'. 54

Figure 3.1 Structure of oxidized 5-deazariboflavin 67

Figure 3.2: Signal increase at 550 nm before and after flash photolysis of 5 μM cytochrome c, 5 mM EDTA and 50 μM $Ru(bpy)_3^{2+}$ in 0.1 M phosphate buffer (pH 7). 73

Figure 3.3: Absorption spectrum of ~ 72 μM 5-Deazariboflavin in 4 mM phosphate buffer, 0.5 mM EDTA (pH 7). 75

Figure 3.4: Absorbance change at 518 nm due to semiquinone ($DRFH^{\cdot}$) disproportionation before and after laser flash photolysis of 120 μM DRF, 0.5 mM EDTA, 92 mM KCl in 4 mM phosphate (pH 7). 76

Figure 3.5: Absorbance change at 518 nm, due to semiquinone ($DRFH^{\cdot}$) decay in the presence of 2.5 μM a_5Ru(His-60)CCP, before and after laser flash photolysis of 120 μM DRF, 0.5 mM EDTA, 92 mM KCl in 4 mM phosphate (pH 7). 77

Figure 3.6: Plot of observed rate constants (k) vs. a_5Ru(His-60)CCP concentration for $DRFH^{\cdot}$ decay in the presence of 2.5-30 μM a_5Ru(His-60)CCP. 78

Figure 3.7: Visible absorption spectra of 5 μM native CCP and compound I of CCP (pH 7). The maximum in the difference spectrum (compound I - CCP) is at ~ 564 nm 82

Figure 3.8: Absorbance change at 564 nm before and after laser flash photolysis of (a) 2.5 μM (b) 10 μM and (c) 40 μM a_5Ru^{3+}(His-60)CCP(Fe^{4+}). 83

Figure 3.9: Plot of rate constants, k vs. a_5Ru^{3+}(His-60)CCP(Fe^{4+}) concentration for Fe^{4+} reduction in the presence of 2.5-30 μM a_5Ru^{3+}(His-60)CCP(Fe^{4+}). 85

Figure 3.10: Plot of rate constants, k vs. [a_5Ru^{3+}(His-60)CCP(Fe^{4+}] due to Fe^{4+} reduction in the presence of 2.5-30 μM a_5Ru^{3+}(His-60)CCP(Fe^{4+}). 86

Figure 3.11: Plot of rate constant, k vs. a_5Ru^{3+}(His-X)CCP(Fe^{4+}) concentration for Fe^{4+} reduction in the presence of 2.5-30 μM a_5Ru(His-60)CCP. 89

Figure 3.12: Intervening amino acid residues between a_5Ru(His-60) and the heme of CCP. 96

Figure 4.1: Computer graphics display of the C_α backbone of CCP showing the location of the heme (red) as well as Trp and Tyr residues (green) 101

Figure 4.2: Fluorescence emission spectra for 1 μM native CCP when excited at 260, 280 and 295 nm. 110

Figure 4.3: Fluorescence emission spectra obtained for 1 μM native CCP, a_5Ru(His-60)CCP and a_5Ru(His-X)CCP. 112

Figure 4.4: Fluorescence emission spectra obtained for 1 μM native CCP and FPLC-purified peak 5c. 120

Figure 4.5: Fluorescence emission spectra obtained for 1 μM native CCP and compound I of CCP when excited at 280 nm 122

Figure 4.6: Fluorescence emission spectra obtained for 1 μM CCP and 1 μM unfolded CCP in the presence of 8 M urea. 123

Figure 4.7: Relative fluorescence intensity of 1 μM CCP vs. urea concentration. 124

Figure 4.8: Increase in the fluorescence intensity at 350 nm of compound I vs. time following addition of 1 μM protein to 8 M urea. 126

Figure 4.9: Fluorescence emission spectra obtained for 1 μM unfolded CCP in 8 M urea. The protein was reacted with a 0:1, 1:1 and 10:1 molar excess of H_2O_2 and unfolded in 8 M urea 15 s after

addition of H_2O_2. 127

Figure 4.10: Time dependence of fluorescence spectra obtained for 1 μM unfolded CCP in 8 M urea. The protein was reacted with a 10-fold molar excess of H_2O_2 and unfolded in 8 M urea at the following times after addition of H_2O_2: 15 s, 5 min, 10 min (open triangles), 20 min and 24 h. 128

Figure 4.11: Time dependence of the percent fluorescence in 8 M urea of CCP, compound I and H_2O_2-oxidized CCP using 3:1, 5:1 and 10:1 molar ratios of H_2O_2/CCP. Fluorescence measurements were recorded at 15 s to 24 h after H_2O_2 addition. 129

Figure 4.12: Time dependence of the percent enzymatic activity of the CCP samples in Figure 4.11 130

LIST OF TABLES

Table 1.1: Summary of intramolecular electron transfer rate constants for some a_5Ru-modified proteins 11

Table 2.1: Reaction conditions for the modification of various proteins with $a_5Ru^{2+}H_2O$ 27

Table 2.2: Characterization of the ruthenium content, activity and compound I stability of species purified from the ruthenation reaction mixture. 45

Table 2.3: Histidine modification by DEPC in various hemoproteins, including two singly-modified a_5Ru(His)CCP derivatives 57

Table 3.1: Observed rate constants (k) for 5-DRFH· semiquinone decay in the presence of a_5Ru(His)CCP derivatives, and calculated bimolecular rate constants (k_2) 80

Table 3.2: Observed rate constants (k) and calculated bimolecular rate constants (k_2) for reduction of Fe^{4+} in the presence of a_5Ru^{3+}(His-60)CCP(Fe^{4+}) under different conditions. 87

Table 3.3: Observed rate constants (k) and calculated bimolecular rate constants (k_2) for reduction of Fe^{4+} in the presence of a_5Ru^{3+}(His-X)CCP(Fe^{4+}) 88

Table 4.1: Relative fluorescence (%) intensities of native CCP in the presence of freely-diffusing quenchers 111

Table 4.2: Relative fluorescence (%) intensity of native CCP and the a_5Ru(His)CCP derivatives 111

Table 4.3: Relative fluorescence (%) intensities of the a_5Ru(His)CCP derivatives in the presence of freely-diffusing quenchers 114

Table 4.4: Overlap integrals (J) and R_o's calculated for Trp to heme fluorescence energy transfer in CCP, CCP-CN and compound I, as well as for Trp to a_5Ru fluorescence energy transfer in a_5Ru(His)CCP 114

Table 4.5: Efficiency of energy transfer from Trp to heme and Trp to a_5Ru for CCP and a_5Ru(His)CCP derivatives 116

Table 4.6: Calculated fluorescence (%) for native CCP and for the attachment of a_5Ru to each of the surface His residues 118

Table 7.1: Summarized data for the time dependence of % fluorescence of CCP, compound I and H_2O_2-oxidized CCP in 8 M urea 144

Table 7.2: Summarized data for the time dependence of % enzymatic activity of CCP, compound I and H_2O_2-oxidized CCP in 8 M urea 144

LIST OF SCHEMES

Scheme 2.1: Reaction of a_5RuH_2O with His 19

Scheme 2.2: Reaction of DEPC with His 20

Scheme 2.3: Reaction of His with > 200-fold excess of DEPC 56

Scheme 3.1: Deazariboflavin semiquinone production and disproportionation 68

Scheme 3.2: The decay mechanism for DRFH· in the absence and presence of CCP or a_5Ru(His-60)CCP 74

LIST OF ABBREVIATIONS

a	NH_3
AA	atomic absorption
apoCCP	CCP from which the heme has been removed
a_4(py)Ru	*trans*-tetraamminepyridineruthenium(III)
a_5Ru	pentaammineruthenium(III)
Arg	arginine
Asp	aspartate
BBQ	7H-benzimidazo[2,1-a]benz[de]isoquinololine-7-one
CAPS	3-[cyclohexylamino]-1-propanesulphonic acid
CCP	cytochrome c peroxidase
CCP-CN	cyanide adduct of CCP
compound I	CCP + 1 equivalent of H_2O_2
cyt c	cytochrome c
DEPC	diethylpyrocarbonate
DRF	5-deazariboflavin
Fe^{4+}=O	oxo ferryl iron
ferricyt c	cyt c(Fe^{3+})
FPLC	Fast protein liquid chromatography
GOx	glucose oxidase
HIPIP	high potential iron-sulphur protein
His	histidine
HRP	horseradish peroxidase
L	(bpy), (DIC) or (DIPS)
Lys	lysine
Mb	myoglobin
NATA	N-acetyl tryptophanamide
PdP	Palladium Protoporphyrin
PMT	photomultiplier tube
$Ru(bpy)_3^{2+}$	tris(2,2'-bipyridine)ruthenium(II)
$Ru(DIPS)_3^{4-}$	tris[4,7-di(phenyl-4-sulphonate)-1,10-phenanthroline]ruthenium(II)
$Ru(DIC)_3^{4-}$	tris(4,4'-dicarboxy-2,2'-bipyridine)ruthenium(III)
Trp	tryptophan
Tyr	tyrosine
TTP	5,10,15,20-tetraphenyl porphyrin iron(III)
ZnP	Zinc Protoporphyrin
X	Surface His residue 6 or 96

1.0 INTRODUCTION

Peroxidases oxidize a number of inorganic and organic compounds with the concomitant reduction of hydrogen peroxide or organic peroxides. These enzymes are found throughout nature in microorganisms, plants and animals.[1] It has been postulated that peroxidases are all involved in cellular defence to prevent oxidative damage to tissue. Physiological roles include prevention of lipid peroxidation (cellular damage), lignin degradation, prostaglandin synthesis and thyroid hormone biosynthesis.[2] Once life was firmly established in an oxygen environment, peroxidases developed more specialized functions such as prostaglandin biosynthesis (prostaglandin H synthase)[3] and phagocytosis (myeloperoxidase).[4] Many peroxidases have protoporphyrin IX as the prosthetic group (Figure 1.1). Non-heme peroxidases include glutathione peroxidase, a tetrameric enzyme, containing one selenium atom per subunit[5] and NADH peroxidase, a flavoenzyme.[6] Recently, a vanadium-containing bromoperoxidase from seaweed has been isolated .[7]

To date, cytochrome c peroxidase (CCP) is the only peroxidase for which there is a high resolution crystal structure.[8] Thus, CCP is an ideal model for investigating structure-function relationships in heme peroxidases. The proposed mechanism for the reaction of CCP (Figure 1.2) shows that heterolytic cleavage of H_2O_2 occurs and an oxo ferryl (Fe^{4+}=O) species is formed upon coordination of O2 of H_2O_2 to the Fe. CCP contains active site amino acid residues which are poised to heterolytically cleave peroxide.[9] Cleavage of the O-O bond is assisted by an Arg residue which stabilizes the negative charge developing on O1, and by a His residue which assists

in the transfer of the O2 proton to O1, which is released as water (Figure 1.2). Proton transfer from O2 is possible, despite the high pK of H_2O_2 (~ 12), because coordination of the O2 to the heme iron weakens the O2-H bond significantly.[9] Initially, an Fe^{5+}=O species is formed which rapidly receives an electron from an amino acid residue to form Fe^{4+}=O. Coordination of the Fe to His-175 which is strongly hyrogen bonded to Asp-235 increases electron donation to the Fe^{4+} centre, thereby stabilizing its high oxidation state.[9] This intermediate with the Fe^{4+}=O and a protein radical centre is commonly known as compound I, and is two oxidizing equivalents above native CCP.

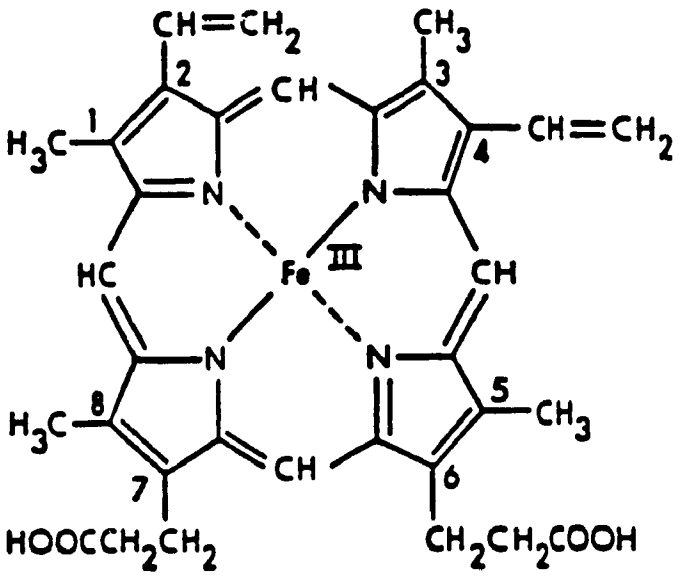

Figure 1.1: Structure of Protoporphyrin IX.[9]

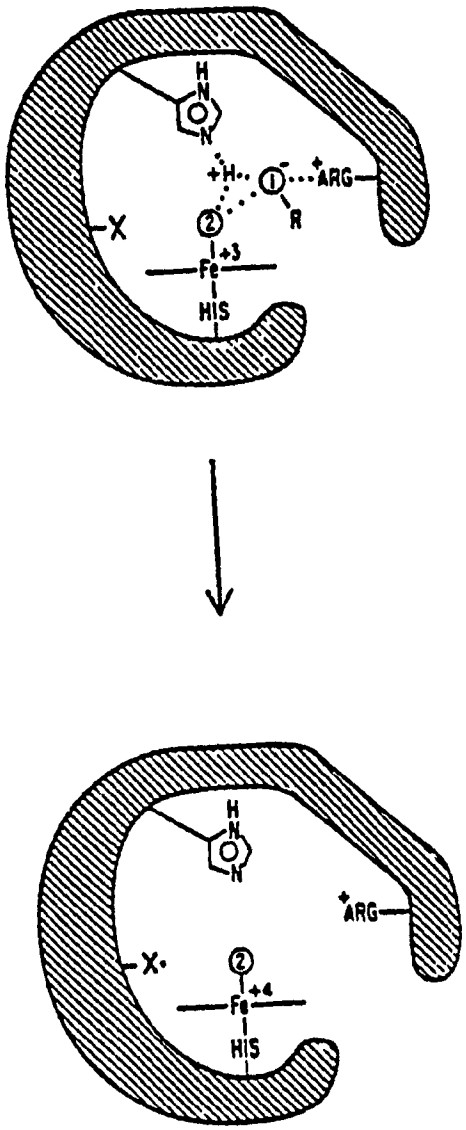

Figure 1.2: Proposed mechanism for heterolytic cleavage of hydrogen peroxide in the active site of CCP.[9]

Compound I is reduced in two one-electron transfer steps from cyt c to generate the native enzyme (eqns 1-3).

$$CCP(Fe^{3+}) + H_2O_2 \longrightarrow \text{Compound I} + H_2O \quad (1)$$

$$\text{Compound I} + e^- \longrightarrow \text{Compound II} \quad (2)$$

$$\text{Compound II} + e^- \longrightarrow CCP(Fe^{3+}) + H_2O \quad (3)$$

The biological role of CCP is thought to be the reduction of H_2O_2 by cyt c to prevent radical formation leading to tissue damage. It may also control the supply of reducing equivalents to the terminal oxidase in yeast mitochondrial respiration. All peroxidases form high oxidation state intermediates, including the selenium atom of glutathione peroxidase which undergoes a two-electron oxidation from Se^{2+} to Se^{4+}.[10] The $Fe^{4+}=O$ species is postulated to be an intermediate in numerous oxygenase proteins, including heme cytochrome P-450[11] and non-heme binuclear oxo-bridged iron proteins such as ribonucleotide reductase and methane monooxygenase,[12] although such intermediates have yet to be observed.

The protein moiety of peroxidases is able to control the reactivity of this highly oxidizing species, as illustrated by comparing metMb and CCP. It is possible to form $Fe^{4+}=O$ in metMb; however, this intermediate is formed much more slowly than compound I formation in CCP ($k = 1.4 \times 10^2$ and 1.4×10^8 M^{-1} s^{-1}, respectively),[13] presumably because Mb which is designed to reversibly bind O_2 to Fe^{2+}, does not contain a distal Arg residue in the active site.[9] A protein radical is also formed in equine metMb, probably on Tyr-103, ~ 18% of which then becomes covalently-linked to the heme.[14]

$Fe^{4+}=O$ in porphyrin model compounds can be stabilized by ligation of strongly basic oxyanions such as hydroxide and methoxide to the Fe in 5,10,15,20-tetraphenylporphyrin iron(III) (TTP).[15] It is then possible to electrochemically generate a $Fe^{4+}=O$ species, which can be followed by a second oxidation producing a porphyrin cation radical, in addition to the ferryl iron.[15] In the absence of Fe-ligated oxyanion substituents in TTP, only porphyrin-based cation radicals can be produced.[15] Recently, a large number of heme model complexes have been synthesized which are able to form a stable $Fe^{4+}=O$ intermediate at temperatures of -120 to -90 °C.[16-19] The absorption spectra of these models have Soret maxima between 406 and 430 nm, which falls in the range seen for the $Fe^{4+}=O$ intermediate of peroxidases. For example, 1-methyl imidazole protoporphyrin IX dimethyl ester, (NMI)$Fe^{4+}=O$(PPDME), has a Soret maximum at 416.[19]

Resonance Raman spectroscopy has become a useful tool in identifying $Fe^{4+}=O$ intermediates in model systems and proteins. Isotopic labelling with ^{18}O has assisted in the assignment of the $Fe^{4+}=O$ stretching vibration in heme models[19] (820-850 cm^{-1}), in several peroxidases (745-787 cm^{-1}),[20,21] in myoglobin (797 cm^{-1}),[22] and in cytochrome c oxidase (790 cm^{-1}).[23] Low temperature transient absorption spectroscopy has identified a $Fe^{4+}=O$ species during catalysis by the hemoprotein prostaglandin H synthase.[24]

Reducing equivalents for the reduction of CCP compound I are provided by cyt c, which forms an electrostatically-stabilized, noncovalent complex with CCP.[8,9] The distance between the heme edges of the proteins has been estimated to be

~ 17 Å,[9] so that long-range intracomplex electron transfer takes place. Electron transfer over long distances plays an important role in numerous biological processes, including the respiratory chain of mitochondria, in which four electrons are transferred to cytochrome c oxidase which reduces oxygen to water; this is coupled to ATP production at various steps. In the reaction centre of green plants and photosynthetic bacteria sunlight initiates a series of electron transfer steps which are coupled to glucose production from water and CO_2.[25] In these systems, electrons rapidly travel large distances (> 10 Å) through the protein matrix between the redox centres.

The factors which control the rates of long-range electron transfer in biological systems are still not fully understood. Important factors include the driving force for the electron transfer process from one redox centre to another. Reorganization energy is required to reduce one redox centre and oxidize the other centre during the inter- or intramolecular electron transfer process. Electrostatic interactions between two redox centres may be important in alignment and recognition when two proteins form an electrostatically-stabilized complex, for example CCP and cyt c. The distance between the two redox centres, as well as the relative orientation of the two redox centres, will also affect the rate of electron transfer.[26] For proteins, the nature of the intervening amino acid residues between the two redox centres is also thought to affect the rate of electron transfer.[27]

The studies to date on protein electron transfer reactions and rates can be divided into two main categories: (a) Intermolecular, where redox partners are free

to diffuse towards each other in solution to form a precursor complex :-

$$A + B \rightleftharpoons AB \dashrightarrow A^+B^- \dashrightarrow A^+ + B^-$$

The observed rate constant (k_{obs}) is dependent on complex formation as well as the rate of electron transfer so, $k_{obs} = k_{et} K_D$, therefore, K_D must be estimated in order to obtain k_{et}. This can be difficult, especially if K_D is in the mM range. Experimental factors such as pH and ionic strength will also play a role in electron transfer; (b) Intramolecular, where the redox partners are at fixed sites in a rigid matrix, ensuring that the distance separating the two sites remains constant. In this case k_{obs} will be equal to k_{et} if electron transfer is the rate-determining step, assuming that there is no conformational gating which controls the rate of electron transfer.[28]

Recent studies have centred on intramolecular electron transfer since K_D does not have to be estimated. Model systems can provide insight into the mechanism of electron transfer and the factors that control the rates. One of the most elegant systems for studying long-range intramolecular electron transfer in proteins was developed by H. B. Gray and coworkers at the California Institute of Technology,[29,30] in which a second redox centre is covalently attached to the surface of structurally well-defined metalloproteins. The attached redox centre should be well-characterized and transfer $1e^-$; for this reason an inorganic metal centre was chosen. A metal centre that proved to be suitable was pentaammineruthenium(III) (a_5Ru).[30] In aqueous solution, in the 2+ oxidation state, the sixth ligand is water ($a_5Ru^{2+}H_2O$) and this species reacts specifically with histidine residues on a protein, which upon

oxidation yields a stable, covalently-linked a_5Ru^{3+}(His)protein complex. Singly-modified a_5Ru(His)protein derivatives can be obtained by ion-exchange chromatography, resulting in a protein structure with two redox centres. Proteins modified with a_5Ru include ribonuclease A,[31,32] lysozyme,[33] α-lytic protease,[33] glucose oxidase,[34] cyt c[29,30] azurin,[37,38] myoglobin,[37,38] c_{551},[39] plastocyanin[40] and a high potential iron-sulphur protein.[41,42] Cyt c was the first protein modified for electron transfer studies, since it is an electron transferase and is commercially available. Cyt c has a 6-coordinate low-spin heme, is redox active in vivo ($Fe^{2+/3+}$), and is stable in both oxidation states. The reorganization energy of the heme is low, calculated to be 27.5 kcal/mol from intramolecular electron transfer data[43] and 25 kcal/mol from Marcus theory.[44] Azurin, a blue copper protein, is of interest because it has a similar function to cyt c in the respiratory chain of bacteria.[37] The reorganization energy of the blue copper centre is also low, yet despite the similarity in distances between the redox centres and a 60 mV higher driving force for azurin, the observed electron transfer is slower than for cyt c (Table 1.1).

The Fe^{2+} state of Mb contains a 5-coordinate high-spin heme, whereas the Fe^{3+} heme, which is not physiologically relevant, is 6-coordinate high-spin.[22] Thus, the reorganization energy of the heme is expected to be higher for electron transfer in Mb compared to cyt c or azurin. The Mb derivative with an a_5Ru attached to His-48 [a_5Ru(His-48)Mb] has been studied most extensively. This derivative has a heme-edge to Ru separation distance of 13 Å (similar to 11.8 Å for cyt c) and the calculated reorganization energy for the heme is 80 kcal/mol, more than twice the

value for either cyt c or azurin. Electron transfer from Ru to the Fe is slightly unfavourable (ΔE° = -20 mV) so k_{et} is small (0.041 s^{-1}).[37,38] Electron transfer was not observed for other a_5Ru-modified Mb derivatives because of the large separation distance between the two redox centres (19-22 Å). It is possible to increase the driving force for electron transfer, so that k_{et} can be measured for other a_5Ru derivatives of Mb by replacing the heme with zinc protoporphyrin (ZnP).[46] ZnP can be photoexcited to give a stable triplet (^{3}ZnP) which is a strong reductant:

$$ZnP \text{ ----> } {}^3ZnP \text{ ----> } ZnP^+ + e^- \qquad E^\circ \sim 900 \text{ mV} \qquad (4)$$

which can then reduce the a_5Ru centre rapidly:

$$^3ZnP\text{---}Ru^{3+} \text{ ----> } ZnP^+\text{---}Ru^{2+} \qquad \Delta E^\circ \sim 800 \text{ mV} \qquad (5)$$

Unlike the heme-containing a_5Ru derivatives of Mb, electron transfer can be observed in four zinc-substituted a_5Ru derivatives of Mb (Table 1.1). All the a_5Ru(His)MbZnP derivatives have the same driving force, yet the distance dependence of electron transfer is not linear. This suggests that the through-space separation distance between redox centres is less important than the actual path available for electron transfer. Computer graphics studies show that the through-bond distances may be more relevant to electron transfer and are often much greater than through-space distance.[27] It is therefore necessary to examine possible electron transfer pathways between the two redox sites using computer graphics and the x-ray structure coordinates for the protein being studied.

Table 1.1

Summary of intramolecular electron transfer rate constants for some a_5Ru-modified proteins.

[a]Distance from the heme edge to the His residue in hemoproteins. Distance from the Fe atom to the His residue in HIPIP and distance from the Cu atom to the His residue in Azurin and plastocyanin.

[b]Driving force

[c]Rate constant for intramolecular electron transfer

[d]Reorganization energy

[e]Genetically engineered cyt c in which an asparagine residue is replaced by a His residue at position 62

[f]Zinc-substituted protoporphyrin

[g]High potential iron-sulphur protein

[h]*trans*-tetraamminepyridineruthenium(III)

[i]Palladium-substituted protoporphyrin

[j]Assuming E° = 80 mV for free $a_5Ru^{3+/2+}(His)$[43] and E° = 1.087 V for $Fe^{4+/3+}$ of CCP[49]

[k]This study

[l]X = His-6 or 96

Protein	Ruthenium centre	His	Dist[a] (Å)	ΔE^{ab} (mV)	k_{et}[c] (s^{-1})	λ[d] (kcal/mol)	Reference
Cyt c	a_5Ru	33	11.8	180	30	30	29,30
Cyt c[e]	a_5Ru	62	15	180	1.7	30	48
ZnP-Cyt c[f]	a_5Ru	33	11.6	980	$7.7x10^5$		45
Cyt c-551	a_5Ru	47	7.9	200	13		39
Azurin	a_5Ru	83	11.8	240	1.9	28	35,36
Plastocyanin	a_5Ru	59	11.9	260	> 0.08		40
HIPIP[g]	a_5Ru	42	7.9	350	18		41,42
Fe-Mb	a_5Ru	48	12.7	20	0.041	80	37
ZnP-Mb	a_5Ru	48	12.7	800	$7x10^4$		46
ZnP-Mb	a_5Ru	81	19.3	800	86		46
ZnP-Mb	a_5Ru	116	20.1	800	89		46
ZnP-Mb	a_5Ru	12	22	800	100		46
Fe-Mb	$a_4(py)Ru^h$	48	12.7	275	2.1		46
PdP-Mb[i]	a_5Ru	48	12.7	750	$9.1x10^3$		47
ZnP-Mb	a_5Ru	48	12.7	800	$7x10^4$		46
PdP-Mb	$a_4(py)Ru$	48	12.7	980	$9x10^4$		47
CCP	a_5Ru	60	21.8	1000[j]	3.2 ± 1.2		TS[k]
CCP	a_5Ru	X[l]	20-23	1000	1.6 ± 0.6		TS

It has also been proposed that the nature of the intervening residues is important in determining intramolecular electron transfer rates. The a_5Ru(His-12)MbZnP derivative has a Trp residue (Trp-14) between the two redox sites which could explain why k_{et} for this derivative is greater than the His-81 and His-116 derivatives, which do not possess any aromatic residues in the electron transfer path.[44] However, this was not found to be the case for a genetically engineered derivative of cyt c in which a surface His residue was introduced at position 62, chosen because a Trp residue (Trp-59) is between the heme and His-62.[48] The a_5Ru(His-62)cyt c derivative gave an intramolecular electron transfer rate over similar distances of 1.7 s^{-1}, slower than the rate of 30 s^{-1} observed for a_5Ru(His-33)cyt c.[48]

Investigation of the effect of driving force on the rate of electron transfer has been possible by replacing the heme of a_5Ru(His-48)Mb with other metal substituted protoporphyrins. Since the distance and path are the same for all derivatives, the effect of driving force on electron transfer rates can be investigated directly. For example, Pd protoporphyrin (PdP) has an excited state oxidation potential:[47]

$$^3PdP \text{ ----> } 1e^- + PdP^+ \qquad E^\circ = 640 \text{ mV}$$

and may replace the heme of Mb:

$$a_5Ru^{3+}(His\text{-}48)Mb^3PdP \text{ ----> } a_5Ru^{2+}(His\text{-}48)MbPdP^+ \qquad \Delta E^\circ = 720 \text{ mV}$$

Alternatively, the driving force may be adjusted by altering the a_5Ru centre. One of the NH_3 groups can be replaced by a pyridine to give a *trans*tetraamminepyridine-ruthenium derivative which gives rise to a $\Delta E^\circ \sim 275$ mV when coupled with the heme:[47]

$a_4(pyr)Ru^{3+}(His\text{-}48)Mb \longrightarrow a_4(pyr)Ru^{2+}(His\text{-}48)Mb \qquad \Delta E^\circ = 275\ mV$

and when coupled to PdP:[16]

$a_4(pyr)Ru^{3+}(His\text{-}48)Mb^3PdP \rightarrow a_4(pyr)Ru^{2+}(His\text{-}48)MbPdP^+ \qquad \Delta E^\circ = 980\ mV$

The rates of electron transfer for substituted a_5Ru(His-48)Mb derivatives are summarized (Table 1.1). An examination of the data in Table 1.1 shows that rates of intramolecular electron transfer are not simply dependent on through-space distances and the driving force for electron transfer.

CCP is also an ideal candidate for modification with a_5Ru because it is well-characterized and has three surface histidine residues.[8] Also, the distance between the three surface histidine residues and the iron atom are similar to the distance between the iron atoms in the electrostatically-stabilized complex between CCP and cyt c (~ 25 Å).[9] Despite the large distances between the two centres, electron transfer is expected to occur between the attached a_5Ru and the Fe^{4+}=O heme of CCP, because the driving force (ΔE°) is ~ 1 V.[49]

Compound I of CCP contains an amino acid radical as well as the Fe^{4+}=O species. The location of this radical has been extensively investigated by site-directed mutagenesis and a variety of residues have been proposed as the radical site (Trp-51,[50-52] Trp-191,[50,52,53] Met-172,[51,54] Met-230 and Met-231[55]) but conflicting results have been obtained. Recently, the radical has been identified as residue Trp-191 by ENDOR spectroscopy.[56] This is supported by recent characterization of the reaction of hydrogen peroxide with a CCP-mutant which has a phenylalanine residue in place of Trp-191.[52] The Phe-191 CCP mutant has only 0.02% enzymatic activity compared

to native CCP, and appears to have a porphyrin radical rather than a protein radical as in CCP.[52] Compound I decay in the presence of excess H_2O_2 results in damage to Tyr and Trp residues.[57,58] Trp fluorescence of CCP is of interest because it may provide useful information regarding the protein radical present in compound I.

Ribonuclease A[31,32] α-lytic protease[33] and lysozyme[33] were first modified with a_5Ru^{2+} to study fluorescence energy transfer between Trp residues and a_5Ru. CCP contains 7 Trp and 14 Tyr residues[59] and exhibits intrinsic fluorescence. Computer-graphics modelling of CCP suggests that 2 Trp residues are close enough to be completely quenched by the heme. Fluorescence energy transfer between Trp residues and a_5Ru will be investigated for a_5Ru(His)CCP derivatives.

In summary, this thesis will discuss the preparation, purification and extensive characterization of two a_5Ru(His)CCP derivatives. The electron transfer reactivity of the $Fe^{4+}=O$ intermediate of these derivatives will be investigated. The fluorescence properties of native CCP and compound I will be discussed, and the effect of freely-diffusing (Cs^+, I^- and acrylamide) and covalently-bound (a_5Ru) quenchers will be examined for native CCP. Fluorescence will be used to probe if the radical site in compound I is on a Trp residue. Also, addition of excess H_2O_2, which is reported to decrease enzymatic activity and cause the destruction of aromatic residues,[57,58] will be investigated by fluorescence.

1.1 REFERENCES

1 Frew, J. E.; Jones, P. *Adv. Inorg. Bioinorg. Mechanisms* ; Ed. Sykes, G. A.;

Academic Press, **1984**, 3, 175.

2 Dunford, H. B. *Adv. Inorg. Biochem.* **1982**, *4*, 41.

3 Samuelson, B.; Goldyne, M.; Grandström, E; Hamberg, M; Hammarström, S.; Malmsten, C. *Ann. Rev. Biochem.* **1978**, *41*, 997.

4 Baboir, B. M.; Kuver, R.; Curnette, J. T. *J. Biol. Chem.* **1988**, *263*, 1713.

5 Lawrence, R. A.; Burk, R. F. *Biochim. Biophys. Res. Commun.* **1976**, *71*, 952.

6 Walker, G. A.; Kilgour, G. L. *Arch. Biochem. Biophys.* **1965**, *111*, 534.

7 Muller-Fahrnow, A.; Hinrichs, W.; Saenger, W.; Vilter, H. *FEBS Letters* **1988**, *239*, 292.

8 Finzel, B. C.; Poulos, T. L.; Kraut, J. *J. Biol. Chem.* **1984**, *259*, 13027.

9 Poulos, T. L.; Finzel, B. C. *Pept. Protein rev.* **1984**, *4*, 115.

10 Wendel, A.; Pilz, W.; Ladenstein, R,; Sawatzki,G.; Weser, U. *Biochim. Biophys. Acta.* **1975**, *377*, 211.

11 Ortiz de Montellano, P. R. *Acc. Chem. Res.* **1987**, *20*, 289.

12 Lippard, S. J. *Angew. Chem. Int. Ed. Eng.* **1988**, *27*, 344.

13 Yonetani, T.; Schleyer, H. *J. Biol. Chem.* **1967**, *242*, 1974.

14 Catalano, C. E.; Choe, Y. S. Ortiz de Montellano, P. R. *J. Biol. Chem.* **1989**, *264*, 10534.

15 Lee, W. A.; Calderwood, S. T.; Bruice, T. C. *Proc. Natl. Acad. Sci.* **1985**, *82*, 4301.

16 Chin, D-H.; Balch, A. L.; La Mar, G. N. *J. Am. Chem. Soc.* **1980**, *102*, 1446.

17 La Mar, G. N.; de Ropp, J. S.; Latos-Grazynski, L.; Balch, A. L.; Johnson, R.

B.; Smith, K. M.; Parish, D. W.; Cheug, R-J. *J. Am. Chem. Soc.* **1983**, *105*, 782.

18 Mizutani, Y.; Hashimoto, S.; Tatsuno, Y.; Kitagawa, T. *J. Am. Chem. Soc.* **1990**, *112*, 6809.

19 Oertling, W. A.; Kean, R.; Babcock, G. T. *Inorg. Chem.* **1990**, *29*, 2633.

20 Palaniappan, V.; Terner, J. *J. Biol. Chem.* **1989**, *264*, 16046.

21 Reczek, C. M.; Sitter, A J.; Terner, J. *J. Mol. Struc.* **1989**, *214*, 27.

22 Sitter, A. J.; Reczek, C. M.; Terner, J. *Biochim. Biophys. Acta.* **1985**, *828*, 229.

23 Varotsis, C.; Babcock, G. T. *Biochemistry* **1990**, *In Press.*

24 Dietz, R.; Nastainczyk, W.; Ruf, H. H. *Eur. J. Biochem.* **1988**, *171*, 321.

25 Deisenhofer,J.; Epp,O.; Miki,K.; Huber,R.; Michel,H. *Nature,* **1985**, *318,* 618.

26 Isied,S.S. *Prog. Inorg. Chem.* **1984**, *32,* 443.

27 Beratan, D. N.; Onuchic, J. N.; Betts, J. N.; Bowler, B. E.; Gray, H. B. *J. Am.Chem. Soc.* **1990**, *112*, 7915.

28 Hoffman, B. M.; Ratner, M. A. *J. Am. Chem. Soc.* **1987**, *109*, 6237.

29 Yocom, K. M.; Shelton, J. B.; Shelton, J. R.; Schroeder, W. A.; Worosila, G.; Isied, S. S.; Bordignon, E.; Gray, H. B. *Proc. Natl. Acad. Sci.* **1982**, *79,* 7052.

30 Yocom, K.M.; "The Synthesis and Characterization of Inorganic Redox Reagent-Modified Cytochrome c", Ph.D. Thesis, California Institute of Technology, **1982.**

31 Matthews, C. R.; Erickson, P. M.; Van Vliet, D. L.; Petersheim, M. *J. Am. Chem. Soc.* **1978**, *100,* 2260.

32 Matthews, C. R.; Erickson, P. M.; Froebe, C. L. *Biochim. Biophys. Acta.* **1980**,

624, 499.

33 Recchia, J.; Matthews, C. R.; Rhee, M.; Horrocks, W. D. *Biochim. Biophys. Acta.* **1982,** *702,* 105.

34 Degani, Y.; Heller, A. *J. Am. Chem. Soc.* **1988,** *110,* 2615.

35 Margalit, R.; Kostic, N. M.; Che, C-M.; Blair, D. F.; Chaing, H-J.; Pecht, I.; Shelton, J. B.; Shelton, J. R.; Gray, H. B. *Proc. Natl. Acad. Sci.* **1984,** 81, 6554.

36 Gray, H. B. *Chem. Soc. Rev.* **1986,** *15,* 17.

37 Crutchley, R. J.; Ellis, W. R.; Gray, H. B. *Frontiers in Bioinorganic Chemistry;* Xavier, A. V. , Ed.; VCH, 1986, p 679.

38 Crutchley, R. J.; Ellis, W. R.; Gray, H. B. J. Am. Chem. Soc. **1985,** *107,* 5002.

39 Osvath, P.; Salmon, G. A.; Sykes, A. G. *J. Am. Chem. Soc.* **1988,** *110,* 7114.

40 Jackman, M. P.; McGinnis, J.; Powls, R.; Salmon, A. G.; Sykes, A. G. *J. Am. Chem. Soc.* **1988,** *110,* 5880.

41 Jackman, M. A.; Lim, M-C.; Salmon, G. A.; Sykes, A. G. *J. Chem. Soc., Chem. Commun.* **1988,** 179.

42 Jackman, M. A.; Lim, M-C.; Sykes, A. G.; Salmon, G. A. *J. Chem. Soc., Dalton Trans.* **1988,** 2843.

43 Nocera, D. G.; Winkler, J. R.; Yocom, K. M.; Bordignon.; Gray, H. B. *J. Am. Chem. Soc.* **1984,** *106,* 5145.

44 Marcus, R. A.; Sutin, N. *Biochim. Biophys. Acta.* **1985,** *811,* 265.

45 Elias, H.; Chou, M. H.; Winkler, J. R. *J. Am. Chem. Soc.* **1988,** *110,* 429.

46 Axup, A. W.; Albin, M.; Mayo, S. L.; Crutchley, R. J.; Gray, H. B. *J. Am.*

Chem. Soc. **1988,** *110,* 435.

47 Karas, J. L.; Lieber, C. M.; Gray, H. B. *J. Am. Chem. Soc.* **1988,** *110,* 599.

48 Bowler, B. E.; Meade, T. J.; Mayo, S. L.; Richards, J. H.; Gray, H. B. *J. Am. Chem. Soc.* **1989,** *111,* 8757.

49 Purcell, W. L.; Erman, J. E. *J. Am. Chem. Soc.* **1976,** *98,* 7033.

50 Hori, H.; Yonetani, T. *J. Biol. Chem.* **1985,** *260,* 349.

51 Goodin, D. B.; Mauk, G. A.; Smith, M. *J. Biol. Chem.* **1987,** *262,* 7719.

52 Erman, J. E.; Vitello, L. B.; Mauro, J. M.; Kraut, J. *Biochemistry* **1989,** *28,* 7992.

53 Scholes, C. P.; Liu, Y.; Fishel, L. A.; Farnum, M. F.; Mauro, J. M.; Kraut, J. *Isr. J. Chem.* **1989,** *29,* 85.

54 Goodin, D. B.; Mauk, G. A.; Smith, M. *Proc. Natl. Acad. Sci. U. S. A.* **1986,** *83,* 1295.

55 Edwards, S.; Xuong, N. H.; Hamlin, R. C.; Kraut, J. *Biochemistry* **1987,** *26,* 1503.

56 Sivaraja, M.; Goodin, D. B.; Smith, M.; Hoffman, B. M. *Science* **1989,** *245,* 738.

57 Coulson, A. F. W.; Yonetani, T. *Biochem. Biophys. Res. Commun.* **1972,** *49,* 391.

58 Erman, J. E.; Yonetani, T. *Biochim. Biophys. Acta.* **1973,** *393,* 350.

59 Takio, K.; Titani, K.; Ericsson, L. H.; Yonetani, T. *Arch. Biochem. Biophys.* **1980,** 203, 615.

2.0 PREPARATION AND PURIFICATION OF $a_5Ru(His)$CCP DERIVATIVES

2.1 INTRODUCTION

A redox centre may be attached specifically to His residues in proteins by a simple substitution reaction using the histidine-specific reagent aquopentaammineruthenium(II) (a_5RuH_2O) shown in scheme 2.1.

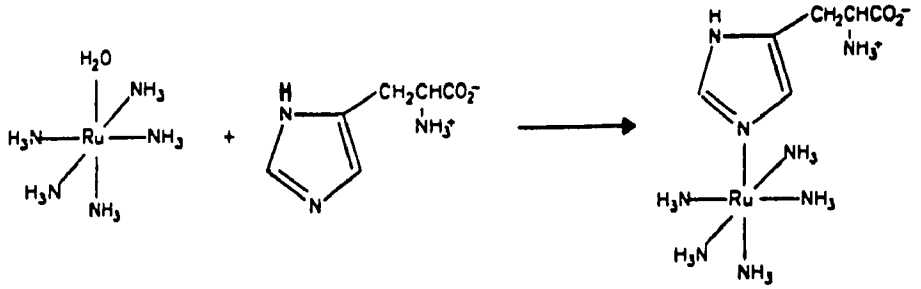

Scheme 2.1: Reaction of a_5RuH_2O with His[1]

The Ru(II) product is labile and is oxidized to the Ru(III) product which is stable.[2] The number of different $a_5Ru(His)$ species formed will depend on the number and accessibility of His residues. Horse heart cyt c only has one buried His residue available for modification, so reaction times of 1-3 days are required.[3,4] Sperm whale myoglobin (Mb), on the other-hand, has four surface His residues which are modified in 30 min.[5]

CCP has six His residues (Figure 2.1), three of which are surface exposed and the most likely candidates for modification (Figure 2.1).[6a] Two of the remaining His residues are buried in the heme pocket; His-175 is coordinated to the heme Fe and His-52 lines the distal pocket.[7] The final His residue, His-181, is not expected to be reactive with the Ru complex at pH 7 since it is an essential component of the H-

bonding network between heme propionate-7 and Asp-37, and is not solvent-exposed.[7] The three surface His residues (His-6, 60 and 96) are expected to show different reactivities with the Ru complex. His-6 and 96 are less exposed than His-60 (Figure 2.2) and the N(3) nitrogen of both His residues appear to be within H-bonding distance of a carbonyl oxygen. Computer graphics analysis suggests that His-60 is the most exposed His residue (Figure 2.2) and does not appear to interact with neighbouring residues.

One possible method of determining the number of Ru-modified His residues in a protein involves use of the His-specific reagent, diethyl pyrocarbonate (DEPC), which reacts specifically with His in model compounds and in proteins.[9] Nucleophilic attack by His N(3) on a carbonyl carbon of DEPC results in the formation of an N-carbethoxyhistidine species:

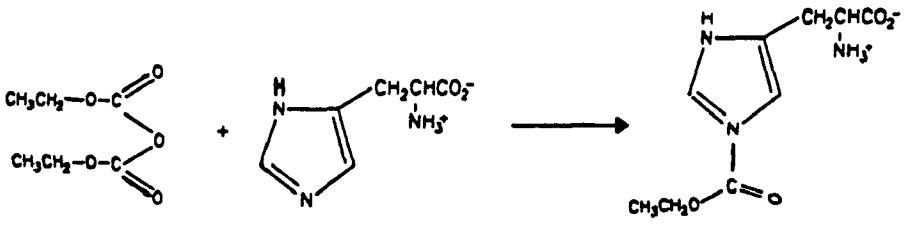

Scheme 2.2: Reaction of DEPC with His[6a]

which may be followed spectrophotometrically as an absorbance increase at 230-250 nm. The three surface His residues of CCP, His-6, 60 and 96 (Figure 2.1), are readily modified by DEPC at pH 7.[6a] At pH 8, the H-bonding network involving His-181,

Figure 2.1: **(a)** Location of His residues in CCP and their distances from the iron centre from the x-ray structure at 1.7 Å resolution;[8] **(b)** Computer graphics display of the C_α backbone of CCP showing the location of the heme and the three surface His residues (His-6, His-60 & His-96).[6b]

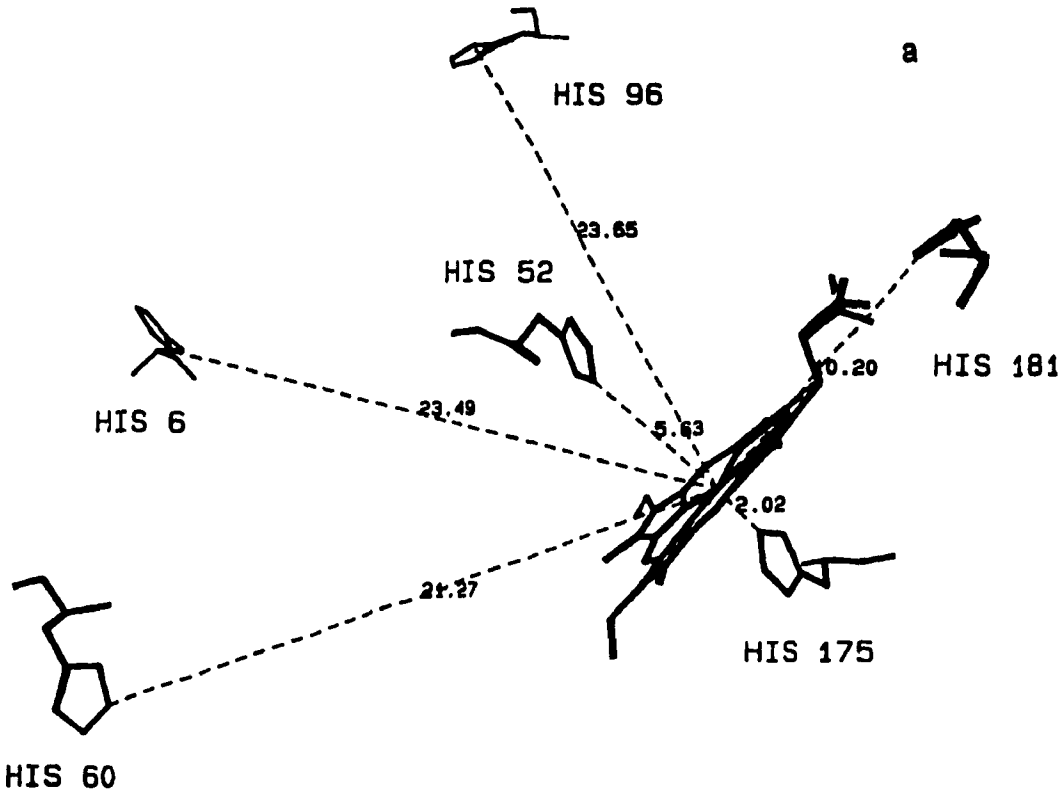
a
HIS 96
23.65
HIS 52
HIS 181
10.20
HIS 6
23.49
5.63
2.02
21.27
HIS 175
HIS 60

b

Figure 2.2: Computer graphics generated space filling models of CCP highlighting in red (a) His-60 and (b) His-6. The remaining surface His residue of CCP (His-96) has similar solvent accessibility to His-6 and is therefore not shown. The CCP coordinates were obtained from the crystal structure.[6b,8]

a

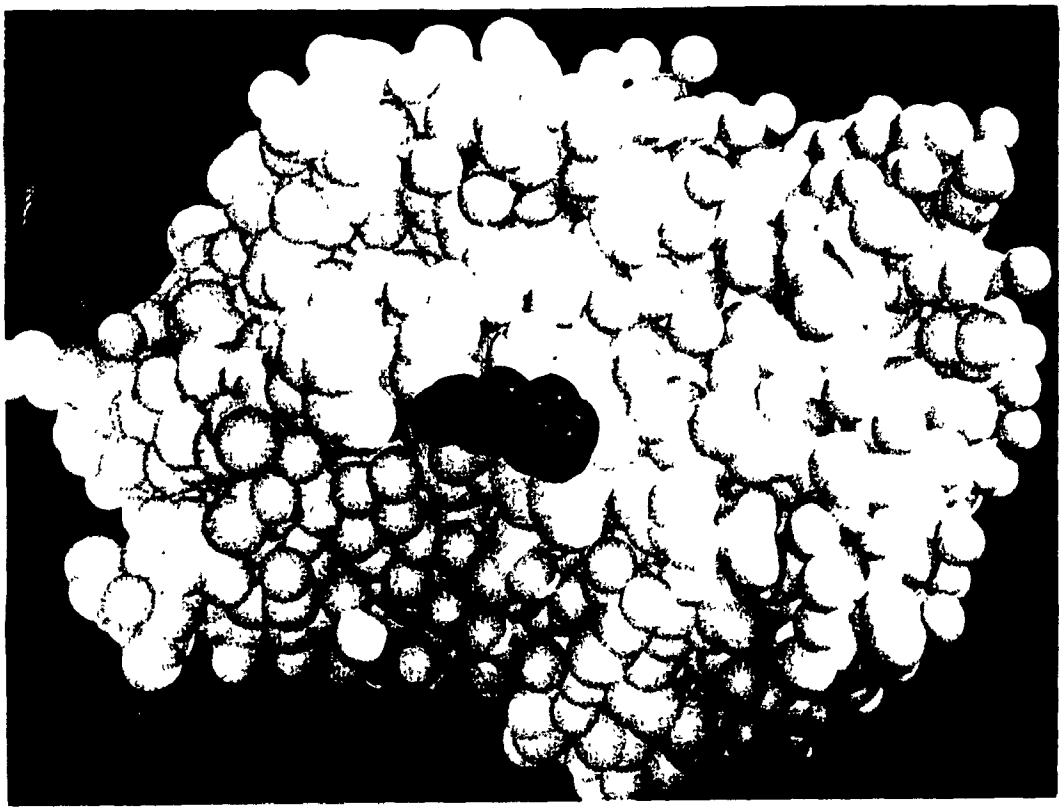

b

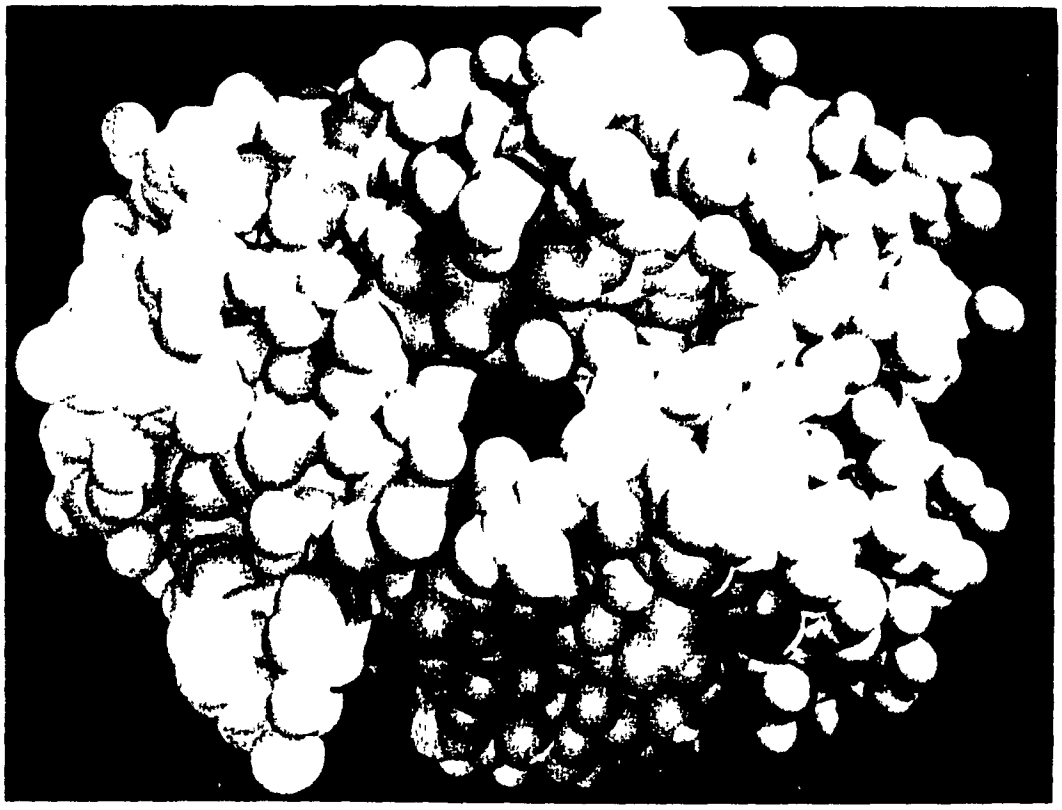

Asp-37 and propionate-7 is broken, which increases access to the heme, allowing DEPC to modify five His residues. Only His-175 remains unmodified because its N(3) atom is coordinated to the Fe atom.[7] The reactivity of DEPC with a_5Ru(His) should be decreased relative to free His because DEPC reacts primarily with the pyridine nitrogen of the imidazole ring (Scheme 2.2). The reactivity of DEPC with His, a_5Ru(His), native and ruthenium-modified CCP derivatives was investigated to see if a His side chain is modified by the ruthenium complex.

It is important that ruthenium-modified CCP derivatives are stable and that the protein structure is not significantly altered by the presence of the ruthenium centre. The enzymatic activity, i.e., the reduction of hydrogen peroxide to water, can be followed spectrophotometrically when coupled to cyt c oxidation.[10] On reaction with H_2O_2, CCP forms a stable intermediate (compound I) which slowly decays to a species spectrally similar to native CCP in the absence of exogenous donors.[11] The rate of decay of compound I is also used as a measure of its relative stability in a_5Ru(His)CCP compared to native CCP.

A survey of reaction conditions for the ruthenation of other proteins (Table 2.1) was used as a guide to determine the most suitable conditions for modifying CCP. Conditions similar to Sperm whale Mb were chosen because it has four surface His residues which are easily modified.[5] After modification, the different species can be separated by chromatography. Some protein may remain unmodified, some may be modified at one or more of the reactive His residues, and some protein may be denatured during modification. The separated species can then be characterized to

identify which species contain one a_5Ru/heme. These species are of particular interest for intramolecular electron transfer studies. This chapter will outline the modification and purification steps leading to the isolation and characterization of singly-modified a_5Ru(His)CCP derivatives, and will also describe other products obtained from the reaction mixture. The location of the a_5Ru centre will be identified by x-ray crystallography for one of the singly-modified CCP derivatives.

Table 2.1

Reaction conditions for the modification of various proteins with $a_5Ru^{2+}H_2O$

Protein	Buffer	Reaction time (h)	Molar excess of a_5Ru salt	Ref.
Ribonuclease	0.1 M Pi[a]	6	20	12,13
α-Lytic protease	0.1 M Pi[b]	10		14
Lysozyme	0.1 M Pi[a]	19		14
Cyt c	0.1 M Pi[a]	24-72	50	2,3,4
Azurin	0.1 M Tris[c]	3	50	15
Myoglobin	0.1 M Tris[c]	0.5	5	5
Cyt c_{551}	0.05 M HEPES[d]	3	15	16
Plastocyanin	0.02 M HEPES[e]	4	45-60	17
GOx[f]	0.1 M Pi[a]	48	1000	18
HIPIP[g]	0.02 M HEPES[e]	0.75	39	19,20
CCP	0.1 M Pi[a]	3	20	TS[h]

[a]Phosphate buffer (pH 7)

[b]Phosphate buffer (pH 8)

[c]Tris buffer (pH 7)

[d]HEPES buffer (pH 7.26)

[e]HEPES buffer (pH 7.5)

[f]Glucose oxidase in 3 M urea (pH 7)

[g]High potential iron-sulphur protein

[h]TS = This study

2.2 EXPERIMENTAL SECTION

2.2.1 Materials

CCP was isolated from bakers yeast (Fleishmans).[21] Cytochrome c (Type III) for the CCP enzymatic activity assay was obtained from Sigma and used without further purification. DEPC, imidazole, L-His and KCN were also obtained from Sigma. Sodium dithionite and $a_5Ru^{3+}Cl$ were purchased from Fisher and Strem, respectively. Ammonium hexafluorophosphate and ruthenium AA standard (1000 ppm) were purchased from Aldrich. Ion-exchange resins including DEAE-Sepharose CL-6B and S-Sepharose CL-6B (fast flow), and molecular exclusion gels including Sephadex G-25 and G-75 were obtained from Pharmacia. Pharmacia was also the manufacturer and supplier of the FPLC system which consisted of an LC-500 controller unit connected to two P-500 pumps and a strip-chart recorder (Mandel). Samples were loaded via a motorized MV-7 valve. All other chemicals were reagent grade and used without purification. Ultrafiltration cells and membranes were purchased from Amicon. Proteins and buffers were filtered using 0.2 & 1.2 μm Acrodisc filters, respectively, supplied by Gelman sciences. Gas-tight syringes were purchased from Hamilton. Serum caps were obtained from Aldrich and cleaned by boiling in 1 N NaOH followed by 1 N HCl. After rinsing, the caps were stored at 4°C. Dialysis tubing (Spectrapor 2, 12-14 KDa cutoff) was obtained from Spectrum Medical Industries. Prior to use, dialysis tubing was boiled for 30 min in 0.5 M EDTA[22] and stored in water at 4°C. Distilled water (specific resistance > 18 MΩ cm) was prepared by a Barnstead Nanopure system. All anaerobic work was performed

under argon gas. Prepurified (Linde, Union Carbide) argon was purged of oxygen by passing it through a chromous scrubbing tower.

2.2.2 Methods

Preparation of Ruthenium Complexes: $[a_5Ru^{2+}H_2O](PF_6)_2$ was prepared by the published procedure[23] in which $a_5Ru^{3+}Cl$ was reduced over Zn/Hg amalgam in 0.1 M H_2SO_4 under argon. After 2 h, when all the ruthenium complex had dissolved, the yellow solution was transferred to a 100 ml round-bottomed flask by a transfer needle. A 5 ml deaerated, saturated solution of ammonium hexafluorophosphate was added to the ruthenium solution using a 5 ml gas-tight Hamilton syringe. This solution was cooled on ice and a yellow precipitate of $[a_5RuH_2O](PF_6)_2$ appeared. This solution was filtered using a medium porosity glass-frit filter (2.5 cm diameter). The precipitate was washed with 10 ml distilled water followed by 10 ml of anhydrous ether, dried on a vacuum line, and stored at 4 °C in a vacuum desiccator for up to 2 months. Preparation of a_5Ru(His) by the published procedure[1] in which L-His (0.6 g) was dissolved in 0.1 N HCl (40 ml) and purged of oxygen using argon for 1 h. A few pieces of Zn-Hg amalgam were added to the solution, followed by $a_5Ru^{3+}Cl$ (0.3 g), and the reaction allowed to proceed under argon for 3 h. The reaction was terminated by diluting the mixture to 100 ml and bubbling with air for 1 h. The resulting dark red solution was adjusted to pH 1 with HCl, and passed through a cation-exchange column (Dowex 50W-X2). a_5Ru^{3+}(His) was eluted by 3 N HCl as an orange band. The solution was evaporated to dryness in a fumehood and the residual solid was crystallized from an acetone-water mixture (1:1).

CCP Isolation: CCP was isolated by the published procedure[21] with the following modifications: a second column packed with DEAE resin was used to purify CCP, instead of gel filtration. The purified CCP was concentrated by ultrafiltration in a stirred cell using a YM-30 membrane (M.W. cutoff of 30 KDa) and dialysed against 0.1 M phosphate (pH 7) to remove any bound acetate, and then against water for crystallization. A previously published cyt c assay[10,21] was used to determine the enzymatic activity of native CCP and of the a_5Ru(His)CCP derivatives. In this assay, the oxidation of ferrocytochrome c is measured by monitoring the absorbance decrease at 550 nm, Δe_{550} = 18 mM^{-1} cm^{-1}.[24] A stock solution of ferricyt c in 0.1 M phosphate buffer (A_{550} ~ 0.5) was reduced with sodium dithionite until A_{550} ~ 1.3-1.4). The volume of the assay solution was 2 ml. A unit of enzymatic activity for this assay is defined as an absorbance decrease of 1.0 at 550 nm per 10 s per 10 µl of enzyme.[10] CCP is fully active if an absorbance change of 1.0 is observed under the conditions described for a 20 µM solution of enzyme. Spectrophotometric measurements were carried out on a Hewlett Packard 8451A diode array spectrophotometer with a response time of 0.1 s.

CCP Modification: CCP was reacted with a 20-fold molar excess of a_5RuH_2O under argon at room temperature in 0.1 M phosphate (pH 7) for 3 h. In a typical preparation 5-100 mg CCP (0.2-0.4 mM) were deaerated by bubbling argon over the protein solution for 1 h. a_5RuH_2O was dissolved in degassed buffer and transferred by gas-tight syringe to the vessel containing the protein. The reaction was terminated by loading the reaction mixture onto a G-25 gel filtration column (2.5 x 20 cm)

equilibrated with reaction buffer to remove any remaining unreacted a_5RuH_2O. The buffer was changed to 50 mM acetate (pH 5.1), by diluting and concentrating the mixture three times in a stirred ultrafiltration cell, with a YM-10 membrane.

Anion-exchange chromatography: Native or ruthenium-modified CCP (2-10 mg) was loaded onto a DEAE-Sepharose column (1 x 10 cm) and eluted by a linear NaCl gradient in 50 mM acetate buffer, pH 5.1 (120 ml buffer and 120 mM buffer + 0.95 M NaCl). A flow rate of 6 ml/h was maintained by an LKB 2132 MicroPerpex peristaltic pump, and fractions of 1 ml were collected using an LKB 2112 RediRac fraction collector. Absorbance at 408 nm was measured for each fraction.

Cation-exchange chromatography: Ruthenium-modified CCP (1-100 mg) was loaded onto a column (1 x 10 cm) packed with S-Sepharose and eluted by the linear NaCl gradient used for anion-exchange chromatography. A linear gradient is required to separate the complex mixture of species present in ruthenium-modified CCP. Typical flow rates were 5-10 ml/h and 1-2 ml fractions were collected and the absorbance at 408 nm measured.

FPLC: Ruthenium-modified CCP samples (0.1-1 mg in volumes ranging from 25-500 μl) were loaded onto a cation-exchange HR 5/5 Mono-S column and eluted using NaCl gradients in 50 mM acetate buffer, pH 5.1. The absorbance at 280 nm was measured using a UV-1 or a UV-M monitor.

Ruthenium content of a_5Ru-modified CCP samples:

(a) Atomic absorption (AA) method: Ruthenium was detected at 349.9 nm

using a Perkin-Elmer (Model 503) AA spectrophotometer equipped with either a flame or graphite furnace attachment.[24] Samples were prepared in 0.1 M phosphate buffer, pH 7.0. Protein samples were prepared to be at least 50-100 μM in an attempt to observe a signal due to ruthenium. Standard curves for 0.5-20 ppm Ru gave linear plots with correlation coefficients, $R > 0.99$.

(b) Spectrophotometric method: The absorption maximum of a_5Ru(His) (ϵ_{303} = 2100 $M^{-1}cm^{-1}$)[1] at pH 5 is increased and red-shifted at pH 10 (ϵ_{370} = 3400 $M^{-1}cm^{-1}$)[14] and is therefore easier to detect at high pH. CCP is unstable above pH 8[26] but may be stabilized by forming the cyanide complex.[27] 10 μM native and modified CCP samples were prepared in 0.1 M CAPS buffer (pH 11) containing 10 mM KCN. All protein concentrations were chosen to be 10 μM assuming ϵ_{422} = 103 mM^{-1} cm^{-1} for the cyanide adducts of both CCP[27] and a_5Ru(His)CCP. The concentration chosen is a compromise between obtaining a large enough absorbance to detect the a_5Ru(His) complex (ϵ_{370} = 3400 M^{-1} cm^{-1}), and using a minimum amount of protein. The absorption spectrum of native CCP-CN was subtracted from the cyanide adduct of each band from cation-exchange chromatography. If the resultant difference spectrum had a broad band with λ_{max} = 370 nm, the protein species present was assumed to be modified with the a_5Ru(His) complex. Subtraction of the spectra of two different samples of native CCP-CN gives a difference spectrum which is devoid of peaks and has a flat baseline.

X-ray crystallization: Growth of crystals suitable for x-ray crystallization was performed by Dr. S. L. Edwards at the University of Maryland following published

procedures.[28]

Diethyl pyrocarbonate modification: A stock solution of 0.1 M DEPC was made fresh daily by adding 0.15 ml DEPC to 10 ml anhydrous ethanol. The concentration of the stock DEPC was determined by adding a known volume to 3 ml of 1 mM His or imidazole and measuring the absorbance increase at 240 nm (ϵ_{240} = 3200 M^{-1} cm^{-1}) for the His derivative or 230 nm (ϵ_{230} = 3300 M^{-1} cm^{-1}) for the imidazole derivative.[9] The concentrations of a_5Ru(His) and CCP were determined spectrophotometrically using published extinction coefficients, ϵ_{303} = 2100 M^{-1} cm^{-1} for a_5Ru(His)[1] and ϵ_{408} = 98 mM^{-1} cm^{-1} for CCP.[29] The concentration of a_5Ru(His)CCP was also determined using ϵ_{408} for CCP since a_5Ru(His) has little absorbance in the Soret region and attachment to surface His residues is not expected to perturb the heme. The time course for the reaction of DEPC with His, a_5Ru(His), CCP and a_5Ru(His)CCP was followed spectrophotometrically. The exposure of samples to uv-light during the measurements was minimized since readings were taken at large time intervals.

Computer graphics: X-ray crystal structure coordinates for CCP, obtained from the Brookhaven data bank, were imported into a graphics programme obtained from UCSF (Midas plus)[6b] which was run on a Silicon Graphics 4D personal IRIS system. Photographs were taken of the screen in a darkened room using a 35 mm camera equipped with a 135 mm telephoto lens. The camera was set up on a tripod ~ 6 ft from the screen, and a cable release was used to avoid moving the camera while taking photographs.

2.3 RESULTS

CCP Modification: Modification of CCP with a 20-fold excess a_5Ru^{2+} did not result in the precipitation of any protein during the reaction. Approximately 95% of the CCP was recovered following the ruthenation procedure. Percent yields of peaks 4a' and 5b' following cation-exchange chromatography were estimated to be 7 and 0.5%, respectively.

Anion-exchange chromatography: a_5Ru-modified CCP shows a different elution profile from native CCP, but both are eluted as single broad bands (Figure 2.3). Anion-exchange chromatography was chosen first because it is used in the isolation procedure for CCP.[21] Modified CCP binds to the DEAE resin but it is eluted at a lower salt concentration than native CCP, presumably because each a_5Ru group introduces a 3+ charge to the protein. However, although a number of bands were expected, the ruthenium-modified CCP reaction mixture was eluted as a single broad band. Lowering the pH to make CCP more cationic and reduce its affinity for the DEAE column, did not improve the separation.

Cation-exchange chromatography: Since native CCP is anionic at pH > 5.1, it does not bind to cation-exchange resins, and is eluted in the void volume. Modified CCP does bind, due to the positive charge introduced by the a_5Ru complex. At least six distinct bands are present in the elution profile of modified CCP from the cation-exchange column (Figure 2.4). Each of the bands in Figure 2.4 were rechromatographed on the same column using shallower salt gradients but the resolution was not improved. Initially, this gave the misguided idea that all the bands

were due to single species. The next section on FPLC shows that, in fact, this is not correct.

FPLC (Cation-exchange chromatography): Elution conditions similar to those for cation-exchange chromatography at ambient pressure were used since both resins possess sulphonate groups. The FPLC elution profile (Figure 2.5) is similar in overall appearance to that at ambient pressure (Figure 2.4). However, FPLC further resolves bands 2 to 5 into a number of peaks. Most notable, is the chromatography of band 3 by FPLC which shows that this band consists of at least 4 distinct peaks (Figure 2.5). The yield of the individual components is very small, so work on band 3 was discontinued. Band 1 is eluted in the void volume like native CCP. Rechromatography of bands 2 to 5 shows that they may be resolved further when shallower gradients are used, although band 2 yields a sharp peak which still accounts for > 50 % of the total protein content of this band. Band 4 is resolved into peaks 4a and 4c, and a definite shoulder 4b using shallower NaCl gradient (50-100 mM) (Figure 2.6a). Peak 4a is the major component and was rechromatographed by holding the NaCl concentration at 70 mM, yielding peak 4a' which can not be resolved any further (Figure 2.6b). Similarly, peak 5 can be resolved using a shallower gradient (150-200 mM) (Figure 2.7a) into peaks 5a, 5b and 5c. Peak 5b is the major component and rechromatography of this peak by holding the NaCl concentration at 170 mM, yielded peak 5b' which can not be resolved any further (Figure 2.7b).

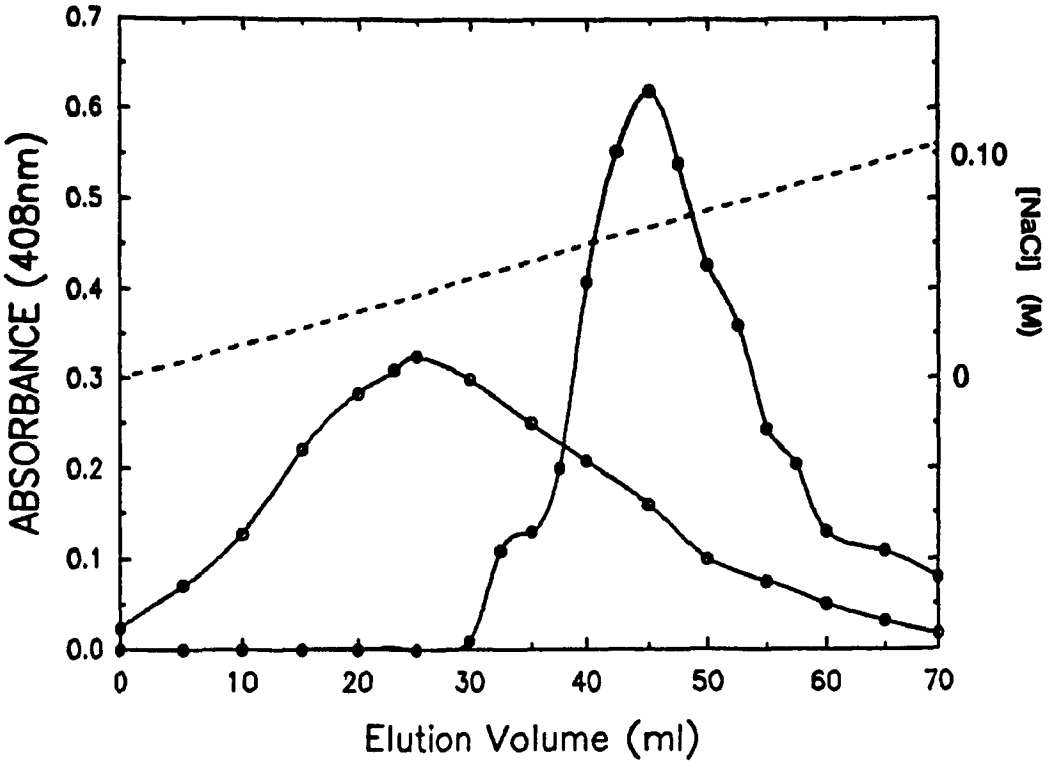

Figure 2.3: Anion-exchange chromatography (DEAE-Sepharose CL-6B) of 2 mg native CCP (solid circles) and a_5Ru modified CCP (open circles). Elution was with a linear 0-500 mM NaCl gradient in 50 mM acetate buffer, pH 5.1 (dashed line), at a flow rate of 5 ml/h.

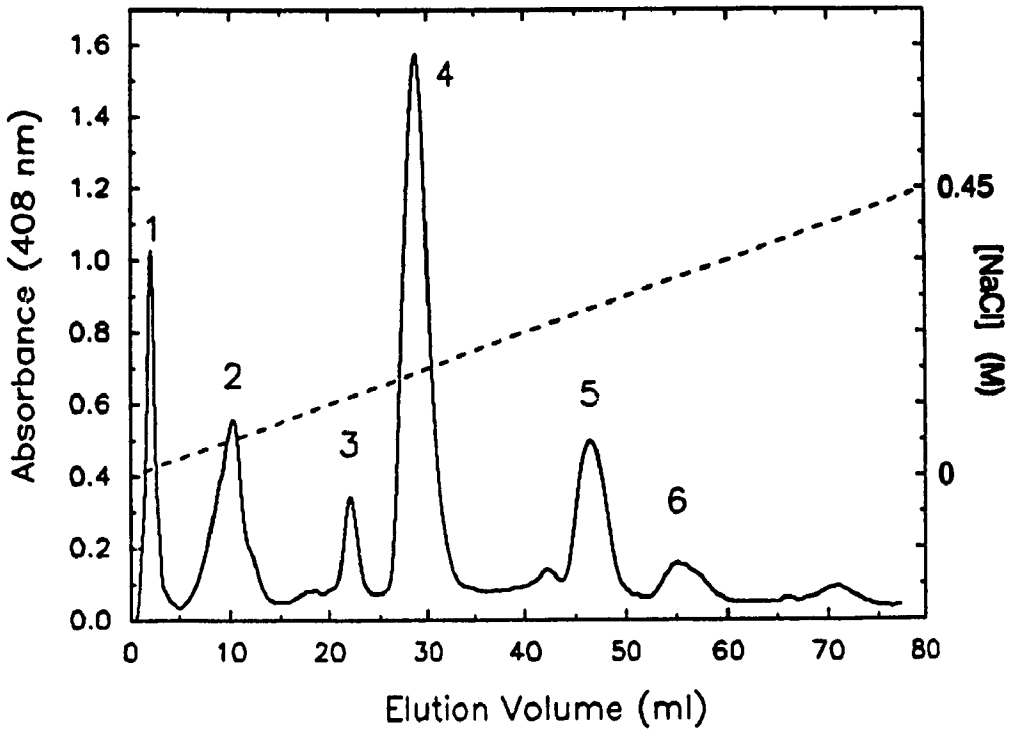

Figure 2.4: Cation-exchange chromatography (S-Sepharose, fast flow) of 10 mg of the CCP species from the a_5Ru reaction mixture at 4°C. Elution was with a linear 0-0.5 M NaCl gradient in 50 mM acetate buffer, pH 5.1 (dashed line), at a flow rate of 6 ml/h, 2 ml fractions were collected.

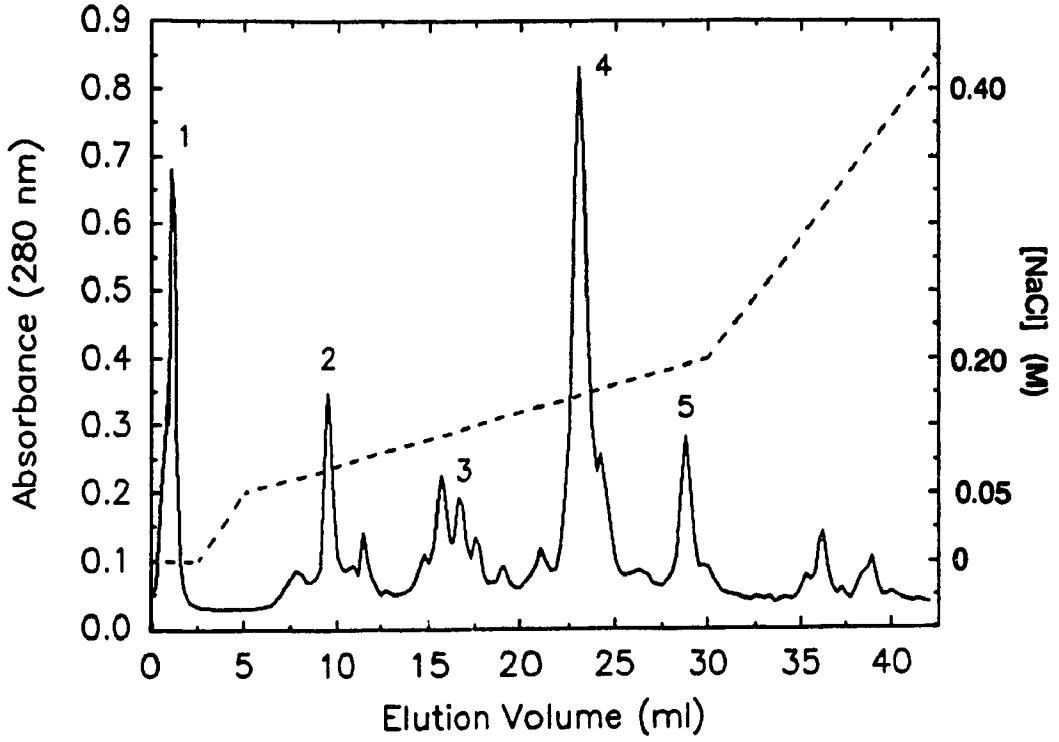

Figure 2.5: FPLC cation-exchange chromatography (Mono S, HR 5/5) of 1 mg of the same sample as Figure 2.4. The column was equilibrated with 50 mM acetate (pH 5.1) and elution was with 0-0.95 M NaCl in 50 mM acetate buffer (pH 5.1) as shown (dashed line). Flow rate: 0.5 ml/min. Fraction size: 0.5 ml. 22°C.

Figure 2.6: (a) FPLC cation-exchange (Mono S, HR 5/5) rechromatography of ~ 1 mg of band 4 in Figure 2.5. Elution was with the NaCl gradient shown (dashed line), and the experimental conditions were the same as in the caption to Figure 2.5 except that a fraction size of 0.25 ml was used. (b) Rechromatography of ~ 0.5 mg of peak 4a in (a) above under identical conditions except that the NaCl concentration of the eluting buffer was held constant at 0.07 M.

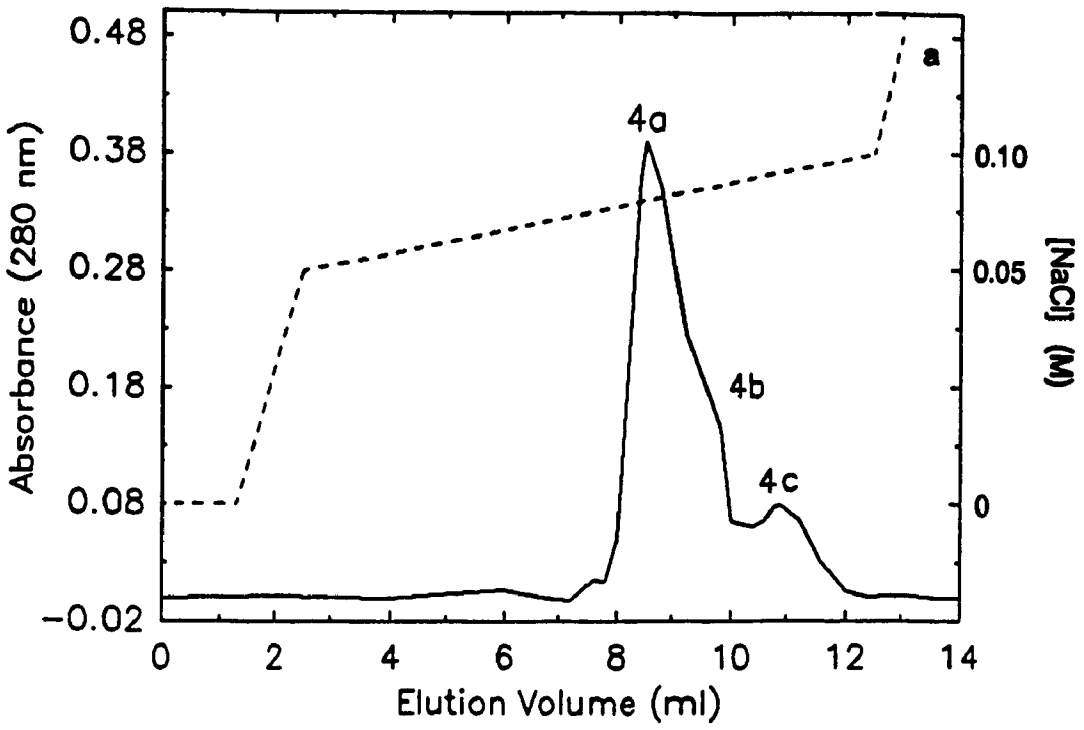
a
4a
4b
4c
0.48
0.38
0.28
0.18
0.08
−0.02
Absorbance (280 nm)
0.10
0.05
0
[NaCl] (M)
0
2
4
6
8
10
12
14
Elution Volume (ml)

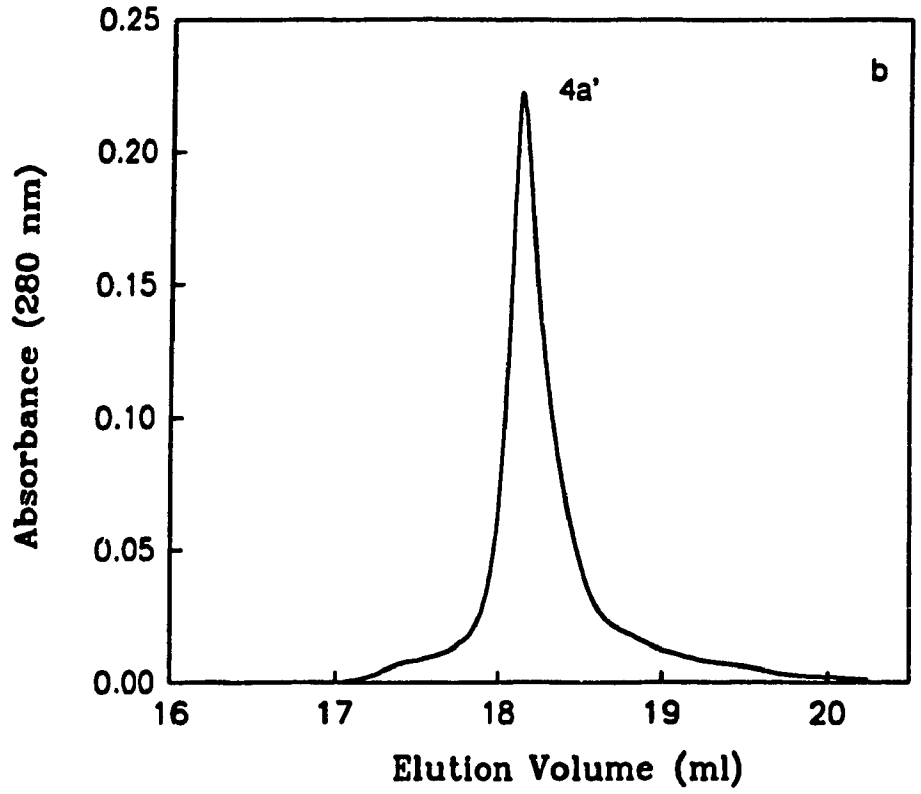
b
4a'
0.25
0.20
0.15
0.10
0.05
0.00
Absorbance (280 nm)
16
17
18
19
20
Elution Volume (ml)

Figure 2.7: (a) FPLC cation-exchange (Mono S, HR 5/5) rechromatography of ~ 1 mg of band 5 in Figure 2.5. Elution conditions were identical to those given in the caption to Figure 2.6(a) except for the NaCl gradient used (dashed line). (b) Rechromatography of ~ 0.5 mg of peak 5b in (a) above under identical conditions except that the NaCl concentration of the elution buffer was held constant at 0.17 M.

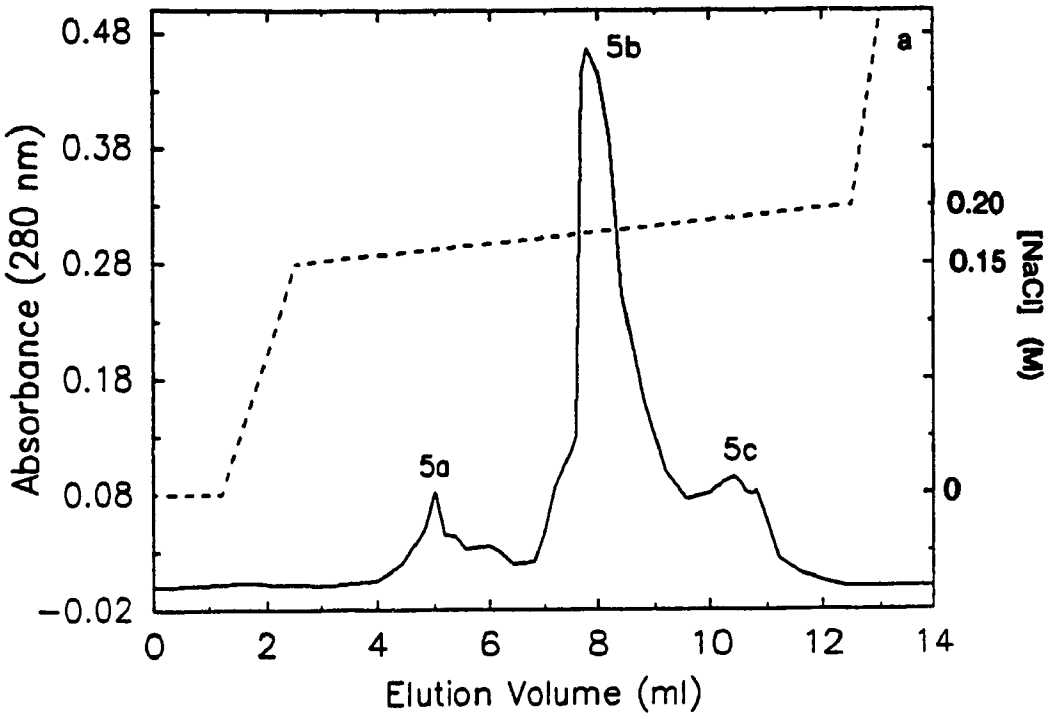
0.48
0.38
0.28
0.18
0.08
−0.02
Absorbance (280 nm)
0
2
4
6
8
10
12
14
Elution Volume (ml)
5a
5b
5c
a
0.20
0.15
0
[NaCl] (M)

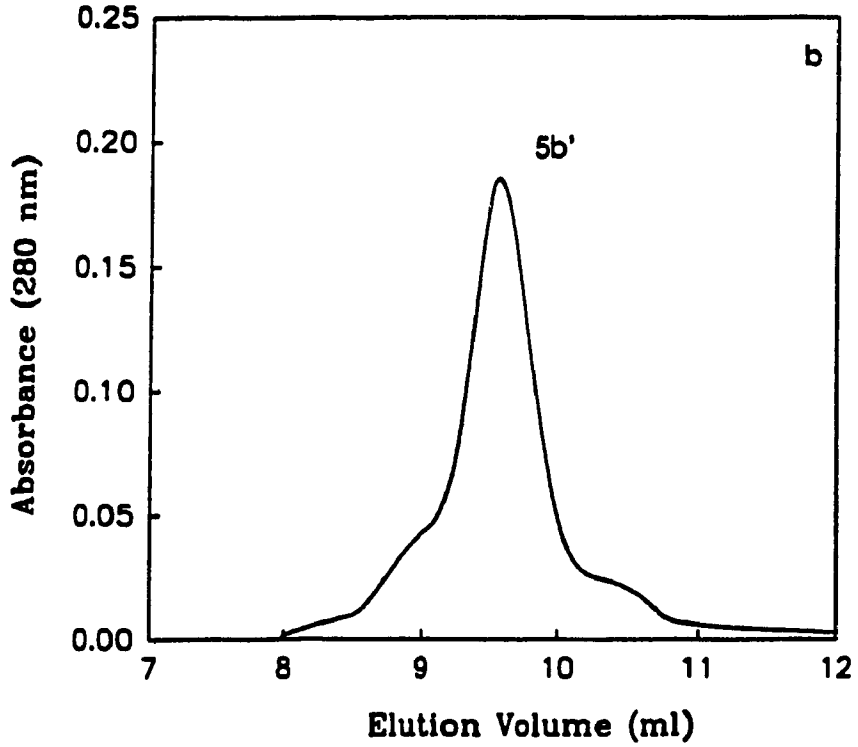
0.25
0.20
0.15
0.10
0.05
0.00
Absorbance (280 nm)
7
8
9
10
11
12
Elution Volume (ml)
5b'
b

Ruthenium content of a_5Ru-modified CCP: Previous studies have used AA to analyze for ruthenium content.[2-4] Our results for AA are not shown as this method was abandoned after preliminary studies because AA is a destructive technique requiring at least 1 mg of purified protein per determination. When cheap, commercially available proteins such as cyt c and Mb are used such losses, although undesirable, can be tolerated.

The method of choice here is uv-vis absorption spectroscopy because only 0.2 mg of protein are required to obtain a spectrophotometric measurement. Figure 2.8 shows the shift in the 303 nm band of a_5Ru(His) at high pH due to ionization of the pyrrole nitrogen which has a pK_a of ~ 14 in free His, and ~ 8.9 in a_5Ru(His).[30] Thus, a pH-induced spectral shift of the 303 nm band will indicate that the a_5Ru(His) is attached to His residues on the protein. Figure 2.9 shows the spectra of native CCP and CCP-CN and Figure 2.10 shows the difference spectra obtained when the spectrum of CCP-CN is subtracted from the cyanide complexes of peak 4a' and 5b'. The difference spectra clearly show a peak due to a_5Ru(His) whereas subtraction of CCP-CN from another sample of CCP-CN yields a difference spectrum with no peaks (Figure 2.10).

The ruthenium content, determined spectrophotometrically, of some of the bands purified by cation-exchange chromatography (Figure 2.5) are listed in Table 2.2. Band 1 is eluted in the void volume from the cation-exchange column (Figure 2.5) as is native CCP. Since this band appears to contain no ruthenium, it probably contains native CCP. Band 2 binds to the cation-exchange column but it does not

appear to have any a_5Ru(His) absorbance (Table 2.2). The ruthenium content of band 3 was determined for protein purified at ambient pressure (Figure 2.4). The Ru/heme ratio for this band is close to 1 but Figure 2.5 indicates that band 3 contains at least four species of low abundance. Peak 4a', and the less abundant 5b', appear to contain single 1:1 Ru/heme derivatives (Table 2.2), so further work was centred on these peaks. Although peak 5b' has a Ru/heme ratio of one, there is a large error of 30% associated with these data (Table 2.2), probably due to the smaller number of samples prepared for ruthenium determination because this peak was not purified from every modification. Also, the difference spectrum obtained for peak 5b' shows sharp minima at 300 nm and 430 nm unlike peak 4a' (Figure 2.10). This suggests that the binding of the a_5Ru has perturbed the protein structure of the species in peak 5b' more than that in peak 4a'.

X-ray crystallization of a_5Ru(His)CCP derivatives: X-ray crystal structure analysis shows that peak 4a' is a singly-modified a_5Ru(His) derivative of CCP and that His-60 is the modified residue (Figure 2.11). This peak is the most abundant one from cation-exchange chromatography (Figure 2.5), and His-60 is expected to be the most likely site for modification on CCP, due to its high solvent accessibility compared to His-6 or 96 (Figure 2.2).

Table 2.2

Characterization of the ruthenium content, activity and compound I stability of species purified from the ruthenation reaction mixture.

Species[a]	a_5Ru/Heme	% Activity[b]	$t_{½}$ for the decay of compound I[c] (h)
CCP[d]	0	100 ± 6	5.5 ± 0.8 (10)[e]
Peak 1 (Figure 2.5)	0	101 ± 9	ND[f]
Peak 2 (Figure 2.5)	0	99 ± 7	ND
Peak 3 (Figure 2.4)	0.80 ± 0.12	88 ± 9	ND
Peak 4a' (Figure 2.6b)	0.92 ± 0.16	100 ± 5	3.0 ± 0.6 (8)
Peak 5b' (Figure 2.7b)	0.97 ± 0.30	93 ± 5	2.9 ± 0.8 (5)

[a]The peaks were purified by cation-exchange chromatography, and the relevant chromatograms are shown in the Figures in parenthesis

[b]Enzymatic activity relative to native CCP

[c]$t_{½}$ obtained from semilog plot for the absorbance decrease at 424 nm due to reduction of Fe^{4+}

[d]Native CCP

[e]Number of measurements of $t_{½}$

[f]ND = not determined

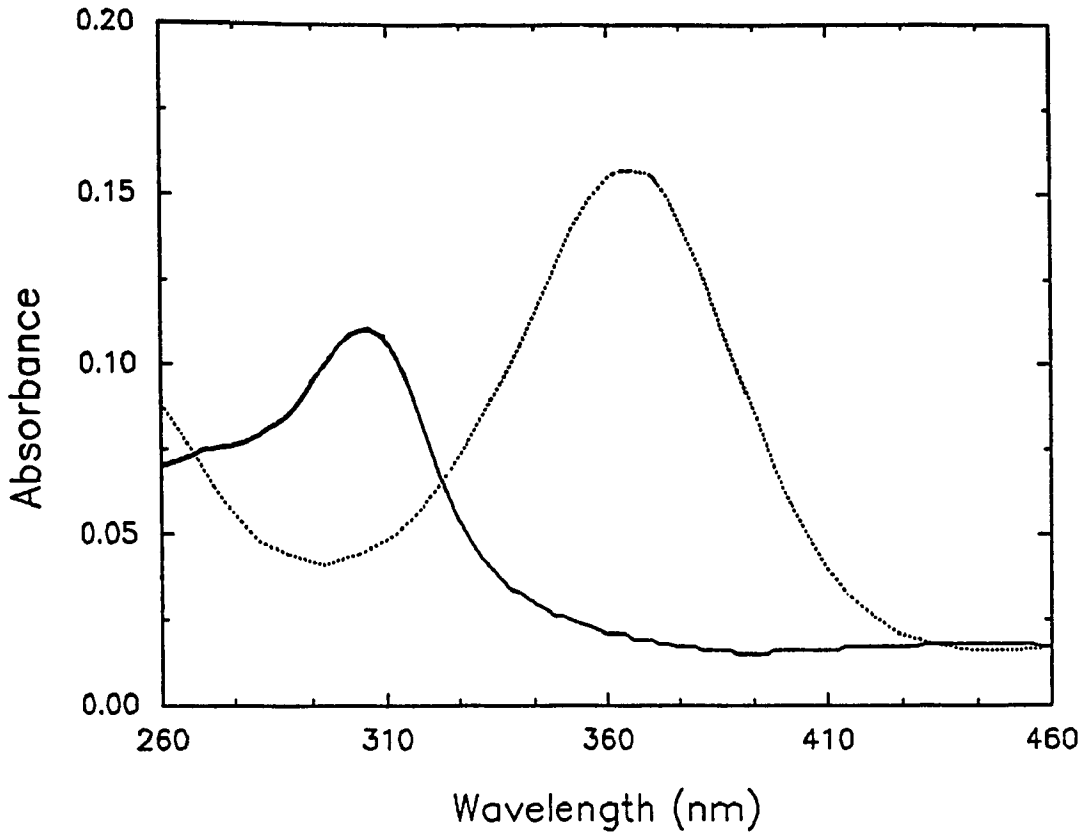

Figure 2.8: Absorption spectra of ~ 60 μM a_5Ru(His) at pH 7 (solid line) in 0.1 M phosphate buffer, and pH 11 (dotted line) in 0.1 M CAPS buffer. Cuvette path length: 10 mm. 22 °C.

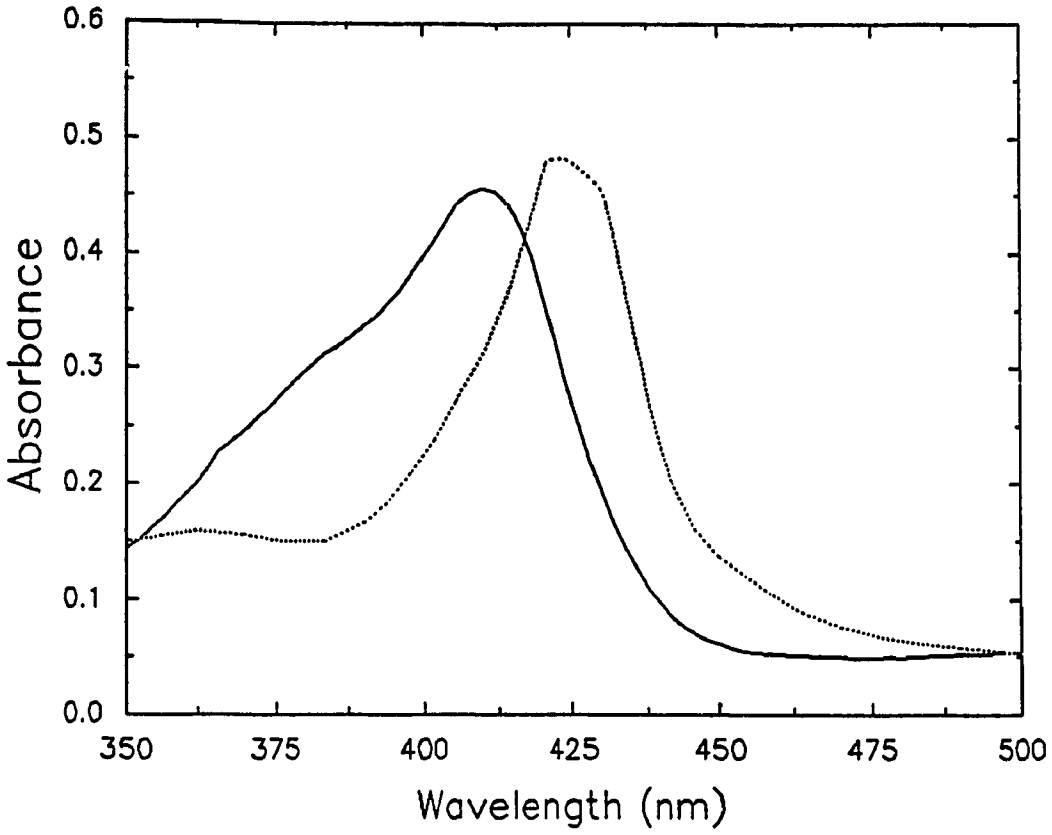

Figure 2.9: Absorption spectra of ~ 4.7 μM native CCP (solid line) in 0.1 M phosphate (pH 7.0) and the cyanide complex of CCP (dotted line) in 0.1 M CAPS, 10 mM KCN (pH 11). Cuvette path length: 10 mm. 22 °C.

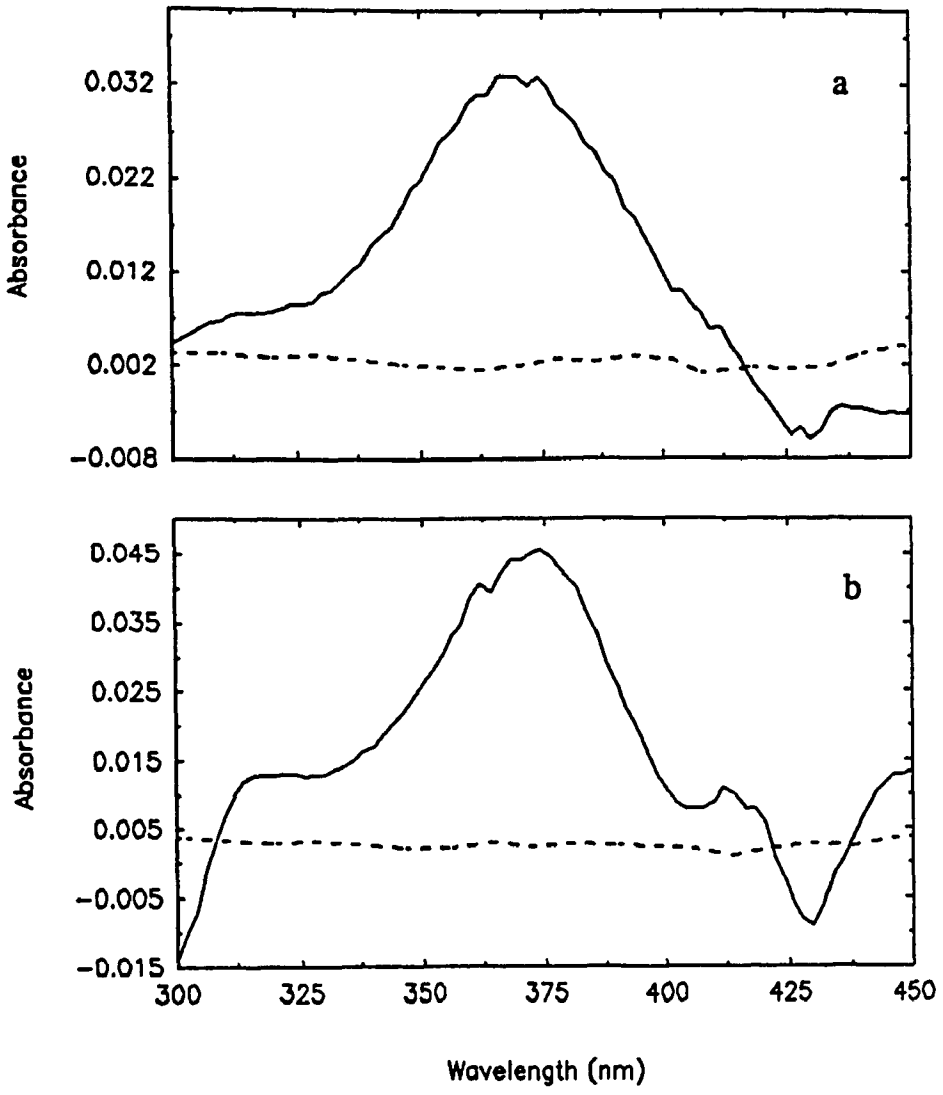

Figure 2.10: Difference spectra of the CCP-CN species of peaks **(a)** 4a' and **(b)** 5b' minus CCP-CN. The dashed line in each panel represents the difference spectrum of two CCP-CN samples showing that no peak is present at 370 nm. All samples contained 10 μM protein in 0.1 M CAPS buffer (pH 11) containing 10 mM KCN. Cuvette path length: 10 mm. 22 °C. Peaks 4a' and 5b' are from the rechromatography by FPLC as shown in Figures 2.6 and 2.7, respectively.

Enzymatic activity & Compound I stability: From Table 2.2 it is interesting to note that the peaks purified by cation-exchange chromatography retain most, if not all, of their enzyme activity when compared to native CCP. From the crystal structure of CCP we know that the heme site is at least 20 Å from any of the surface His residues (Figure 2.1). Also, from computer graphics and a Brownian dynamics study, the proposed cyt c binding regions on CCP do not appear to be close to any of the surface His residues.[31] Therefore, it is not surprising that the a_5Ru(His)CCP derivatives have enzymatic activities comparable to CCP.

The catalytic cycle of CCP, discussed in Chapter 1, involves the formation of a stable intermediate, compound I (Figure 1.2) in the presence of H_2O_2. This intermediate contains an Fe^{4+}=O heme which spontaneously decays back to a Fe^{3+} species with a half-life ($t_{½}$) of ~ 5 h for native CCP. Typical semilog plots for the absorbance change at 424 nm due to the decay of Fe^{4+}=O in native CCP, and in peaks 4a' and 5b' are shown in Figure 2.12. The decays were followed over 2-3 half-lives and fit to a single exponential with correlation coefficients > 0.99. Peaks 4a' and 5b' both decay with a half-life of ~ 3 h, thus, although the decay of the Fe^{4+}=O in both derivatives is faster than in native CCP, the Fe^{4+}=O species are stable enough to be used in electron transfer experiments.

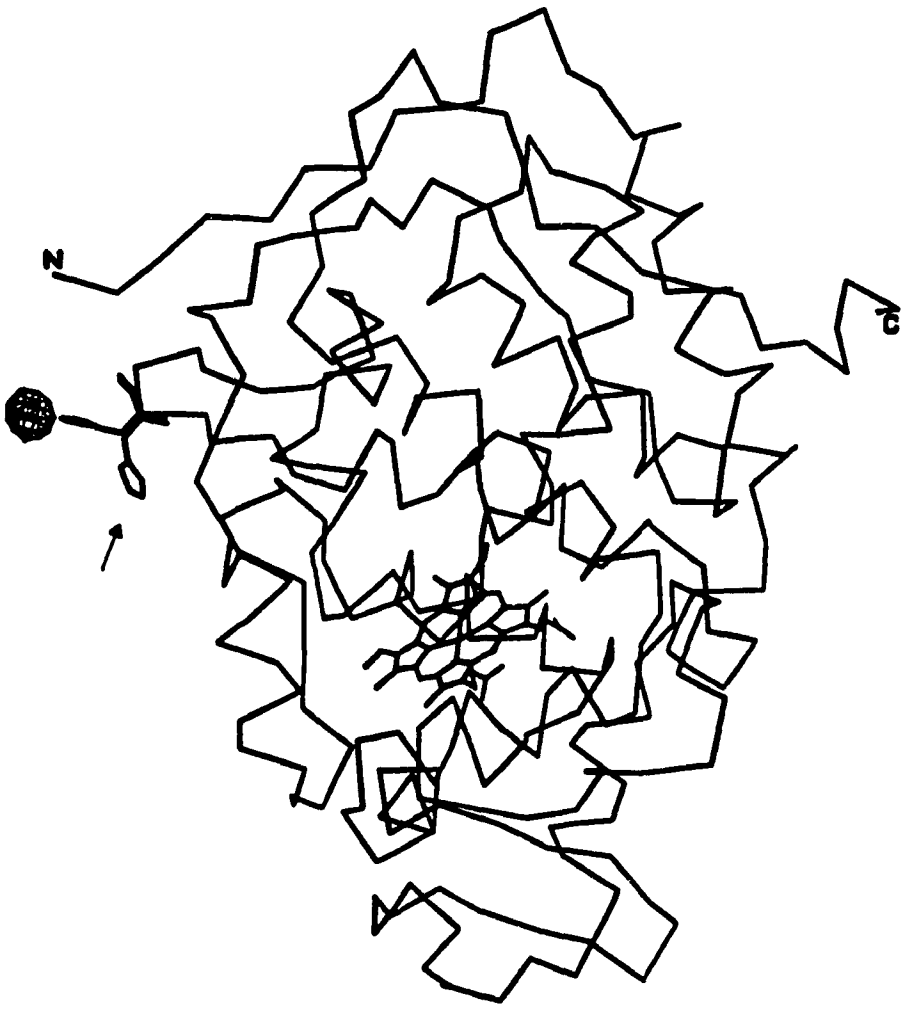

Figure 2.11: A 2 Å density difference map [a_5Ru(His-60)CCP - native CCP] contoured at 5-times above background superimposed on the CCP model. The position of His-60 prior to attachment of a_5Ru is indicated by the arrow. Attachment of a_5Ru causes reorientation of the His-60 residue to accommodate the a_5Ru as indicated by the new position of His-60 with the a_5Ru complex designated by the hatched sphere. The x-ray structure was carried out by Dr. S. L. Edwards following published procedures.[28]

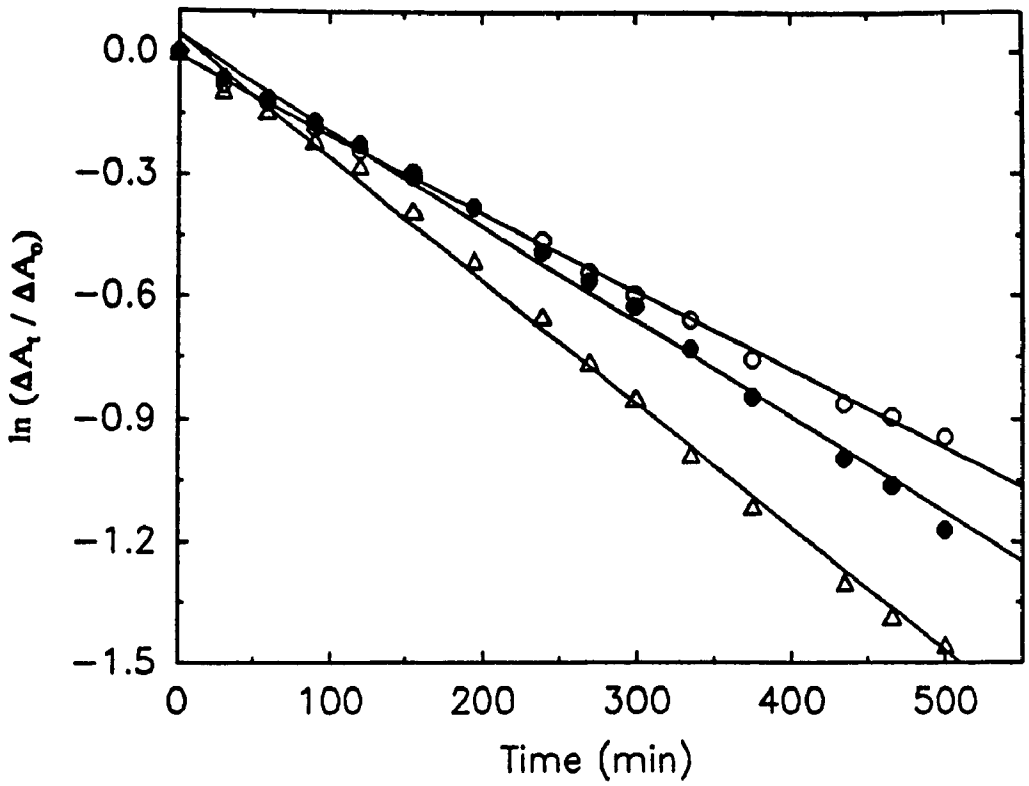

Figure 2.12: Absorbance decrease at 424 nm due to the decay of compounds I of CCP (open circles), peak 4a' (solid circles) and peak 5b' (open triangles). Semilog plot of the ratio of the absorbance change at time, t ($\Delta A_t = A_t - A_\infty$) to the total absorbance change ($\Delta A_o = A_o - A_\infty$) vs. time. Conditions: 4 μM protein in 0.1 M phosphate buffer (pH 7). Reactions were performed at 22 °C.

DEPC reactivity with His, a_5Ru(His), native CCP and the a_5Ru(His)CCP derivatives: The reactivity of DEPC with His and a_5Ru(His) was investigated to see if the coordination of a_5Ru to N(3) of the imidazole inhibits N-carbethoxyhistidine formation. The results (Figure 2.13) clearly show that DEPC is much less reactive with a_5Ru(His) than free His, although a small amount of the N-carbethoxyhistidine is formed. DEPC reacts with both nitrogen atoms of the imidazole ring[9] when there is a large excess (> 200-fold) of DEPC over His (Scheme 2.3), but DEPC is not present in such a large excess here, so little modification of the pyrrole nitrogen is expected, although this can not be ruled out. Modification of the pyrrole nitrogen causes an absorbance change at 240 nm, although the magnitude of the absorbance increase appears to be smaller than for modification of the pyridine nitrogen.[9] The observed absorbance increase when DEPC is reacted with a_5Ru(His) may also be due to small amounts of free His present due to ruthenium loss in the a_5Ru(His) complex. It is also possible that substitution of the ruthenium in the a_5Ru(His) complex by DEPC takes place, to form N-carbethoxyhistidine. Reaction of DEPC with $a_5Ru^{3+}H_2O$, where His is replaced by an aquo ligand, yielded no absorbance change at 240 nm over 30 min, but incubation of DEPC with a 1:1 mixture of $a_5Ru^{3+}H_2O$ and His yielded the same absorbance increase at 240 nm as in the reaction of DEPC and His alone. Thus, if DEPC reacts with $a_5Ru^{3+}H_2O$ there is no contribution to the absorbance increase at 240 nm, and its reaction with free His is unaltered.

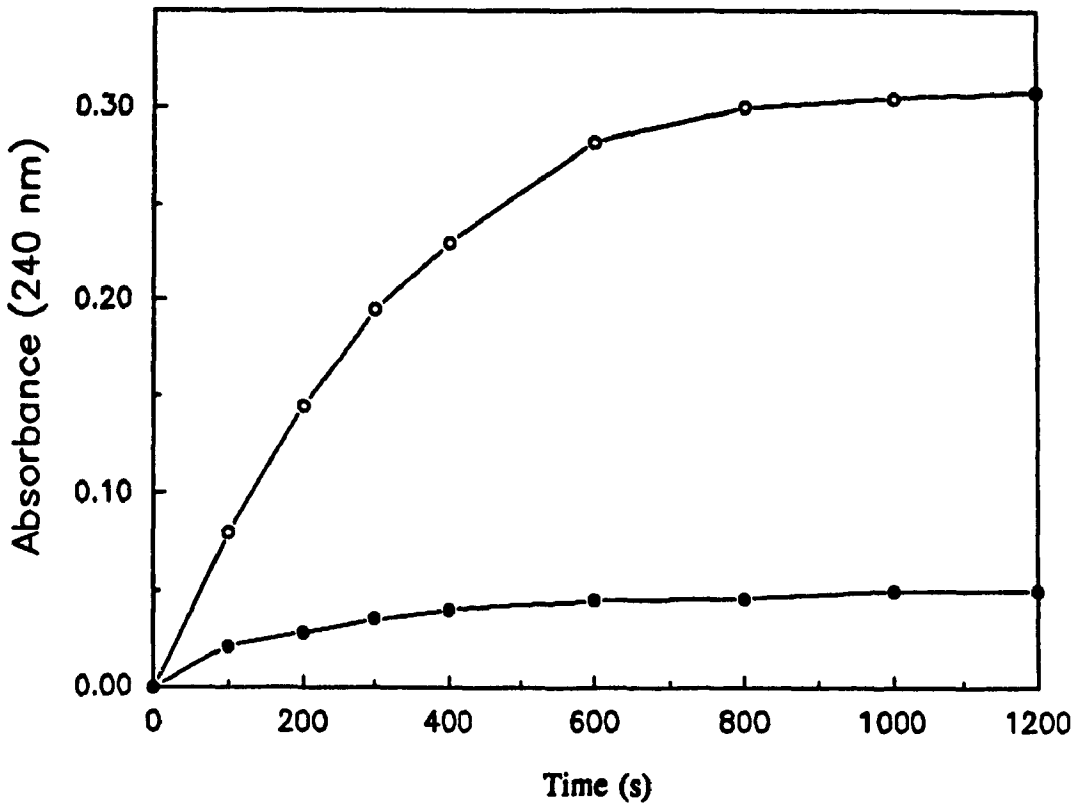

Figure 2.13: Observed absorbance change at 240 nm following the mixing of DEPC with free His (open circles) and a_5RuHis (closed circles). A 10-fold molar excess of DEPC was added to 100 μM solutions of the His and a_5Ru(His) samples in 0.1 M phosphate (pH 7). Reactions were performed at 22 °C.

Figure 2.14: Observed absorbance change at 240 nm following the mixing of DEPC with 10 μM (a) native CCP (open circles) and peak 4a' (open triangles), and (b) native CCP (open circles) and peak 5b' (closed circles). The absorbance change is expressed as the number of His residues modified using the published extinction coefficient, $\Delta\epsilon_{240}$ = 3300 M^{-1} cm^{-1}. A 50-fold molar excess of DEPC over protein was added to samples, which were 10 μM in 0.1 M phosphate (pH 7). Reactions were performed at 22 °C.

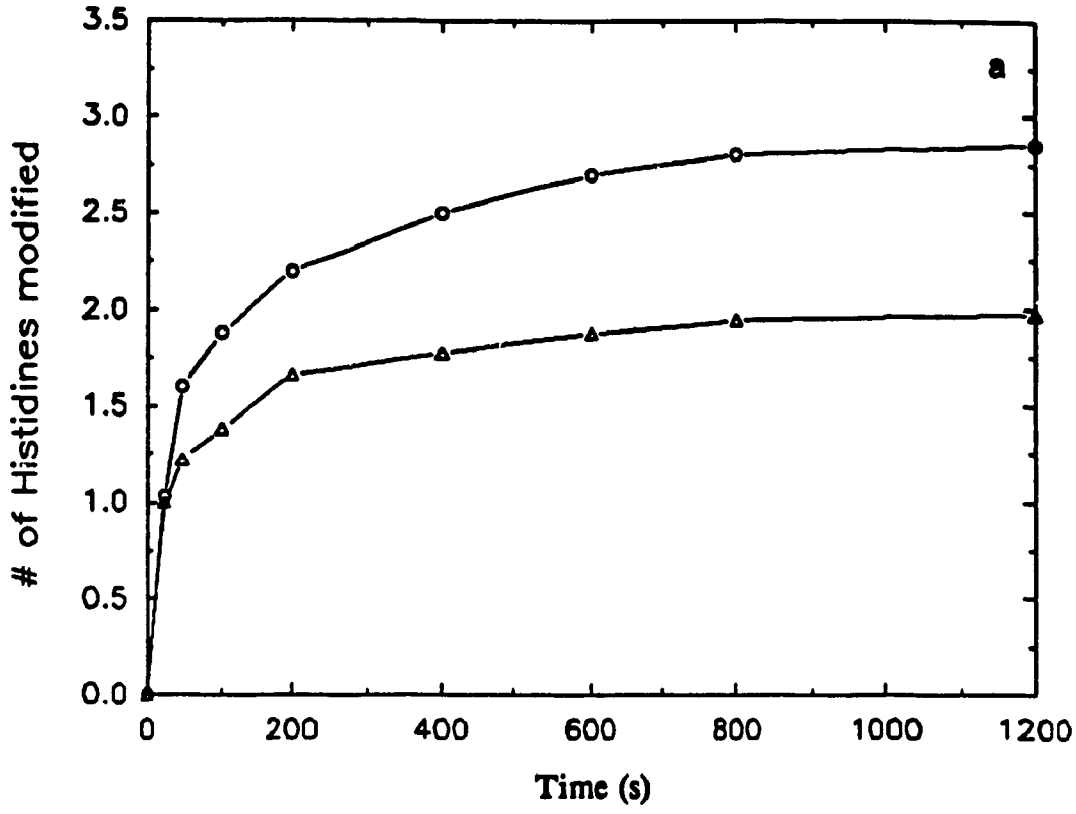
a
# of Histidines modified
Time (s)
0.0
0.5
1.0
1.5
2.0
2.5
3.0
3.5
0
200
400
600
800
1000
1200

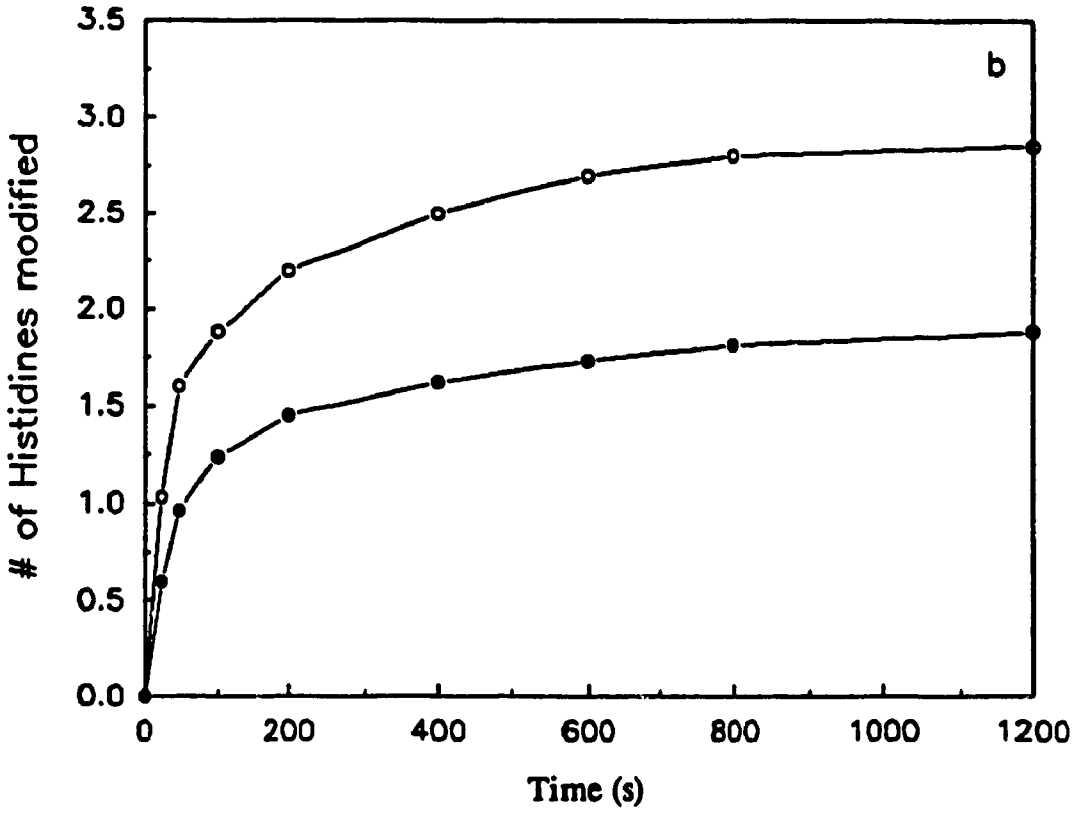
b
# of Histidines modified
Time (s)
0.0
0.5
1.0
1.5
2.0
2.5
3.0
3.5
0
200
400
600
800
1000
1200

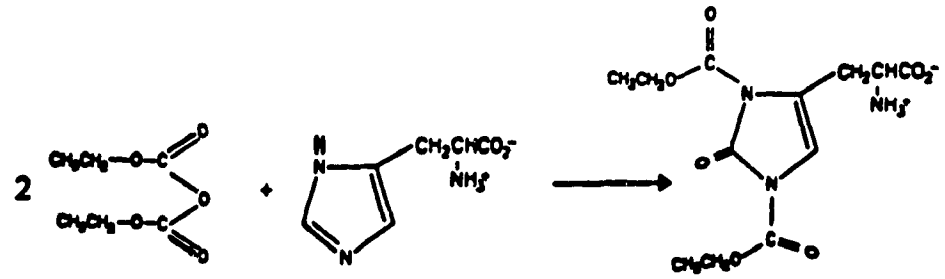

Scheme 2.3: Reaction of His with > 200-fold excess of DEPC[9]

DEPC is rapidly hydrolysed in aqueous solution, having a $t_{½}$ of 9 min in 37 mM phosphate buffer (pH 7).[9] For this reason excess DEPC (10 to 100-fold) is generally required. A 50-fold excess of DEPC over CCP was used here which corresponds to a 17-fold excess over His residues at pH 7, since 3 His residues are reactive at this pH.[6a] As with a_5Ru(His), the covalent attachment of a_5Ru to CCP decreases its reactivity with DEPC (Figure 2.14). At pH 7, DEPC modifies three His residues in native CCP, while only two His are modified in the CCP species present in peaks 4a' and 5b' (Figure 2.14). Also, the absorbance increase at 240 nm is reversed by addition of hydroxylamine which removes the carbethoxy group from N-carbethoxyhistidine.[9] This suggests that the a_5Ru is coordinated to the pyridine N(3) nitrogen of His (Scheme 2.2), in each of these modified CCP species.

To compare the relative reactivities of His residues in other proteins towards DEPC and a_5Ru, the reaction of DEPC with horse heart cyt c and horse Mb was investigated. Horse cyt c has only one His residue accessible to a_5RuH_2O and Table 2.3 shows that DEPC can only access a single His. The crystal structure of sperm whale Mb is known and it has twelve His residues, four of which are surface

Table 2.3

Histidine modification by DEPC in various hemoproteins, including two singly-modified a_5Ru(His)CCP derivatives

Protein	# of histidine residues modified by DEPC
Native CCP	3.03 ± 0.34 (36)[a]
Peak 4a' (Figure 2.6b)	2.09 ± 0.28 (15)
Peak 5b' (Figure 2.7b)	1.98 ± 0.17 (10)
Cytochrome c[b]	1.03 ± 0.31 (3)
Myoglobin[c]	8.12 ± 0.34 (4)

All samples contain 10 μM protein in 0.1 M phosphate buffer (pH 7), with a 50-fold molar excess of DEPC over protein.

[a]Number of measurements in parentheses.

[b]Horse heart (Sigma, Type VI)

[c]Horse heart (Sigma, Type III)

exposed residues. Horse Mb has identical His residues to sperm whale Mb, with the exception of His-12, which is absent. This residue is one of the surface-exposed residues in sperm whale Mb. DEPC appears to react with eight His residues on horse Mb (Table 2.3), suggesting that the majority of His residues are exposed to solvent. The ruthenation of horse Mb has not been investigated, but ruthenation of sperm whale Mb yields four singly-modified a_5Ru(His)Mb derivatives including a_5Ru(His-12)Mb which is absent in horse Mb. Therefore, horse Mb is expected to yield at least three singly-modified derivatives corresponding to three surface His residues.

2.4 DISCUSSION

Two singly-modified a_5Ru(His) derivatives of CCP are obtained when a_5RuH_2O is reacted with CCP at room temperature for 3 h in phosphate buffer (pH 7). This reaction time is short compared to the 1-3 days required for cyt c, but longer than the 30 min required for Mb, which is consistent with the accessibility of His residues in these proteins. Both Mb and CCP have surface His residues which are easily modified, whereas cyt c has only one buried His which is difficult to modify. DEPC is an excellent probe for the modification of His residues by a_5Ru, since both reagents react primarily with the pyridine nitrogen of the imidazole ring (Scheme 2.2) as shown above with a_5Ru(His) and free His. At pH 7, three His residues are accessible on native CCP, while only two are accessible in both peaks 4a' & 5b'. This suggests that a ruthenium centre is attached to a surface His in each derivative, and since peaks 4a' & 5b' have different chromatographic properties, it is reasonable to

assume that the covalently-attached ruthenium centre is located at different His residues in each derivative. The attachment of a_5Ru to His residues is supported by the difference spectra for a_5Ru(His)CCP-CN and CCP-CN which yields a peak at 370 nm at pH > 10, which is similar to the peak observed for the model complex, a_5Ru(His). Furthermore, this method of ruthenium determination will not detect a_5Ru bound to residues other than His because they are not expected to have the same spectroscopic properties as a_5Ru(His) such as the pH-induced spectral shift from 303 to 370 nm. Since the absorbance spectrum for peak 5b' yields minima at ~ 430 nm and below 300 nm, as well as the characteristic a_5Ru(His) peak at 370 nm, the heme may be more perturbed in this species. The x-ray crystal structure of CCP shows that His-6 and 96 are less solvent-exposed than His-60 (Figure 2.2), so attachment of an a_5Ru centre to either of these residues is expected to perturb the protein structure more than modification of residue His-60. The relative accessibility of the three surface His residues may also explain the higher yield (7% and 0.5%, respectively) of peak 4a' which is modified at His-60, compared to peak 5a', which is probably modified at either His-6 or 96.

DEPC and a_5RuH_2O both appear to react with one His in horse cyt c, although DEPC is able to access the His residue in 20 min, compared to 1-3 days for the ruthenium complex. Reactivity of DEPC with horse Mb does not give an accurate measure of the number of surface-exposed His residues, as was the case for horse cyt c and CCP. This is probably because DEPC is uncharged and is more hydrophobic than $a_5Ru^{2+}H_2O$ and can access His residues not accessible to a_5Ru

during the short reaction time of ~ 30 min used for Mb. Longer reaction times may allow the ruthenium complex to access more buried His residues in horse Mb, although it is unlikely that only singly-modified derivatives will be present due to the high reactivity of the three surface His residues which are modified within 30 min.

Separation of the ruthenation reaction mixture by cation-exchange chromatography was possible because of the introduction of 3+ charge for each a_5Ru centre attached. Presumably, the attached a_5Ru centre is solvent-exposed so it can interact with the negatively-charged sulphonate groups of the cation-exchange matrix. Table 2.2 summarizes some of the properties of the various species isolated by cation-exchange chromatography. The enzymatic activities of all purified peaks are similar to that of native CCP. For the singly-modified a_5Ru(His)CCP derivatives (peaks 4a' & 5b') this is consistent with the fact that the surface His are (Figure 2.1) at least 20 Å from the active site of CCP. The activity of other proteins that have been modified using a_5Ru (ribonuclease A, α-lytic protease, lysozyme and GOx) was found to decrease depending on the extent of modification. This is clearly demonstrated for ribonuclease which retains 65% activity when one a_5Ru centre is attached, but only 22% activity when two a_5Ru centres are present.[13] Lysozyme retains 70% activity when a single a_5Ru is covalently attached,[14] whereas α-lytic protease is completely inactive when its single His, which is thought to play a key role in catalysis,[14] is ruthenated. GOx was modified in an attempt to observe direct electrochemical communication between GOx and an electrode. The modification was carried out in 3 M urea to expose buried His residues, resulting in the

attachment of 14 ruthenium centres. Remarkably, this derivative of GOx retains 70% of the activity of native GOx.[18] Since no CCP derivatives with Ru/heme ratios > 1 were isolated, the effect of modification with two or more a_5Ru centres on the activity of CCP is not known.

The half-life for compound I decay in the absence of exogenous reducing equivalents is ~ 5 h for native CCP, and ~ 3 h for peaks 4a' and 5b'. Considering that the surface His residues are all > 20 Å from the active site (Figure 2.1) there is no obvious explanation for the decrease in stability of compound I for peaks 4a' & 5b'. Reduction of Fe^{4+}=O by an endogenous donor requires charge migration through the polypeptide and will be dependent on conformational changes, H-bonding and electrostatic interactions. However, Fe^{4+}=O is stable enough in both singly-modified derivatives for electron transfer studies.

Identification of the site of modification by a_5Ru can be achieved by cleaving the modified protein at Arg and Lys residues with trypsin, followed by peptide mapping.[3] However, high resolution crystal structure data is available for native CCP,[8] so it is logical to crystallize peaks 4a' & 5b' and identify each site of modification from a difference map between native CCP and each derivative. Crystals of peak 4a' are isomorphous with native CCP and the a_5Ru is located specifically at residue His-60 (Figure 2.11). The a_5Ru centre appears to be highly solvent-exposed, and the orientation of His-60 is changed to accommodate the a_5Ru centre, such that the distance from the a_5Ru centre to the heme edge is increased to 21.8 Å from 16.6 Å in native CCP.[7,8] The crystal structure for peak 5b' has not been

determined, so the site of modification is not known. It is assumed from the results of the DEPC modification that the a_5Ru is attached to either residue His-6 or 96, which are the two remaining surface His residues.

An interesting point noticed during this study is that these derivatives, particularly peak 5b', crystallize more readily than native CCP. Thus, it is possible that this modification procedure could help in the crystallization of other proteins for x-ray crystal structure analysis.

2.5 REFERENCES

1 Sundberg, R. J.; Gupta, G. *Bioinorg. Chem.* **1973,** 3, 39.

2 Yocom, K. M.; The Synthesis and Characterization of Inorganic Redox Reagent-Modified Cytochrome c, Ph.D. Thesis, California Institute of Technology, 1982.

3 Yocom, K. M.; Shelton, J. B.; Shelton, J. R.; Schroeder, W. A.; Worosila, G.; Isied, S. S.; Bordignon, E.; Gray, H. B. *Proc. Natl. Acad. Sci.* **1982,** *79,* 7052.

4 Yocom, K. M.; Winkler, J. R.; Nocera, D. G.; Gray, H. B. Chemica. Scripta. **1983,** *21,* 29.

5 Crutchley, R. J.; Ellis, W. R.; Gray, H. B. *J. Am. Chem. Soc.* **1985,** 107, 5002.

6a Bosshard, H. R.; Banziger, J.; Hasler, T.; Poulos, T. L. *J. Biol. Chem.* **1984,** *259,* 5683.

6b Ferrin, T, E.; Huang, C. C.; Jarvis, L. E.; Langridge, R. *J. Mol. Graphics* **1988,** *6,* 13.

7 Poulos, T. L.; Finzel, B. C. *Pept. Protein Rev.*; **1984**, *4*, 115.

8 Finzel, B. C.; Poulos, T. L.; Kraut, J. *J. Biol. Chem.* **1984**, *259*, 13027.

9 Miles, E. W. *Methods Enzymol.* **1977**, 47, 431.

10 Yonetani, T.; Ray, G. S.; *J. Biol. Chem.* **1965**, *240*, 4503.

11 Erman, J. E.; Yonetani, T. *Biochim. Biophys. Acta.* **1975**, *393*, 350.

12 Matthews, C. R.; Erickson, P. M.; Van Vliet, D. L.; Petersheim, M. *J. Am. Chem. Soc.* **1978**, *100*, 2260

13 Matthews, C. R.; Erickson, P. M.; Froebe, C. L. *Biochim. Biophys. Acta.* **1980**, *624*, 499.

14 Recchia, J.; Matthews, C. R.; Rhee, M.; Horrocks, W. D. *Biochim. Biophys. Acta.* **1982**, *702*, 105.

15 Margalit, R.; Kostic, N. M.; Che, C-M.; Blair, D. F.; Chaing, H-J.; Pecht, I.; Shelton, J. B.; Shelton, J. R.; Gray, H. B. *Proc. Natl. Acad. Sci.* **1984**, 81, 6554.

16 Osvath, P.; Salmon, G. A.; Sykes, A. G. *J. Am. Chem. Soc.* **1988**, *110*, 7114.

17 Jackman, M. P.; McGinnis, J.; Powls, R.; Salmon, A. G.; Sykes, A. G. *J. Am. Chem. Soc.* **1988**, *110*, 5880.

18 Degani, Y.; Heller, A. *J. Am. Chem. Soc.* **1988**, *110*, 2615.

19 Jackman, M. A.; Lim, M-C.; Salmon, G. A.; Sykes, A. G. *J. Chem. Soc., Chem. Commun.* **1988**, 179.

20 Jackman, M. A.; Lim, M-C.; Sykes, A. G.; Salmon, G. A. *J. Chem. Soc., Dalton Trans.* **1988**, 2843.

21 English, A. M.; Laberge, M.; Walsh, M. *Inorg. Chim. Acta* **1986**, *123*, 113.

22 Cooper, T. G.; *The Tools of Biochemistry;* Wiley Interscience, **1980,** p 379.

23 Callahan, R. W.; Brown, G. M.; Meyer, T. J. *Inorg. Chem.* **1985,** 14, 1443.

24 Margoliash, E.; Frohwirt, N. *Biochem. J.* **1959,** *71,* 570.

25 *Cathodeon Hollow Cathode Lamps for Atomic Absorption Spectrophotometers,* Perkin-Elmer, 1976.

26 Dowe, R. J.; Erman, J. E. *Biochim. Biophys. Acta.* **1985,** *827,* 183.

27 Erman, J. E. *Biochemistry* **1974,** *13,* 39.

28 Edwards, S. L.; Xuong, N. H.; Hamlin, R. C.; Kraut, J. *Biochemistry* **1987,** *26,* 1503.

29 Balny, C.; Anni, H.; Yonetani, T. *Fed. Eur. Biochem. Soc.* **1987,** *221,* 349.

30 Sundberg, R. J.; Bryan, R. F.; Taylor, I. F.; Taube, H. *J. Am. Chem. Soc.* **1974,** *96,* 381.

31 Northrup, S. H.; Boles, J. O.; Reynolds, J. C. L. *Science (Washington, D. C.)* **1988,** *241,* 67.

3.0 ELECTRON TRANSFER KINETICS OF a_5Ru(His)CCP DERIVATIVES

3.1 INTRODUCTION

The heme Fe of CCP can exist in the +2, +3 and +4 oxidation states, providing two redox couples ($Fe^{2+/3+}$ and $Fe^{3+/4+}$) for electron transfer studies.[1a] Possible intramolecular electron transfer schemes using the a_5Ru(His)CCP derivatives are shown in eqns (1-4):

Ru^{2+}---Fe^{3+} ----> Ru^{3+}---Fe^{2+} $\Delta E^\circ \sim -278$ mV (1)[1b]

Ru^{3+}---Fe^{2+} ----> Ru^{2+}---Fe^{3+} $\Delta E^\circ \sim +278$ mV (2)[1b]

Ru^{2+}---Fe^{4+}, $P^{+\cdot}$ ----> Ru^{3+}---Fe^{3+}, $P^{+\cdot}$ $\Delta E^\circ \sim +900$ mV (3)[1b]

Ru^{2+}---Fe^{4+} ----> Ru^{3+}---Fe^{3+} $\Delta E^\circ \sim +900$ mV (4)[1b]

Eqn (1) is not feasible due to the unfavourable driving force for this reaction. The driving force for intramolecular electron transfer illustrated in eqn (2)-(4) indicate that all three reactions should be feasible. $P^{+\cdot}$ represents the protein radical present in compound I of CCP and is thought to be located on residue Trp-191. The x-ray crystal structure of CCP shows that Trp-191 is not located on the electron transfer pathways between any of the surface His residues (6, 60 or 96) and the heme. Consequently, $P^{+\cdot}$ is probably not involved in the intramolecular electron transfer so we assume that eqns (3) and (4) are equivalent here. Since we could not detect the protein radical, its fate was not investigated in this study. Investigation of the protein radical would require a technique such as EPR, which was not available to us.

It is desirable to reduce rapidly, in situ, the centre which is to be the reductant to ensure that the intramolecular electron transfer is rate limiting. For example, in eqn (4) above reduction of Fe^{4+} should be slower than the initial in situ reduction of the Ru^{3+} centre. Techniques for studying rapid kinetics include flash photolysis and pulse radiolysis. In pulse radiolysis a high energy electron generator produces $OH^{\cdot}$ radicals in aqueous solution. High concentrations of a radical acceptor (AH) results in the formation of $A^{\cdot}$ radicals, where $A^{\cdot}$ is often a strong reductant.

$$H_2O + e^-_{(aq)} \longrightarrow + OH^{\cdot} + H^{\cdot} \qquad (5)$$

$$AH + OH^{\cdot} \longrightarrow A^{\cdot} + H_2O \qquad (6)$$

The formate radical was found to be a useful reductant for a_5Ru(His-33)cytochrome c since the a_5Ru centre is reduced three times more selectively than the heme, 5.4×10^9 vs 1.8×10^9 M^{-1} s^{-1}.[2,3] This is desirable when following intramolecular electron transfer from the a_5Ru to the heme Fe as in eqn (1) above. Pulse radiolysis has also been successfully used to study electron transfer in HIPIP[4], cyt c_{551}[5] and plastocyanin.[6]

Flash Photolysis was used exclusively in this study. A laser or flash-tube provides a short pulse of light which generates the reactants in situ. For protein electron transfer studies $Ru(bpy)_3^{2+}$ is a useful photoredox reagent because it is excited by visible light so uv damage to proteins is avoided. Also, photoexcitation of $Ru(bpy)_3^{2+}$ produces a strong reductant, $^{\bullet}Ru(bpy)_3^{2+}$. $^{\bullet}Ru(bpy)_3^{2+}$ rapidly reduces the a_5Ru and heme centres of a_5Ru(His-33)cytochrome c with rates of 6.6×10^8 M^{-1} s^{-1} and 1.2×10^8 M^{-1} s^{-1}, respectively, i.e. the a_5Ru is reduced ~ 5.5 times more

selectively than the heme.[7-9] The product of photoreduction, $Ru(bpy)3^{3+}$, is a strong oxidant ($E^\circ \sim 1.3$ V)[23] and must be reduced quickly to avoid re-oxidation of the redox centres on the protein. EDTA can be added as a sacrificial electron donor because it does not quench the excited state ($^*Ru(bpy)_3^{2+}$) efficiently ($k_q < 10^7\ M^{-1}\ s^{-1}$).[10] Other polypyridine complexes (RuL_3) were also used to change the electrostatic interactions between the RuL_3 and the two redox centres of the protein. For example, complexes with negatively charged ligands such as $Ru(DIPS)_3^{4-}$ where DIPS = 4,7-di(phenyl-4-sulphonate)-1,10-phenanthroline and $Ru(DIC)_3^{4-}$, where DIC = 4,4'-dicarboxy-2,2'-bipyridine, were used in an attempt to reduce interactions with the negatively charged heme environment of CCP and enhance interactions with the surface-bound, positively charged a_5Ru centre.

Tollin and coworkers at the University of Azirona have used flavins to study electron transfer in cyt c,[11] flavodoxins,[11,12] ferredoxin,[13] cyt c_{551},[14] cytochrome c oxidase,[15] CCP,[16-18] and in CCP-cyt c complexes.[19-21] Figure 3.1 gives the structure of 5-deazariboflavin:

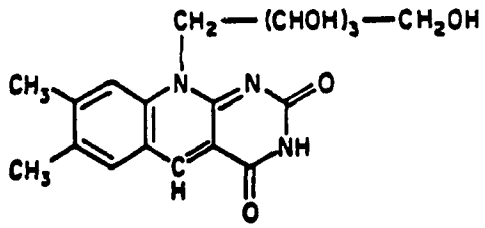

Figure 3.1 Structure of oxidized 5-deazariboflavin

The flavin quinone is photoexcited by visible light to rapidly generate a singlet

which decays to a triplet (^{3}DRF) in ~ 10 ns. The flavin triplet abstracts H· from a donor such as EDTA to form a flavin semiquinone in ≤ 1 μs. The semiquinone is the reactive species, and in the absence of an oxidant it slowly disproportionates ($k = 1 \times 10^6\ M^{-1}s^{-1}$)[16] to yield the fully reduced and oxidized species. Using 5-deazariboflavin as an example, Scheme 3.2 shows photoexcitation of the flavin quinone and hydrogen atom abstraction to yield the semiquinone which is followed by disproportionation in the absence of electron acceptors.

$$DRF + h\upsilon \longrightarrow {}^1DRF \longrightarrow {}^3DRF \qquad (7)$$

$$^3DRF + EDTA \longrightarrow DRFH\cdot + EDTA_{ox} \qquad (8)$$

$$DRFH\cdot + DRFH\cdot \longrightarrow DRFH_2 + DRF \qquad (9)$$

Scheme 3.1: Deazariboflavin semiquinone production and disproportionation

DRFH· exhibits low reactivity with the heme of CCP, but it reduces the heme of cyt c with a rate constant, $k = 2 \times 10^9\ M^{-1}\ s^{-1}$.[18] Like cyt c, a_5Ru is positively charged and is expected to be reduced rapidly and selectively by DRFH·.

This chapter presents the results of investigations on the reduction of ferryl iron in a_5Ru(His)CCP derivatives by inter- and intramolecular (eqn 3) processes. The in situ reduction of the a_5Ru centre was attempted using both Ru polypyridine complexes and DRFH· and results for electron transfer are presented. For the purpose of this Chapter, compound I will be referred to as CCP(Fe^{4+}) since the fate of the protein radical ($P^{+\cdot}$) during flash photolysis is unknown. The electron transfer pathway between the ruthenium and heme centre will be examined and discussed for the well-characterized a_5Ru(His-60)CCP derivative.

3.2 EXPERIMENTAL SECTION

3.2.1 Materials

Tris(2,2'-bipyridine)ruthenuim(II) dichloride hexahydrate [$Ru(bpy)_3^{2+}$], EDTA and hydrogen peroxide were obtained from GFS chemicals, Sigma and ACP chemicals. $Ru(DIC)_3^{4-}$ and $Ru(DIPS)_3^{4-}$ were synthesized by coworkers in this laboratory. 5-deazariboflavin was synthesized at the University of Arizona by the published procedure.[22]

Instrumentation: At Concordia, spectrophotometric measurements were made on a Hewlett Packard HP 8451A diode array spectrophotometer. The flash photolysis system consisted of a high voltage power supply connected to two xenon flash tubes of ~ 25 μs duration (Xenon Corp.). Absorbance changes were monitored using monochromatic light from a tungsten-halogen illuminator (Oriel, Model 77503) through a monochromator (Oriel, Model 77250) which was focused onto a photomultiplier tube (Hamamatzu, Model 77341) via fibre optic cable (Oriel). The PMT was connected to a storage oscilloscope (Phillips, Model 3320A) which was interfaced to a PC XT-computer. Kinetic data were analyzed using Asystant plus software (Asyst Corp.). At Arizona, spectroscopic measurements were made on a Cary 2200 spectrophotometer. The flash photolysis system in Arizona consisted of a pulsed (1 ns pulse duration) nitrogen laser (PRA LN100) which was used to pump a dye (BBQ) and excite DRF at 386 nm. Absorbance changes were monitored by focusing a monitoring beam from a Tungsten-halogen illuminator (Oriel, Model 6129) to a photomultiplier tube (RCA 4463).[25] Signals were amplified using an amplifier

constructed at the University of Arizona. 4-6 traces were collected on a Nicolet 1170 signal adder and transferred both to a strip chart recorder and to a PC AT computer interfaced to the signal adder.

3.2.2 Methods

Sample preparation:

(i) RuL_3 complexes: RuL_3 samples were prepared in 0.1 M phosphate buffer (pH 7). Concentrations were determined spectrophotometrically ($e_{445} \sim 16\ mM^{-1}\ cm^{-1}$).[23] All flash photolysis studies involving RuL_3 complexes were performed at Concordia using a 12 cm path length cylindrical cell purchased from Xenon Corp. Argon (Linde, prepurified) was bubbled through 12 ml of a solution containing 50-100 μM RuL_3 and 1-10 mM EDTA for at least 2 h. Appropriate volumes of 0.5-1 mM protein were then added to the deaerated polypyridine solution using a gas-tight Hamilton syringe and argon was passed over the solution for another 30 min before flash photolysis studies were performed.

(ii) Flavin solutions: All flavin studies were performed at the University of Arizona in Gordon Tollin's laboratory. DRF solutions were prepared by dissolving solid DRF in 4 mM phosphate buffer (pH 7) and 0.5 mM EDTA (μ = 8 mM) for low ionic strength work, or in 4 mM phosphate (pH 7), 0.5 mM EDTA and 0.92 M KCl (μ = 100 mM) for high ionic strength work. The solution was stirred overnight in the dark and filtered the following day with a 1.2 μm filter. DRF concentrations of 80-120 μM were used, as determined spectrophotometrically (e_{398} = 12000 $M^{-1}cm^{-1}$). Argon (Linde, prepurified) was bubbled through a 1 ml sample of DRF for 1 h in a

stoppered cuvette (path length of 5 mm) in the dark. Stock solutions of 0.5-1 mM native CCP, a_5Ru(His-60)CCP, a_5Ru(His-X)CCP and cyt c were prepared, so small volumes of protein were added to the flavin sample. After addition of protein to the DRF solution, using Hamilton syringes, argon was passed over the sample for a further 5 min. A buffered 5 mM solution of H_2O_2 was bubbled with argon for 1-2 h. Protein samples were titrated spectrophotometrically (500-600 nm) with deaerated H_2O_2 to form compound I.

Reaction Kinetics:

(i) **RuL_3 complexes:** RuL_3 solutions were photoexcited with white light using xenon flash tubes (~ 25 μs duration). Cutoff filters (420 nm) were used to protect protein samples from uv light. Monitoring beams at 550 or 565 nm were used to follow reduction of cyt c or compound I of CCP, respectively.

(ii) **Flavin solutions:** Laser excitation at 386 nm, close to the absorption maximum for DRF at 398 nm (Figure 3.3), initiates semiquinone formation. The concentration of the reactive semiquinone species (Scheme 3.1) generated is ≤ 0.6 μM in the laser beam.[25] Protein concentrations were ≥ 2.5 μM, so most experiments were performed under pseudo first-order conditions. The kinetics of semiquinone decay were followed at 518 nm, an isosbestic point for CCP(Fe^{4+}) and CCP(Fe^{3+}).[26] The kinetics of Fe^{4+} reduction to Fe^{3+} in CCP and in the a_5Ru(His)CCP derivatives were monitored at 564 nm, a maximum in the CCP(Fe^{4+}) - CCP(Fe^{3+}) difference spectrum (ϵ_{564} = 8.2 $mM^{-1}cm^{-1}$).[26] In the presence of ferricyt c, Fe^{4+} reduction was followed at 557 nm, an isosbestic point for ferri- and ferrocyt c.[27]

3.3 RESULTS

Photoreduction by $Ru(L)_3$: Reduction of cyt c by $Ru(bpy)_3^{2+}$ was examined to test the system at Concordia and provides a good control to ensure that $Ru(bpy)_3^{2+}$ is photoexcited and is not quenched by oxygen. The observed signal increase at 550 nm (Figure 3.2) clearly shows that $^*Ru(bpy)_3^{2+}$ reduces cyt c and the 10-20 ms timescale for reduction is similar to that reported previously.[7] When a sample of $CCP(Fe^{4+})$ or $a_5Ru(His\text{-}60)CCP(Fe^{4+})$ containing $Ru(bpy)_3^{2+}$ and EDTA was flashed up to 20 times in 2 min, reduction of Fe^{4+} occurred. However, this occurred even in the absence of $Ru(bpy)_3^{2+}$ and EDTA, suggesting photoreduction of Fe^{4+} by an endogenous donor, although 420 nm cutoff filters were used to prevent uv irradiation of the protein samples. Negatively charged polypyridine complexes (where L = DIC or DIPS) were also used, however, they yielded similar results to those obtained for $Ru(bpy)_3^{2+}$.

Photoreduction by 5-Deazariboflavin: This was chosen as an alternative to the $Ru(bpy)_3^{2+}$/EDTA system because it has been successfully used to study electron transfer between cyt c and CCP.[16] The absorption spectrum of DRF (Figure 3.3) has a λ_{max} = 395 nm, hence the choice of 386 nm for flavin excitation.

(a) Reactions of DRFH·: Figure 3.4 shows the absorption change due to semiquinone (DRFH·) disproportionation, yielding bimolecular rate constants as expected for a disproportionation reaction (Scheme 3.1). The decay mechanisms for DRFH· under different conditions are given in Scheme 3.2. Figure 3.5 shows the

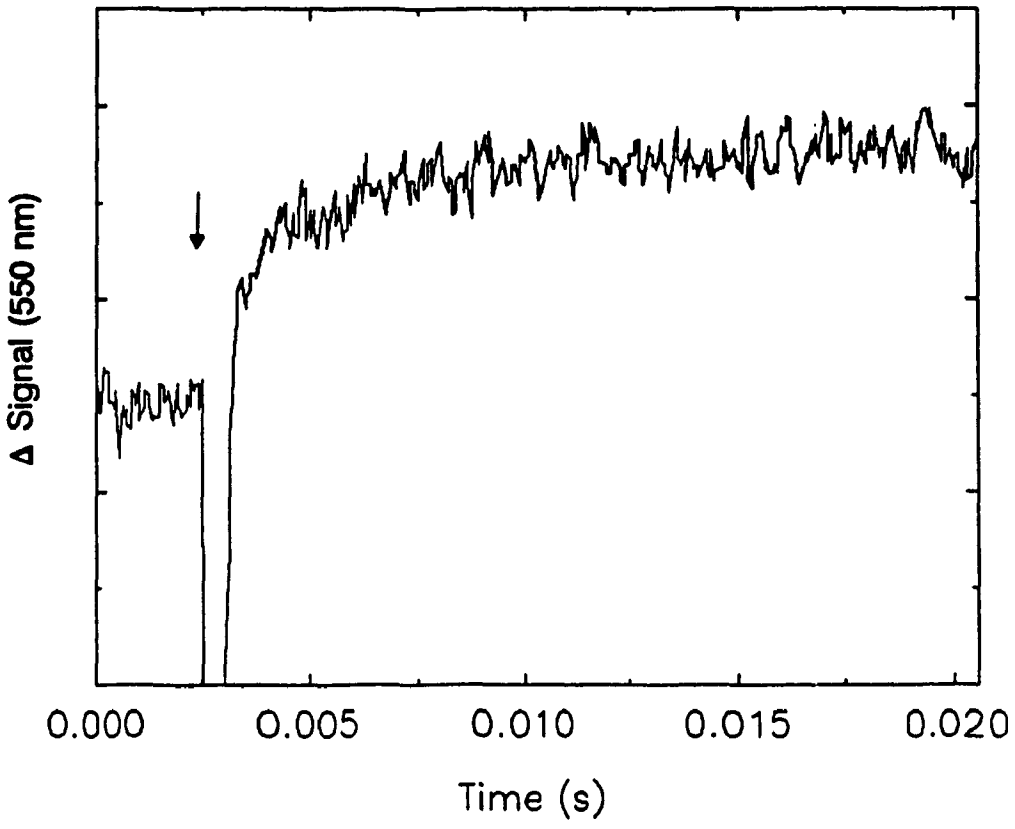

Figure 3.2: Signal increase at 550 nm before and after flash photolysis of 5 μM cytochrome c, 5 mM EDTA and 50 μM $Ru(bpy)_3^{2+}$ in 0.1 M phosphate buffer (pH 7). The arrow indicates the time at which the flash was applied, and the spike following the arrow is due to light from the flash tubes.

spectrophotometric decay of the flavin semiquinone in the presence of 2.5 μM a_5Ru(His-60)CCP. Since this rapid decay does not occur in the presence of native CCP (Scheme 3.2) it is attributed to the reduction of the surface-bound a_5Ru centre. Semiquinone decay, in the presence of a_5Ru(His-60)CCP or a_5Ru(His-X)CCP, follows pseudo first-order kinetics (Figure 3.6) with bimolecular rates of $k_2 = 2 \times 10^9$ M^{-1} s^{-1} and 3×10^9 M^{-1} s^{-1} respectively. These rates are the same for both Fe^{3+} and Fe^{4+} oxidation states of the a_5Ru(His)CCP derivatives. Table 3.1 summarizes the rate constants for semiquinone decay in the presence of either a_5Ru(His-60)CCP or a_5Ru(His-X)CCP. For a_5Ru(His-60)CCP, the rate of semiquinone decay was also investigated at low ionic strength (8 mM) and in the presence of yeast iso-1 cyt c (Table 3.1).

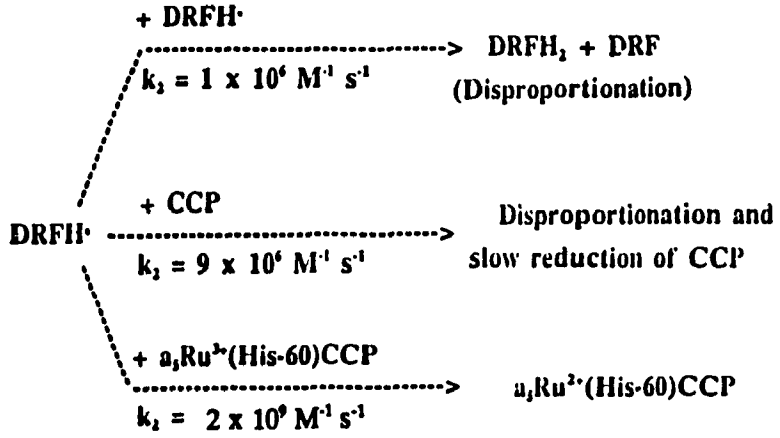

Scheme 3.2: The decay mechanism for DRFH· in the absence and presence of CCP or a_5Ru(His-60)CCP

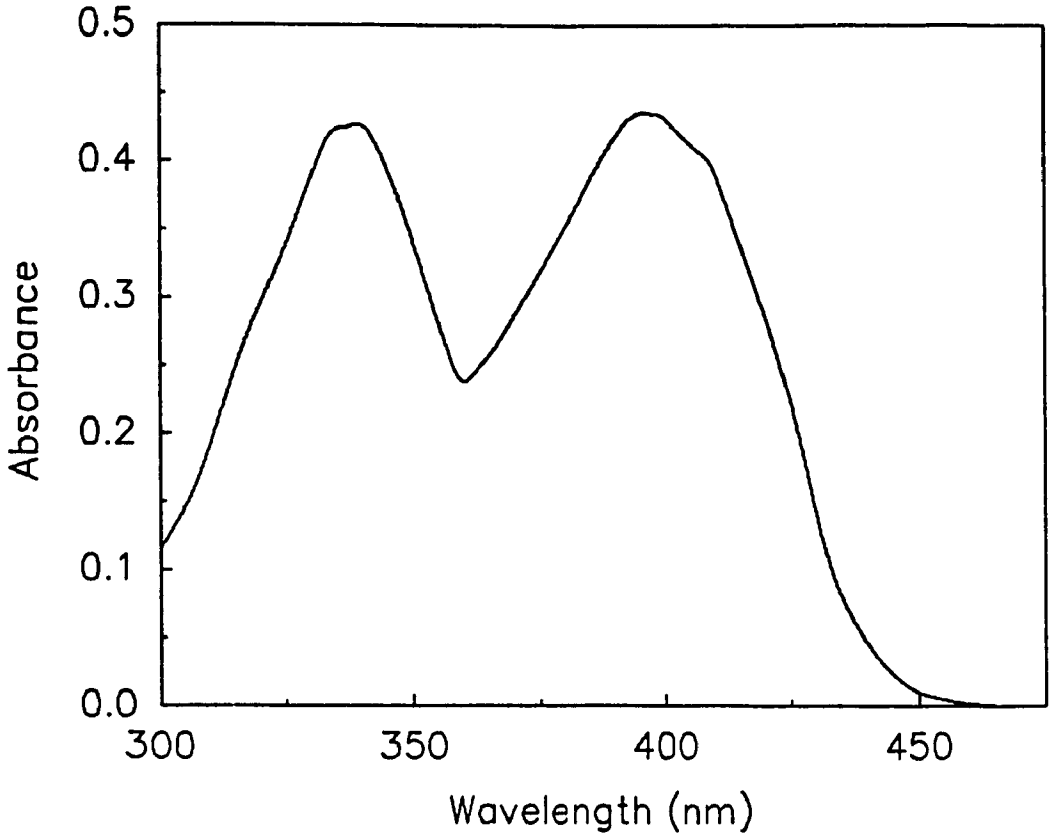

Figure 3.3: Absorption spectrum of ~ 72 μM 5-Deazariboflavin in 4 mM phosphate buffer, 0.5 mM EDTA (pH 7). Path length: 5 mm. 22 °C.

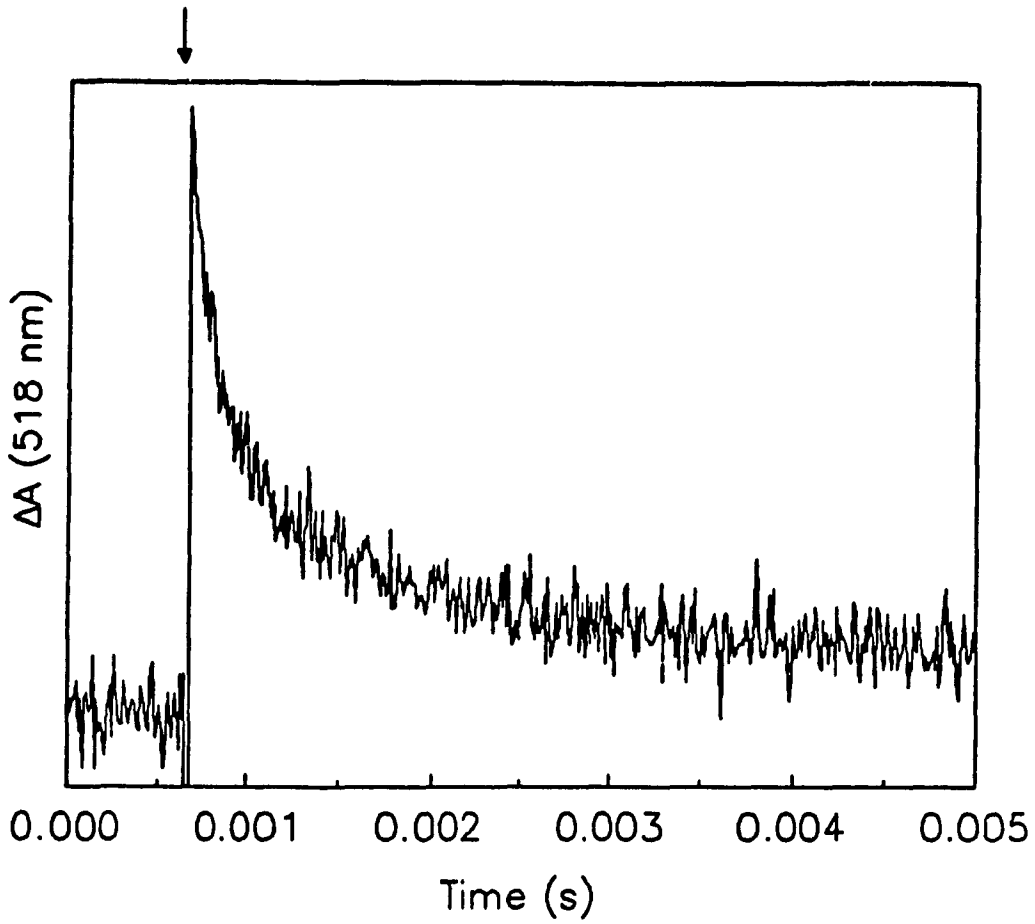

Figure 3.4: Absorbance change at 518 nm due to semiquinone ($DRFH^{\cdot}$) disproportionation before and after laser flash photolysis of 120 μM DRF, 0.5 mM EDTA, 92 mM KCl in 4 mM phosphate (pH 7). The arrow on the trace indicates the time at which the laser flash was applied.

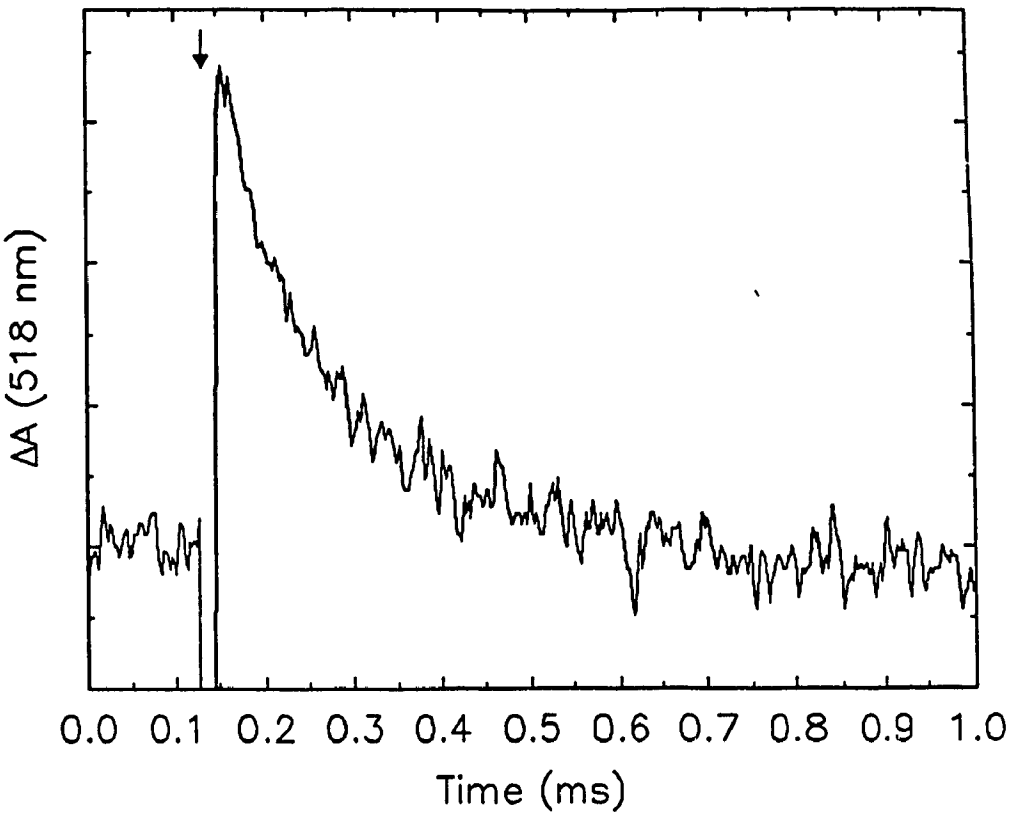

Figure 3.5: Absorbance change at 518 nm, due to semiquinone (DRFH·) decay in the presence of 2.5 μM a_5Ru(His-60)CCP, before and after laser flash photolysis of 120 μM DRF, 0.5 mM EDTA, 92 mM KCl in 4 mM phosphate (pH 7). The arrow on the trace indicates the time at which the laser flash was applied.

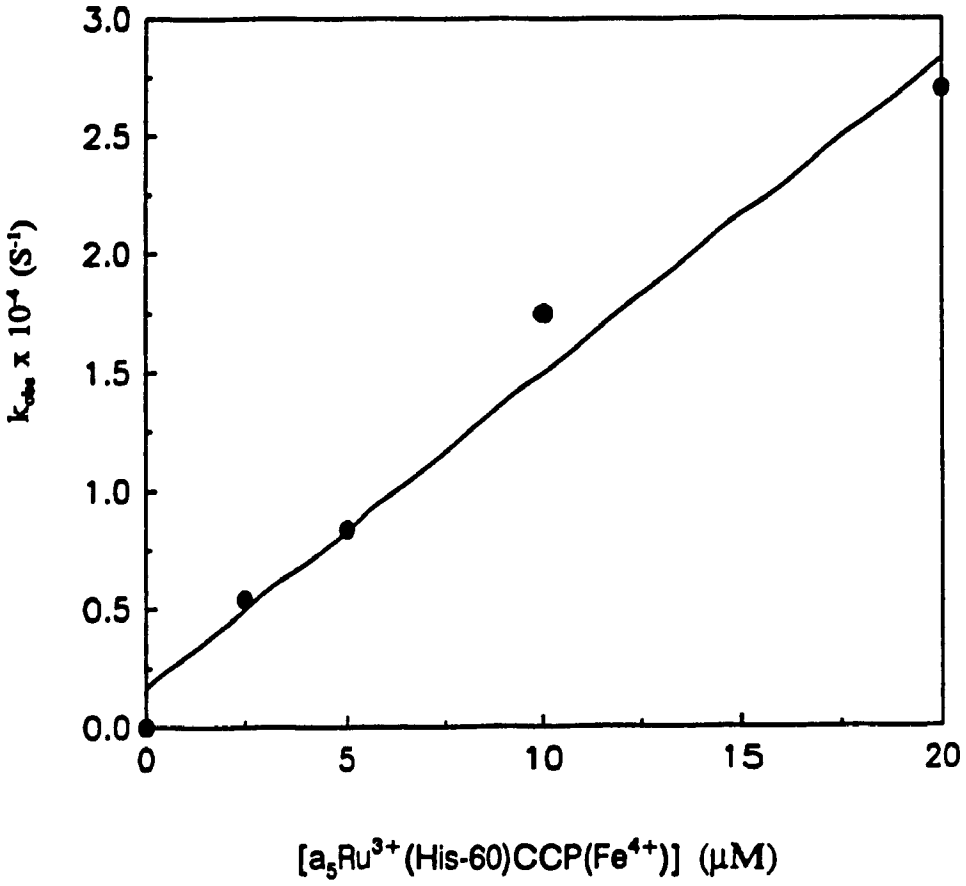

Figure 3.6: Plot of observed rate constants (k) vs. a_5Ru(His-60)CCP concentration for DRFH· decay in the presence of 2.5-30 μM a_5Ru(His-60)CCP. Experimental conditions were: 120 μM DRF, 0.5 mM EDTA, 92 mM KCl in 4 mM phosphate (pH 7)

(b) (i) Intra- and Intermolecular electron transfer in a_5Ru(His-60)CCP(Fe^{4+}) following excitation of DRF: Figure 3.8 shows that the kinetics of reduction of the heme centre in a_5Ru(His-60)CCP(Fe^{4+}) appear to fit a single exponential process at a protein concentration of 2.5 μM. The trace appears to be biphasic at concentrations ≥ 10 μM. Using non-linear regression software (Kinfit) and semilog plots the data were fit to single or double exponential curves, depending on the protein concentration of each sample. The rate of the faster, dominant phase is clearly concentration dependent (Figure 3.9) giving a bimolecular rate constant (k_2 = 1.2 x 10^6 $M^{-1}s^{-1}$) which is assigned to the intermolecular electron transfer rate from surface-bound a_5Ru^{2+} to the ferryl iron of a second protein molecule:

$$a_5Ru^{2+}(His\text{-}60)CCP(Fe^{4+}) + a_5Ru^{3+}(His\text{-}60)CCP(Fe^{4+}) \xrightarrow{k_2} a_5Ru^{3+}(His\text{-}60)CCP(Fe^{4+}) + a_5Ru^{3+}(His\text{-}60)CCP(Fe^{3+}) \qquad (10)$$

The faster phase also shows a dependency on ionic strength (Table 3.2 and Figure 3.10) since the bimolecular rate constant (k_2 = 1.2 x 10^6 M^{-1} s^{-1}) obtained at an ionic strength of 100 mM , increases by a factor of two (k_2 = 2.5 x 10^6 M^{-1} s^{-1}) when the ionic strength is decreased to 8 mM. This is consistent with the fact that CCP is negatively charged, whereas a_5Ru is positively charged, so electrostatic interactions between the surface-bound a_5Ru^{2+} and heme of other CCP molecules are enhanced at low ionic strength. In the presence of yeast ferricyt c (μ = 8 mM), the bimolecular rate constant decreases to 0.62 x 10^6 M^{-1} s^{-1}, presumably because cyt c binding hinders access of the a_5Ru centre to the CCP heme, thus decreasing the intermolecular reduction rates (Figure 3.10).

Table 3.1

Observed rate constants (k) for 5-DRFH· semiquinone decay in the presence of a_5Ru(His)CCP derivatives, and calculated bimolecular rate constants (k_2)

Protein	Ionic strength (mM)	[Protein] (μM)	$k^a \times 10^{-4}$ (s^{-1})	$k_2{}^b \times 10^{-9}$ (M^{-1} s^{-1})
a_5Ru(His-60)CCP	100	2.5 5 10 20	0.54 0.84 1.75 2.70	2
a_5Ru(His-60)CCP	8	2.5 5 7.5 10	0.84 1.30 1.53 2.20	2
a_5Ru(His-60)CCP + cyt c[c]	8	5 10 15	0.80 1.65 2.02	1
a_5Ru(His-X)CCP	100	2.8 5 10	1.00 1.54 2.90	3

[a]Rate constants were calculated from kinetic analysis of the absorbance change at 518 nm. Experimental conditions are as given in the caption to Figure 3.6.

[b]k_2 is obtained from the slope of a plot of k vs. [a_5Ru^{3+}(His)CCP] (Figure 3.6).

[c]Yeast iso-1 ferricyt c (equimolar)

The rate constant of the slower phase (k_1) is concentration independent (Figure 3.9) over the range 2.5-30 μM and is assigned to intramolecular reduction of Fe^{4+} by surface-bound a_5Ru^{2+}:

$$a_5Ru^{2+}(His\text{-}60)CCP(Fe^{4+}) \xrightarrow{k_1} a_5Ru^{3+}(His\text{-}60)CCP(Fe^{3+}) \quad (11)$$

At high protein concentrations (≥ 40 μM) the slow phase disappears because it is unable to compete with the dominant, concentration-dependent fast phase. The rate constant (k_1) for intramolecular reduction of the Fe^{4+} in a_5Ru(His-60)CCP is 3.2 ± 1.2 s^{-1}. Unlike the fast phase, ionic-strength has no effect on the slow rate constant, also consistent with intramolecular electron transfer. The results of the kinetic analysis of reduction of Fe^{4+} in a_5Ru(His-60)CCP(Fe^{4+}) are summarized in Table 3.2.

(ii) **Intra- and intermolecular electron transfer in a_5Ru(His-X)CCP:** The kinetics of Fe^{4+} reduction in a_5Ru(His-X)CCP(Fe^{4+}) are similar to those seen for a_5Ru(His-60)CCP(Fe^{4+}). Monophasic kinetics occur at a protein concentration of 2.8 μM, while biphasic kinetics occur at protein concentrations > 10 μM. The faster phase is concentration dependent and has a bimolecular rate constant, k_2 = 0.64 x 10^6 M^{-1} s^{-1} (Figure 3.11), attributed to intermolecular electron transfer from surface-bound a_5Ru^{2+} to the ferryl iron of another protein molecule:

$$a_5Ru^{2+}(His\text{-}X)CCP(Fe^{4+}) + a_5Ru^{3+}(His\text{-}X)CCP(Fe^{4+}) \longrightarrow$$
$$a_5Ru^{3+}(His\text{-}X)CCP(Fe^{4+}) + a_5Ru^{3+}(His\text{-}X)CCP(Fe^{3+}) \quad (12)$$

The slower phase is assigned to intramolecular reduction of Fe^{4+} since its rate

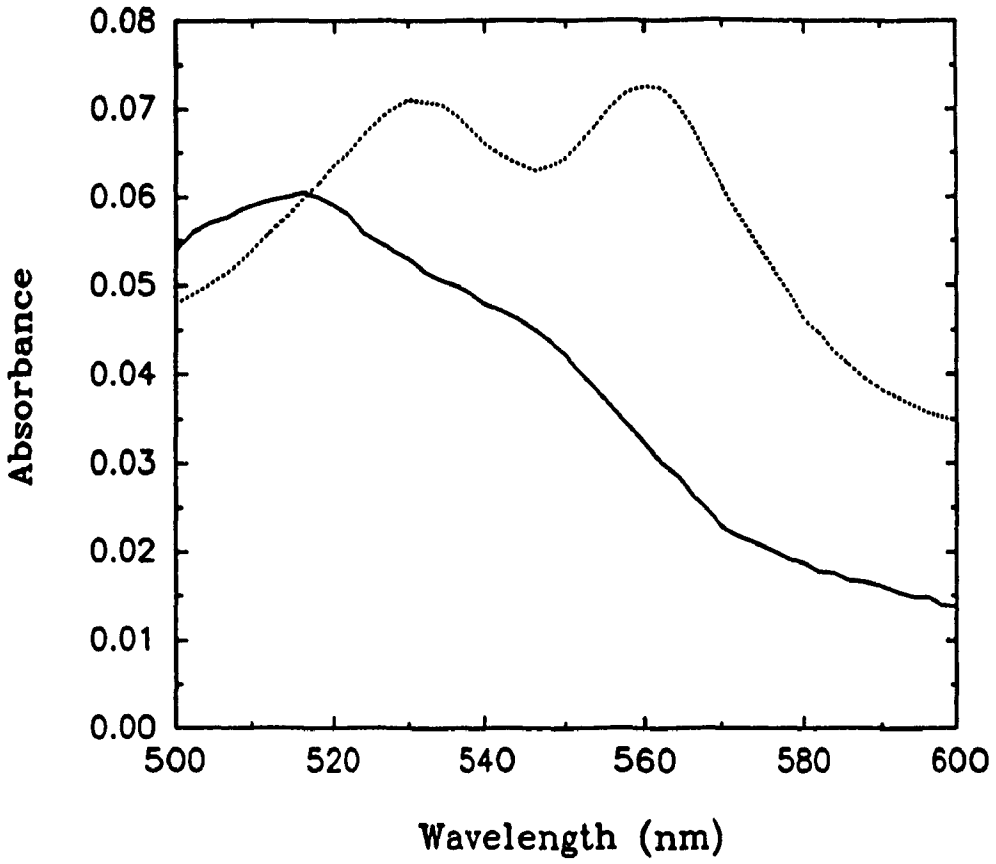

Figure 3.7: Visible absorption spectra of 5 μM native CCP (solid line) and compound I of CCP (dotted line) in 0.1 M phosphate buffer (pH 7). The maximum in the difference spectrum (compound I - CCP) is at ~ 564 nm.

Figure 3.8: Absorbance change at 564 nm before and after laser flash photolysis of (a) 2.5 μM (b) 10 μM and (c) 40 μM a_5Ru^{3+}(His-60)CCP(Fe^{4+}), 120 μM DRF, 0.5 mM EDTA, 92 mM KCl in 4 mM phosphate (pH 7). The arrow on each trace indicates the time at which the laser flash of 1 ns duration was applied to the sample. The dashed line though each trace represents the best fit though the data points. Each trace is the sum of the absorbance changes following 4-6 laser flashes, which gave rise to total absorbance at 564 nm of ~0.01-0.3, corresponding to the reduction of 1-4 μM Fe^{4+} *in the laser beam* during each experiment.

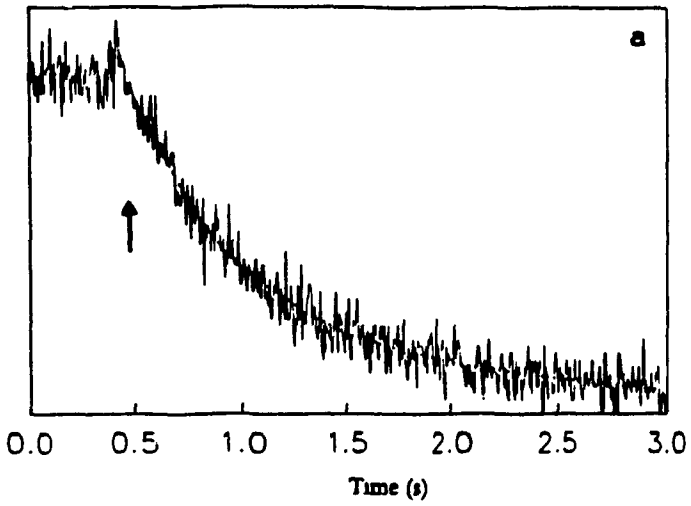
a
0.0
0.5
1.0
1.5
2.0
2.5
3.0
Time (s)

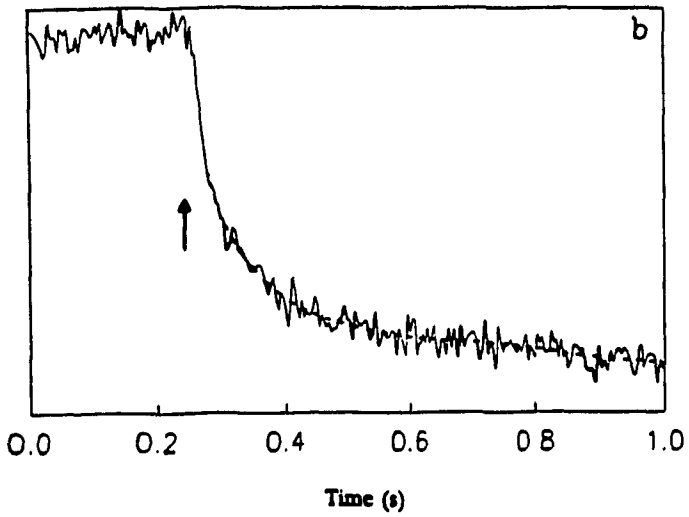
b
0.0
0.2
0.4
0.6
0 8
1.0
Time (s)

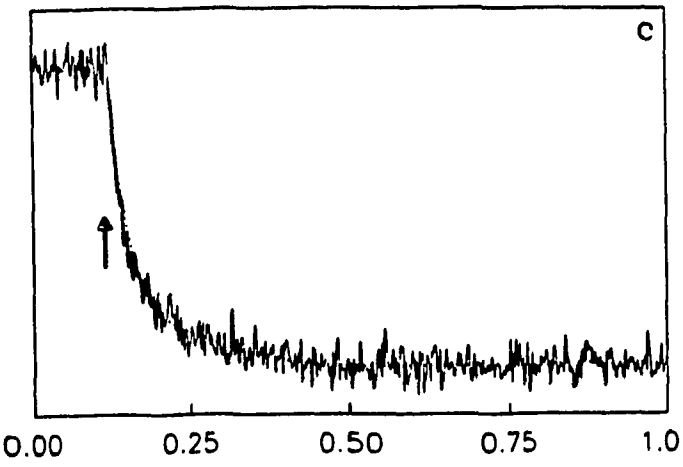
c
0.00
0.25
0.50
0.75
1.0
Time (s)

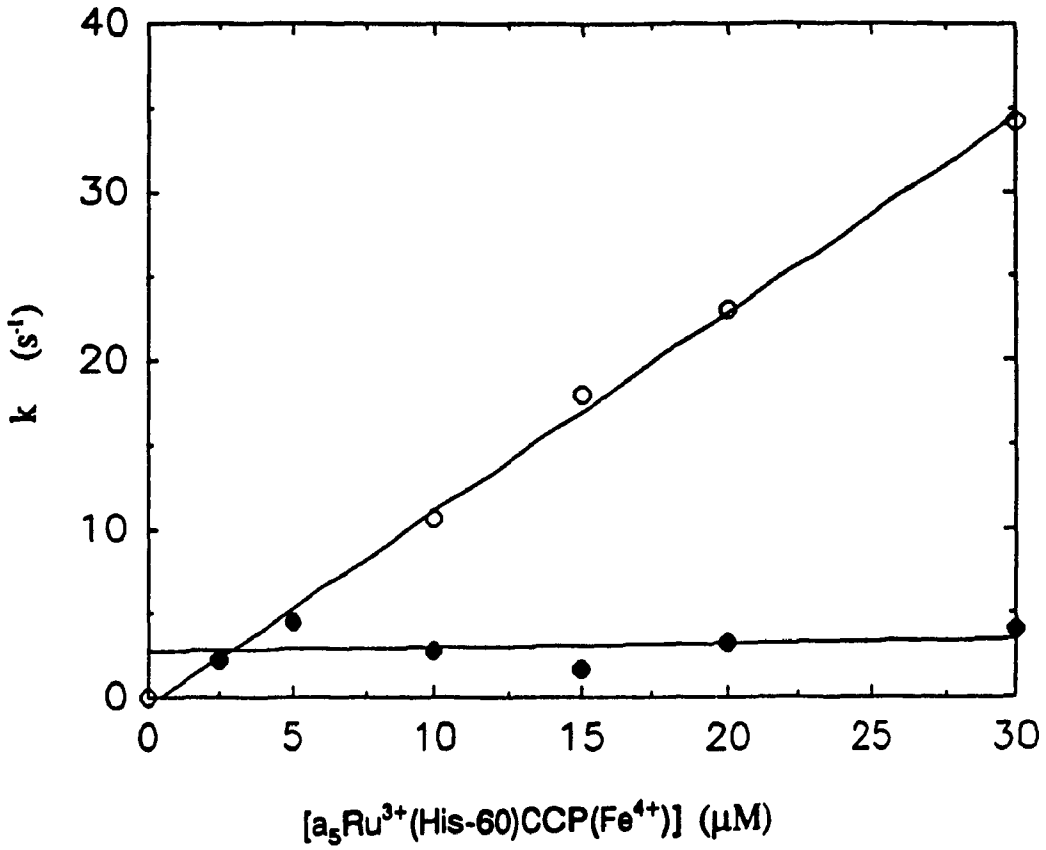

Figure 3.9: Plot of rate constants, k vs. a_5Ru^{3+}(His-60)CCP(Fe^{4+}) concentration for Fe^{4+} reduction in the presence of 2.5-30 μM a_5Ru^{3+}(His-60)CCP(Fe^{4+}). k values were determined from kinetic analysis of the absorbance change due to Fe^{4+} reduction (Figure 3.8). Solid circles represent the slow phase and open circles represent the fast phase. Experimental conditions were the same as those in the caption for Figure 3.8.

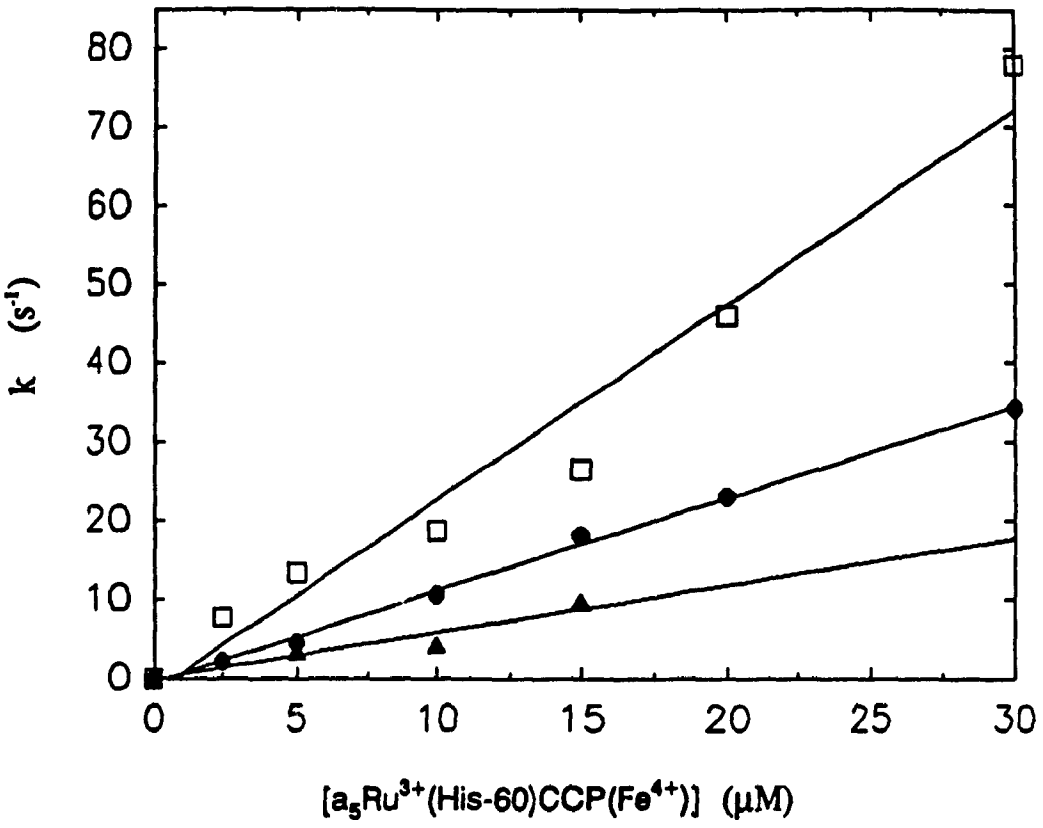

Figure 3.10: Plot of rate constants (k) vs. $[a_5Ru^{3+}(His\text{-}60)CCP(Fe^{4+}]$ for Fe^{4+} reduction in the presence of 2.5-30 μM $a_5Ru^{3+}(His\text{-}60)CCP(Fe^{4+})$. Buffer ionic strength is 8 mM (open squares), 100 mM (closed circles) and 8 mM in the presence of equimolar yeast ferricyt c (triangles). k values were determined from kinetic analysis of the absorbance change due to Fe^{4+} reduction (Figure 3.8). Experimental conditions were as in the caption for Figure 3.8 expect that KCl was omitted to obtain a buffer ionic strength of 8 mM.

Table 3.2:

Observed rate constants (k) and calculated bimolecular rate constants (k_2) for reduction of Fe^{4+} in a_5Ru^{3+}(His-60)CCP(Fe^{4+}) by surface-bound a_5Ru^{2+} under different conditions

Ionic strength (mM)	[Protein] (μM)	k[a] (sec^{-1})		k_2[b] (M^{-1} s^{-1})
		Slow	Fast	
100	2.5	2.2	2.2	1.2×10^6
	5	4.5	4.5	
	10	2.8	10.6	
	15	1.7	18.0	
	20	3.2	23.0	
	30	4.0	34.2	
8	2.5	2.6	7.8	2.5×10^6
	5	6.3	13.4	
	7.5	2.3	18.7	
	10	3.7	26.5	
	20	-	46.0	
	30	-	78.0	
8 + cyt c[c]	5	3.5	3.5	0.64×10^6
	10	4.3	4.3	
	15	3.0	9.6	
	30	2.2	-	

[a]Rate constants were calculated from kinetic analysis of the absorbance change at 564 nm, or 557 nm in the presence of ferricyt c. Experimental conditions are given in Figure 3.8.

[b]k_2 is obtained from the slope of a plot of k vs [a_5Ru^{3+}(His)CCP(Fe^{4+})] (Figure 3.9)

[c]Yeast iso-1 ferricyt c, which was equimolar with a_5Ru^{3+}(His)CCP(Fe^{4+}).

shows no dependence on protein concentration over the range 2.8-20 μM (Figure 3.11):

$$a_5Ru^{2+}(His\text{-}X)CCP(Fe^{4+}) \xrightarrow{k_1} a_5Ru^{3+}(His\text{-}X)CCP(Fe^{3+}) \quad (13)$$

As seen for a_5Ru(His-60)CCP, at ~ 40 μM protein, the slow phase disappears because it can no longer compete with the fast phase. The rate constant (k_1) for intramolecular reduction of the Fe^{4+} in a_5Ru^{2+}(His-X)CCP(Fe^{4+}) is 1.6 ± 0.6 s^{-1}. The results of the kinetic analysis of reduction of Fe^{4+} in a_5Ru(His-X)CCP(Fe^{4+}) are summarized in Table 3.3.

Table 3.3

Observed rate constants (k) and calculated bimolecular rate constants (k_2) for reduction of Fe^{4+} in a_5Ru^{3+}(His-X)CCP(Fe^{4+}) by surface-bound a_5Ru^{2+}

Ionic strength (mM)	[Protein] (μM)	k (sec^{-1})		k_2[a] (M^{-1} s^{-1})
		Slow	Fast	
100	2.8	2.4	2.4	0.64×10^6
	5	1.0	3.0	
	10	1.3	9.0	
	20	1.6	13.9	
	30	-	18.9	

[a]Rate constants were calculated from kinetic analysis of the absorbance change at 564 nm. Experimental conditions are given in Figure 3.8.

[b]k_2 is obtained from the slope of a plot of k vs. [a_5Ru^{3+}(His-X)CCP(Fe^{4+})] (Figure 3.11)

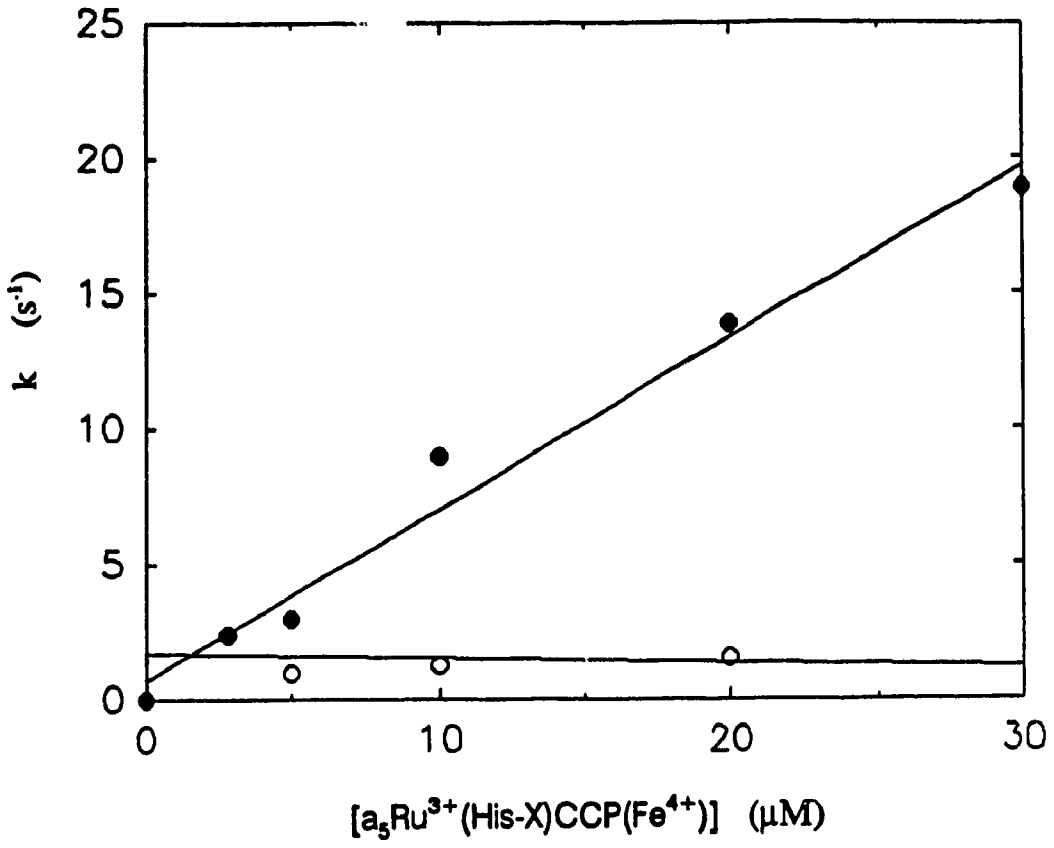

Figure 3.11: Plot of rate constant, k vs. a_5Ru^{3+}(His-X)CCP(Fe^{4+}) concentration for Fe^{4+} reduction in the presence of 2.5-30 μM a_5Ru^{3+}(His-60)CCP(Fe^{4+}). k values were determined from kinetic analysis of the absorbance change due to Fe^{4+} reduction under the experimental conditions given in the caption for Figure 3.8. Open circles represent the slow phase and closed circles represent the fast phase.

3.4 DISCUSSION

The photoexcited $Ru(bpy)_3^{2+}$/EDTA system has been used in electron transfer studies of numerous ruthenated proteins (Table 1.1), so, this was the method of choice for ruthenated CCP. $^*Ru(bpy)_3^{2+}$ is rapidly quenched by native CCP(Fe^{3+}) and compound I ($k = 2\text{-}6 \times 10^9\ M^{-1}\ s^{-1}$, depending on the ionic strength).[28] Therefore, selective reduction of a_5Ru^{3+} is not expected in a_5Ru(His)CCP. Other RuL_3 compounds having negatively-charged ligands were used instead of $^*Ru(bpy)_3^{2+}$ in an attempt to decrease rapid quenching by the negatively-charged CCP heme. However, $Ru(DIPS)_3^{4-}$ and $Ru(DIC)_3^{4-}$ also do not appear to selectively reduce the a_5Ru^{3+} centre of a_5Ru(His)CCP. Consequently, different photoreductants were sought to selectively reduce a_5Ru^{3+} of a_5Ru(His)CCP. Use of a laser instead of xenon flash tubes would allow excitation at a specific wavelength using less light which is focused on a small area of the sample.

Selective reduction using flavins has been shown to be a valuable tool in studying electron transfer in proteins.[11-21] It is possible to monitor flavin semiquinone decay at ~ 500-550 nm, and determine whether or not in situ reduction by the flavin semiquinone is more rapid than intramolecular electron transfer. This is important since one can establish which is the rate limiting step in the electron transfer process. 5-Deazariboflavin was the flavin of choice because it is not an efficient reductant for the heme of CCP (Scheme 3.2)[16,19] either in the absence or presence of cyt c. DRFH$^\cdot$ directly reduces the heme of native CCP with a rate constant of $9 \times 10^6\ M^{-1}\ s^{-1}$, and it reduces the surface-bound a_5Ru ~ 200 times faster

than the heme.

Reduction of Fe^{4+} in a_5Ru(His-60)CCP by a_5Ru^{2+} can occur by inter- and intramolecular processes. The rate of intermolecular reduction in a_5Ru(His-60)CCP is 1.2×10^6 M^{-1} s^{-1} which is comparable to the published reduction of CCP(Fe^{4+}) by freely diffusing a_5Ru^{2+}pyr ($k = 9.5 \times 10^6$ M^{-1} s^{-1}).[29] This suggests that the surface-bound ruthenium complex is highly exposed, consistent with the computer graphics photographs of native CCP (Figure 2.2) showing that His-60 is solvent exposed,[30] and the crystal structure of a_5Ru(His-60)CCP (Figure 2.11) which shows the high solvent-accessibility of the ruthenium centre. The observed ionic strength dependence of intermolecular electron ransfer in a_5Ru(His-60)CCP(Fe^{4+}) is probably due to electrostatically-favourable interactions between the a_5Ru^{2+} centre of one molecule and the heme of another molecule, which gives rise to a doubling of the rate of electron transfer at low ionic strength. The presence of stoichiometric yeast iso-1 ferricyt c at low ionic strength allows complex formation between a_5Ru(His-60)CCP and cyt c, which decreases the rate of intermolecular reduction of Fe^{4+} due to steric hinderance of the CCP heme by bound cyt c. Furthermore, the positively-charged a_5Ru centre may be repelled by the complexed cyt c which is also positively charged.

Intermolecular reduction of Fe^{4+} in a_5Ru(His-X)CCP is slower ($k = 0.62 \times 10^6$ M^{-1} s^{-1}) than seen for the His-60 derivative. This is consistent with the crystal structure of native CCP which shows that His-6 and 96 are much less exposed than His-60 (Figure 2.2). Thus, the a_5Ru(His-X) centre may be less exposed than a_5Ru(His-60), or the slower rate of intermolecular reduction in the His-X derivative

could be due to less favourable electrostatic interactions. The effect of ionic strength or yeast cyt c complexation on the rate of intermolecular electron transfer were not investigated due to insufficient quantities of a_5Ru(His-X)CCP.

The rates for intramolecular electron transfer from the a_5Ru^{2+} centre to the Fe^{4+} heme are 3.2 ± 1.2 and 1.6 ± 0.6 s^{-1} for a_5Ru(His-60)CCP and a_5Ru(His-X)CCP, respectively. These rates are slower than expected, considering the large driving force ($\Delta E^\circ \sim 1$ V)[31] and the 20-23 Å separation distance from the heme edge to the three surface histidine residues. At a lower driving force ($\Delta E^\circ \sim 0.8$ V), intramolecular rates of 85-100 s^{-1} were observed from the Zn-protoporphyrin triplet state (^{3}ZnP) to the surface-bound a_5Ru^{3+} centres in three different a_5Ru^{3+} derivatives of Zn-substituted myoglobin with 19-22 Å separation between the two redox centres (Table 1.1).[32] Similarly, rapid (260 s^{-1}) intracomplex electron transfer has been observed in the electrostatically stabilized complex between yeast cyt c and CCP(Fe^{4+}), which are natural biological partners.[19] A computer-graphics model has estimated the heme edge-to-edge distance between the two proteins to be ~ 17 Å.[1] Intracomplex electron transfer between yeast cyt c and Zn-substituted CCP, yields a rate of 1.1 x 10^4 s^{-1}.[34] However, these studies show that intracomplex electron transfer rates are highly dependent on the cyt c source (yeast, horse, etc.) and on ionic strength.[34,35] This suggests that changes at the protein-protein interface play a dominant role in the control of intracomplex electron transfer. Since no protein-protein interface is crossed during intramolecular electron transfer within a_5Ru(His)CCP, this can not explain the slow intramolecular electron transfer rates

observed for a_5Ru(His)CCP derivatives.

Resonance Raman spectroscopy has shown that Fe^{4+} in compound I of CCP is 6-coordinate low-spin,[36] while in the ferric state the iron of CCP is 5-coordinate high-spin.[37] The reorganization energy associated with the change in spin state and coordination number, which involves dissociation of the Fe^{4+}=O bond, may be large. A temperature-dependence study of intramolecular electron transfer would allow an investigation of the reorganization energy involved in ferryl iron reduction since from Marcus theory:[38]

$$k_{et} = A \exp[-(\Delta G + \lambda)^2/4\lambda kT] \qquad (14)$$

where k_{et} is the rate of intramolecular electron transfer, A is a pre-exponential factor, ΔG is the reaction free energy, λ is the reorganization energy , k is the Boltzman constant and T the temperature. Therefore, a temperature dependence study of intramolecular electron transfer will allow the determination of the reorganization energy (λ). A temperature dependence study would be difficult for a_5Ru(His)CCP because the inter- and intramolecular processes occur on overlapping timescales at the lowest protein concentrations required to obtain a signal with an acceptable signal-to-noise ratio (> 1 μM). The rate of intermolecular electron transfer is dependent on the protein concentration whereas the intramolecular rate is not. Hence, decreasing the protein concentration 20-fold will decrease the intermolecular rate 20-fold, while leaving the intramolecular rate unaffected. Furthermore, the inter- and intramolecular processes will not longer be on overlapping timescales, instead, intramolecular electron transfer will be the dominant rate. However, to achieve this,

the protein concentration must be decreased from 2.5 μM to ~ 0.125-0.25 μM. Under the conditions used, the absorbance change for a protein concentration of 0.125-0.25 μM would probably be too small to be observed.

In addition to a high reorganization energy, it is also possible that the intervening amino acid residues between the two redox centres may not favour rapid electron transfer. A Brownian dynamics computer simulation of the association of cyt c and CCP shows possible binding sites for cyt c, on the surface of CCP.[39] There does not appear to be a suitable binding site near any of the three surface His residues, so a productive pathway for electron transfer from any of these residues to the heme of CCP is not physiologically necessary. Also, addition of cyt c at low ionic strength does not affect the rate of reduction of the a_5Ru^{3+} centre by the flavin semiquinone in the His-60 derivative, indicating that cyt c does not interact with CCP in this region. Hence, even with a high driving force, intramolecular electron transfer rates might be expected to be slow. Furthermore, the intramolecular electron transfer rate does not change on cyt c binding, which eliminates the possibility of cyt c acting as a conformational gating switch to allow facile electron transfer from non-specific surface regions.

A pathway search algorithm has been developed to predict the most efficient pathways for electron transfer in proteins. Factors which affect the rates of electron transfer such as covalent and hydrogen bonding and localized through-space regions are incorporated into this model.[40,41] What is already clear from this model is the importance of H-bonding in shortening electron transfer pathways and also for

providing bridges between gaps in the protein structure. It also appears that through-space couplings only occur when they significantly shorten electron transfer paths, and there are usually only 1-2 such couplings in any given pathway. Mb contains ~ 70% α-helix in its structure, and the number of electron paths in a_5Ru(His-48)Mb is calculated to be about ~ 200. However, many of the pathways differ in minor ways, such as in the details of the through space connections, so it is possible to identify a few of the most probable pathways for electron transfer.[40,41] Such a systematic identification of the electron transfer pathways for a_5Ru(His)CCP has not yet been carried out since the necessary software is not currently available at Concordia. However, from a first examination there appears to be no obvious direct path (Figure 3.12) which is consistent with the slow rate of intramolecular electron transfer. However, since Figure 3.12 provides no information on any bonding or through-space interactions, little can yet be concluded about the electron transfer pathway available for a_5Ru(His-60)CCP.

3.5 REFERENCES

1a Poulos, T. L.; Finzel, B. C. *Pept. Protein rev.* **1984**, *4*, 115.

1b Assuming E° = - 194mV for $Fe^{3+/2+}$ [Conroy, C. W.; Tyma, P; Daum, P. H.; Erman, J. E. *Biochim. Biophys. Acta* **1978**, *537*, 62], E° = 80 mV for $a_5Ru^{3+/2+}$ [Ref. 9] and E° = 1087 mV for $Fe^{4+/3+}$ [Ref. 31].

2 Isied, S. S.; Worosila, G.; Atherton, S. J. *J. Am. Chem. Soc* **1982**, *104*, 7659.

3 Isied, S. S.; Kuehn, C.; Worosila, G. *J. Am. Chem. Soc.* **1984**, 106, 1722.

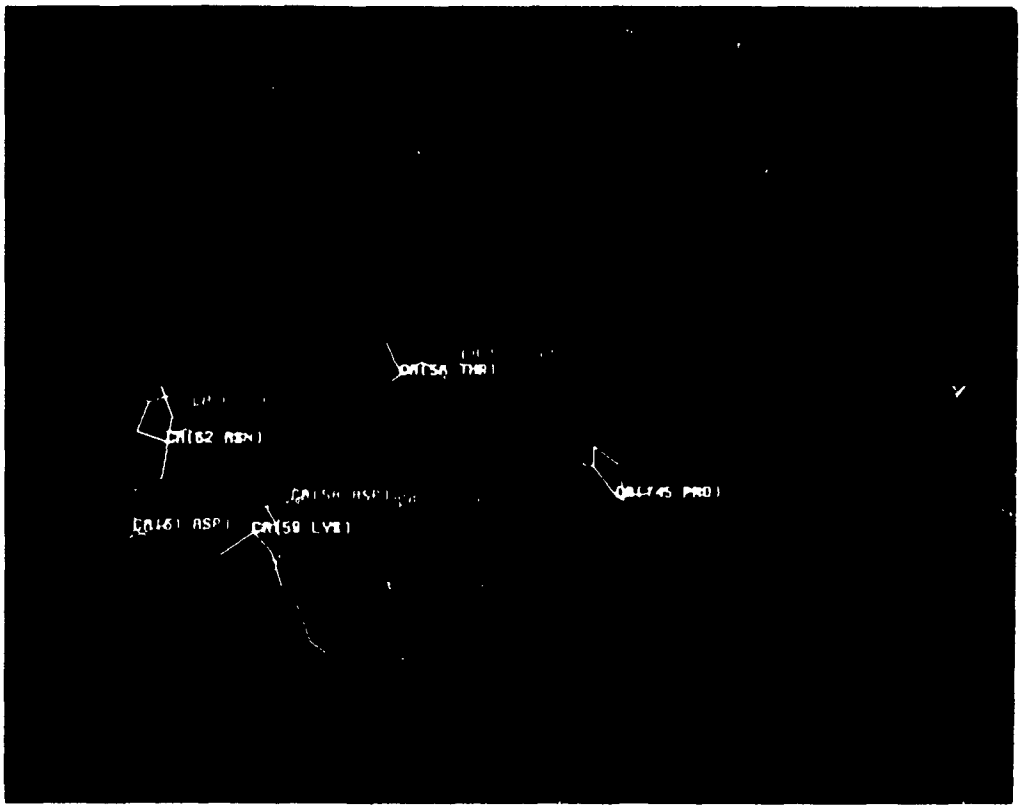

Figure 3.12: Intervening amino acid residues between a_5Ru(His-60) and the heme of CCP. The crystal structure coordinates of native CCP[27] were displayed using Midas software.[6b]

4 Jackman, M. A.; Lim, M-C.; Sykes, A. G.; Salmon, G. A. *J. Chem. Soc., Dalton Trans.* **1988**, 2843.

5 Osvath, P.; Salmon, G. A.; Sykes, A. G. *J. Am. Chem. Soc.* **1988**, *110*, 7114.

6 Jackman, M. P.; McGinnis, J.; Powls, R.; Salmon, A. G.; Sykes, A. G. *J. Am. Chem. Soc.* **1988**, *110*, 5880.

7 Winkler, J. R.; Nocera, D. G.; Yocam, K. M.; Bordignon, E.; Gray, H. B. *J. Am. Chem. Soc.* **1982**, *104*, 5798.

8 Yocom, K. M.; Winkler, J. R.; Nocera, D. G.; Gray, H. B. Chemica. Scripta. **1983**, *21*, 29.

9 Nocera, D. G.; Winkler, J. R.; Yocom, K. M.; Bordignon.; Gray, H. B. *J. Am. Chem. Soc.* **1984**, *106*, 5145.

10 Whitten, D. G. *Acc. Chem. Res.* **1980**, *13*, 83.

11 Simondsen, R. P.; Weber, P. C.; Salemme, F. R.; Tollin, G. *Biochemistry* **1982**, 21, 6366.

12 Hazzard, J. T.; Cusanovich, M. A.; Tainer, J. A.; Getzoff, E. D.; Tollin, G. *Biochemistry* **1986**, 25, 3318.

13 Bhattacharyya, A. K.; Meyer, T. E.; Tollin, G. *Biochemistry* **1986**, 25, 4655.

14 Cusanovich, M. A.; Tollin, G. *Biochemistry*, **1980**, *19*, 3343.

15 Ahmad, I.; Cusanovich, M. A.; Tollin, G. *Biochemistry* **1982**, 21, 3122.

16 Hazzard, J. T.; Poulos, T. L.; Tollin, G. *Biochemistry* **1987**, 26, 2836.

17 Hazzard, J. T.; McLendon, G.; Cusanovich, M. A.; Tollin, G. *Biochim. Biophys. Res.* Commun. **1988**, 151, 429.

18 Hazzard, J. T.; Moench, S. J.; Erman, J. E.; Satterlee, J. D.; Tollin, G. *Biochemistry* **1988**, 27, 2002.

19 Hazzard, J. T.; McLendon, G.; Cusanovich, M. A.; Das, G.; Sherman, F.; Tollin, G. *Biochemistry* **1988**, 27, 4445.

20 Mauro, J. M.; Fishel, L. A.; Hazzard, J. T.; Meyer, T. E.; Tollin, G.; Cusanovich, M. A.; Kraut, J. *Biochemistry*, **1988**, *27*, 6243.

21 Miller, M. A.; Hazzard, J. T.; Mauro, M.; Edwards, S. L.; Simon, P. C.; Tollin, G.; Kraut, J. *Biochemistry* **1988**, 27, 9081.

22 Smit, P.; Stork, G. A.; van der Plas, H. C.; den Harlog, J. A.; van der Marel, G. A.; van Boom, J. H. *Rech. J. R. Neth. Chem.* **1986**, *105*, 538.

23 Szentrimay, R.; Yeh, P.; Kuwana, T. *Electrochemical Studies of Biological Systems*, Sawyer, D. T. Ed.; ACS Symposium series Vol. 38, 1977, p 162.

24 Penzer, G. *An Introduction to Spectroscopy for Biochemists*; Brown, S. B. Ed.; Academic Press; New York, 1980, p 70.

25 Simondsen, R. P.; Tollin, G. *Biochemistry* **1983**, 22, 3008.

26 Yonetani, T. *The Enzymes Vol 18*; Boyer, P. D., Ed.; Academic Press; New York, 1976; p 345.

27 Margoliash, E.; Frohwirt, N. *Biochem. J.* **1959**, *71*, 570.

28 Ann English, personal communication.

29 Yandell, J. K.; Yonetani, T. *Biochim. Biophys. Acta* **1983**, *748*, 263.

30 Finzel, B. C.; Poulos, T. L.; Kraut, J. *J. Biol. Chem.* **1984**, *259*, 13027.

31 Purcell, W. L.; Erman, J. E. *J. Am. Chem. Soc.* **1976**, *98*, 7033.

32 Axup, A. W.; Albin, M.; Mayo, S. L.; Crutchley, R. J.; Gray, H. B. *J. Am. Chem. Soc.* **1988,** *110,* 435.

33 Gray, H. B.; Malmstrom, B. G. *Biochemistry* **1989,** 28, 7499.

34 Liang, N.; Kang, C. H.; Margoliash, E.; Hoffman, B. M. *J. Am. Chem. Soc.* **1986,** *108,* 4665.

35 Ho, P. S.; Sutoris, C.; Liang, N.; Margoliash, E.; Hoffman, B. M. *J. Am. Chem. Soc.* **1985,** *107,* 1070.

36 Reczek, C. M.; Sitter, A J.; Terner, J. *J. Mol. Struc.* **1989,** *214,* 27.

37 Smulevich, G.; Mantini, A. R.; English, A. M.; Mauro, J. M. *Biochemistry* **1989,** 28, 5058.

38 Marcus, R. A.; Sutin, N. *Biochim. Biophys. Acta.* **1985,** *811,* 265.

39 Northrup, S. H.; Boles, J. O.; Reynolds, J. C. L. *Science (Washington, D. C.)* **1988,** *241,* 67.

40 Beratan, D. N.; Onuchic, J. N.; Gray, H. B. *Metal Ions in Biological Systems Vol 27*; Sigel, H. & Sigel, A., Ed.; Marcel Dekker, New York, 1990, pp1-25.

41 Beratan, D. N.; Onuchic, J. N.; Betts, J. N.; Bowler, B. E.; Gray, H. B. *J. Am. Chem. Soc.* **1990,** *112,* 7915.

4.0 FLUORESCENCE PROPERTIES OF CCP, COMPOUND I AND a_5Ru(His)CCP DERIVATIVES

4.1 INTRODUCTION

Intrinsic fluorescence in proteins is due to tryptophan (Trp), tyrosine (Tyr) and phenylalanine (Phe) residues.[1a] CCP contains 7 Trp residues,[2] and since Trp fluorescence is highly sensitive to environment, these residues are useful structural probes.[3] In addition to Trp residues, CCP also contains 14 Tyr residues (Figure 4.1) and 18 Phe residues[2] which can also fluoresce on uv-excitation. However, fluorescence from Tyr and Phe residues is quenched by energy transfer to Trp,[1b] so steady-state fluorescence from proteins is dominated by Trp emission. CCP is a hemoprotein and it is well documented that heme is an efficient quencher of intrinsic protein fluorescence.[4] The crystal structure of CCP shows that Trp-51 and Trp-191 are within 5 Å of the heme, therefore, these residues are expected to have fluorescence quantum yields close to zero due to extensive energy transfer to the heme.[5,6] Four of the remaining Trp residues are 15-19 Å from the heme and their fluorescence should also be substantially quenched.[4] Therefore, Trp-101, which is 28 Å from the heme, is expected to be the main contributor to the steady-state fluorescence.

The relative accessibility of different Trp residues in a protein can be determined by the sensitivity of their fluorescence to a variety of freely-diffusing quenchers.[7,8] Studies with hydrophilic quenchers can provide information on the amount of intrinsic fluorescence arising from water-accessible Trp residues.[9] Since

Figure 4.1: Computer graphics display of the C_α backbone of CCP showing the location of the heme (red) as well as Trp and Tyr residues (green)

Trp-101 appears to be buried, freely-diffusing ionic quenchers are not expected to quench the fluorescence of CCP significantly. The uncharged, nonpolar quencher acrylamide can penetrate to some extent the hydrophobic interior of proteins and quench the more hydrophobic fluorophores.[8]

It has been observed that covalent attachment of pentaammineruthenium(III) (a_5Ru) to histidine residues efficiently quenches Trp fluorescence in α-lytic protease and lysozyme.[10] Fluorescence may be a useful probe of the environment around the sites of modification in the two singly-modified a_5Ru(His)CCP derivatives. Analysis of the structure of CCP indicates that modification of any of the three surface histidine residues should lead to efficient fluorescence quenching of nearby Trp residues. Since the location of all His and Trp residues in CCP is known from the crystal structure, the efficiency of energy transfer can be calculated for derivatives containing a_5Ru at any of the surface His residues. Thus, a comparison of the calculated and observed quenching of Trp fluorescence by a_5Ru may help identify the site of modification in a_5Ru(His-X)CCP where X = His-6 or His-96 (Chapter 2).

Compound I contains an Fe^{4+}=O heme and a radical species.[11] The radical in horseradish peroxidase (HRP) is present on the porphyrin, which is consistent with the fact that the reducing substrates are small, organic molecules which can access the heme.[12] Compound I of CCP does not have a porphyrin radical, instead the radical is centred on an amino acid residue.[11] CCP is one of a small but growing number of enzymes which reportedly make use of stable amino acid radicals. For example, ribonucleotide reductase,[13,14] prostaglandin H synthase[15] and photosystem

II,[16] utilize a Tyr radical. The location of the radical in CCP has long been sought, and several amino acid residues have been implicated, including Trp-51,[5,17-19] Trp-191,[17,19,20] Met-172,[18,21] Met-230 and Met-231.[22] Recently, using ENDOR,[23] a Trp residue has been definitely identified as the radical site and Trp-191 was considered the most likely candidate. Specifically altering this residue to Phe causes changes in the kinetics of CCP turnover, and compound I of the Phe-191 mutant transiently shows a porphyrin radical like HRP.[20] Trp-51, which is only 4 Å from the heme, was eliminated as the radical site since the Phe-51 mutant of CCP causes only minor changes in the ^{1}H ENDOR pattern.[17] CCP is the first protein which purportedly uses a stable Trp radical.[6]

Previously it was observed that CCP can reduce up to 10 equivalents of H_2O_2 in the absence of exogenous donors. Amino acid analysis shows that this is accompanied by the destruction of ~ 3-4 Tyr and ~ 2 Trp, and loss of enzyme activity over 24 h at pH 7.[24,25] Under the same conditions, direct oxidation of Trp and Tyr residues by H_2O_2 in apoCCP does not occur,[26] therefore, the peroxide must be cycled through the heme. The destruction of Trp residues presumably occurs because no reducing equivalents are provided to reduce the endogenous donors.

Because of efficient energy transfer from Tyr --> Trp, the fluorescence intensity should be most sensitive to the loss of Trp residues during reduction of H_2O_2. Therefore, protein fluorescence should be able to identify Trp and Tyr as endogenous donors. Since Trp residues are efficiently quenched by the heme, observation of fluorescence from Trp residues close to the heme requires unfolding

of the polypeptide chain. High concentrations of urea (8 M) relieves heme quenching significantly since it unfolds the polypeptide chain.[1c] Thus, examination of the fluorescence of the unfolded protein may permit a correlation of Trp loss with number of H_2O_2 molecules reduced by endogenous donors. Also, if the H_2O_2-oxidized enzyme is allowed to stand for various times following reaction with H_2O_2 before unfolding, we may be able to probe the migration and quenching of amino acid radicals in CCP. If enzyme activity is measured just prior to unfolding it may be possible to correlate loss of enzyme activity with loss of fluorescence intensity.

This Chapter investigates the fluorescence properties of native CCP, the a_5Ru(His)CCP derivatives and other products from the ruthenation reaction mixture. The accessibility of fluorescent residues in CCP to freely-diffusing (Cs^+, I^- and acrylamide) and covalently-bound quenchers (a_5Ru) is also reported. The fluorescence properties of unfolded CCP in 8 M urea are used to probe the reduction of H_2O_2 by CCP in the absence of exogenous electron donors. Loss of fluorescence is correlated to loss of enzymatic activity when CCP reacts with up to 10 equivalents of H_2O_2 in the absence of exogenous electron donors.

Note: Compound I is formed when 1 equivalent of H_2O_2 is added to CCP. When > 1 equivalent of H_2O_2 is added to CCP, the product is referred to as H_2O_2-oxidized CCP.

4.2 Experimental section

4.2.1 Materials

Analytical grade N-acetyl tryptophanamide (NATA) and KCN were purchased from Sigma. Sodium thiosulphate was obtained from BDH. Electrophoresis grade urea and acrylamide were obtained from Bio-rad. Analytical grade KI, CsCl, NaCl and 30% (w/v) hydrogen peroxide (~ 6.8 M) were supplied by ACP. Sodium ascorbate was purchased from Fisher and concentrations were determined by weight.

4.2.2 Methods

(a) Sample preparation: All stock solutions were prepared in sodium phosphate buffer (pH 7, 0.1 M). The concentrations of stock solutions (5 or 10 μM) of ferric CCP and a_5Ru(His)CCP were determined spectrophotometrically using ϵ_{408} = 98 mM^{-1} cm^{-1}.[27] CCP-CN was prepared as described in Chapter 2. Stock solutions of 5 N KI, CsCl, NaCl and acrylamide were prepared in the phosphate buffer and the pH readjusted to pH 7. Iodine precipitation was prevented by including 1 mM sodium thiosulphate in the KI stock solution. The salt concentration of samples containing the ionic quenchers was adjusted to 0.73 M by adding NaCl. A total of 120 μl of stock salt solution (KI or CsCl + NaCl) and 70 μl stock CCP (10 μM) was added to 630 μl phosphate buffer to give a final volume of 820 μl in a semi-micro cuvette (10 x 5 mm).

(b) Unfolded CCP and H_2O_2-oxidized CCP: 10 M urea was prepared in 0.1 M phosphate buffer and the pH re-adjusted to 7. 30% H_2O_2 was diluted to give a

20 mM H_2O_2 solution which was further diluted to 0.2-1 mM, depending on the final concentration of H_2O_2 required. For all samples, 150 µl CCP, compound I or H_2O_2-oxidized CCP (5 µM) was added to 600 µl urea (10 M) in a semi-micro cuvette to give final CCP and urea concentrations of 1 µM and 8 M, respectively, in a total volume of 750 µl. All amino acid analyses on CCP, compound I and H_2O_2-oxidized CCP (10-fold excess H_2O_2) were performed by B. Gibbs at the Biotechnology Research Institute, Montreal.

Enzymatic activity measurements: CCP, compound I and H_2O_2-oxidized CCP activity measurements were performed on 5 µM samples, prior to unfolding in 8 M urea, following the procedure outlined in the methods for Chapter 2. Measured activities were made relative to a 5 µM stock solution of CCP stored at 4 °C for the duration of the experiment.

Fluorescence measurements: Steady-state fluorescence measurements were carried out using a Shimadzu spectrofluorophotometer (Model RF-5000) with the sample compartment maintained at 22 ± 1 °C. All emission spectra were recorded using the "very slow" scan speed of the fluorometer (114 nm/min). An excitation wavelength of 280 nm and an emission range of 300-450 nm were used. Excitation and emission slits were 5 nm unless otherwise indicated. The Raman peak of water was subtracted from all fluorescence emission spectra, and inner-filter effects were corrected using the formula:[1d]

$$F_c = F \text{ Antilog}[(A_{ex} + A_{em})/2] \qquad (1)$$

where F_c is the corrected fluorescence intensity, F the measured intensity, A_{ex} the absorbance of the solution at the excitation wavelength, and A_{em} the absorbance at the emission wavelength. The fluorescence quantum yields for the CCP samples relative to NATA were calculated from a ratio of the areas of the emission bands normalized for their relative absorbances at the excitation wavelength. The efficiency of energy transfer (E) between the donor (Trp) and acceptor (heme or a_5Ru) was determined using the Förster theory of resonance energy transfer:

$$E = 1 - Q_p/Q_a \qquad (2)$$

where Q_p is the quantum yield in the presence of the acceptor and Q_a is the quantum yield in the absence of the acceptor. The value of Q_a for Trp has been determined to be 0.2.[28] However, this value has been questioned[29] and recalculated to be 0.13. The latter investigator concludes that Weber and Teale[28] do not list experimental conditions such as temperature and pH, factors which affect the observed quantum yields. Both numbers were used in calculations shown here. The efficiency of energy transfer is related to the distance between the acceptor and donor groups by:

$$E = r^{-6}/(r^{-6} + R_o^{-6}) \qquad (3)$$

where r is the distance between the acceptor and donor groups and R_o is the distance at which the donor fluorescence is quenched by 50%. R_o is defined by:

$$R_o = 9.79 \times 10^3 (\kappa^2 n^{-4} Q_a J)^{1/6} \qquad (4)$$

where κ^2 is the orientation factor which is 0.67 for random orientation between the donor and acceptor.[9] The orientation factor could be calculated from the x-ray

structure; however, Trp residues have rotational mobility in proteins and peptides.[30] The refractive index of the medium between the donor and acceptor is given by n, and a value of 1.4 is generally used for proteins.[31] The spectral overlap integral, J, between the donor emission and the acceptor absorption is given by:

$$J = \frac{\int F_\lambda \epsilon_\lambda \lambda^4 \, d\lambda}{\int F_\lambda \, d\lambda} \qquad (5)$$

where F_λ is the fluorescence emission intensity of the donor at wavelength λ (nm) and ϵ_λ is the acceptor extinction coefficient at λ (nm). Overlap integrals were determined between 300 and 400 nm, using eqn (5), as previously described.[32] Values for J and for R_o were calculated for energy transfer from Trp ----> heme and from Trp ----> a_5Ru (Table 4.4).

4.3 RESULTS

Native CCP fluorescence: Figure 4.1 above shows the location of the Trp and Tyr residues and the heme of CCP, mapped on the C_α backbone. Clearly, a number of these residues are close to the heme so extensive fluorescence quenching is expected. Figure 4.2 shows the steady-state fluorescence from native CCP excited at 260, 280 and 295 nm. The emission maximum is at 324 ± 2 nm indicating that the average Trp environment is hydrophobic[1e] since free Trp in aqueous solution has an emission maximum of 350 nm. The emission maximum is independent of the excitation wavelength, and the excitation spectrum is characteristic of Trp absorption

with a maximum at 280 nm. These spectral properties are consistent with the steady-state fluorescence being dominated by emission from Trp residues. The quantum yield relative to NATA is 5.2 ± 0.2% indicating that in native CCP, quenching by the heme is a highly efficient process, as expected.

Quenching of native CCP fluorescence by Cs^+, I^- and acrylamide: Table 4.1 summarizes the observed quenching of CCP fluorescence at 324 nm by these freely-diffusing quenchers. Fluorescence quenching was determined from the decrease in intensity since the emission maximum remained at 324 nm. At a concentration of 0.73 M the hydrophilic quenchers, Cs^+ and I^- give rise to 5% and 7% fluorescence quenching, respectively (Table 4.1). Within experimental error, the emission maximum of CCP is not shifted in the presence of Cs^+ and I^-. This result, together with the relatively high quenching efficiency of acrylamide, is consistent with a buried hydrophobic environment for the fluorescent Trp residues. This is also indicated by the short wavelength position of the emission maximum of CCP.

Fluorescence of singly-modified a_5Ru(His)CCP derivatives: Figure 4.3 compares the fluorescence intensities of native CCP and the a_5Ru-modified derivatives. The data in Table 4.2 indicate that the fluorescence intensity at 324 nm is decreased for a_5Ru(His-60)CCP and a_5Ru(His-X)CCP by 14 ± 2% and 50 ± 5%, respectively, compared to native CCP. Since a 1:1 noncovalent mixture of native CCP and a_5Ru(His) has a fluorescence intensity similar to that of CCP alone, the quenching observed for a_5Ru-modified CCP is due to the covalently-bound a_5Ru, and the extent of quenching depends on the site of attachment of the metal

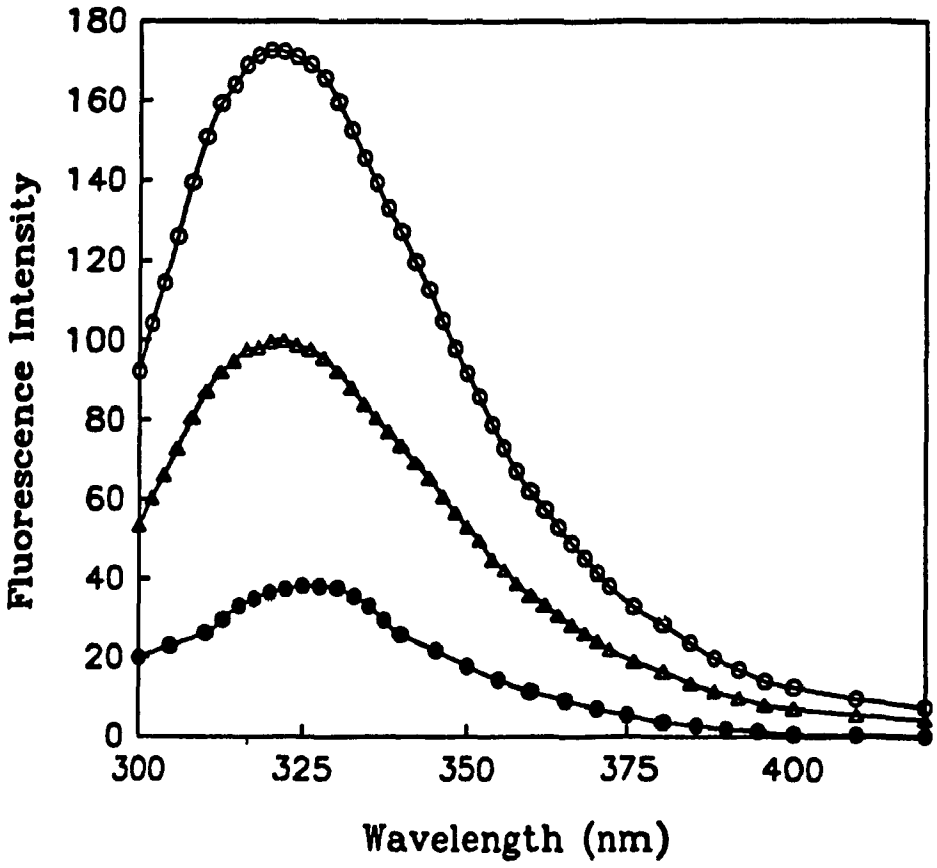

Figure 4.2: Fluorescence emission spectra for 1 μM native CCP in 0.1 M phosphate buffer (pH 7) at 22 °C when excited at 260 (triangles), 280 (open circles) and 295 nm (closed circles). Excitation and emission slit widths were 10 and 5 nm, respectively, and the scan speed was 114 nm/min.

Table 4.1:

Relative fluorescence (%) intensities of native CCP in the presence of freely-diffusing quenchers

0.73 M quencher	% fluorescence intensity
None	100 ± 2
Cs^+	95 ± 2
I^-	93 ± 2
Acrylamide	68 ± 3

Fluorescence intensities were measured at the emission maximum which was centred at 324 nm for all species. Excitation was at 280 nm and the excitation and emission slits were 10 and 5 nm, respectively. Scan speed: 114 nm/min. 22 °C

Table 4.2

Relative fluorescence (%) intensity of native CCP and the a_5Ru(His)CCP derivatives

Protein	% fluorescence intensity
Native CCP	100 ± 2
Native CCP + a_5Ru(His)	100 ± 3
a_5Ru(His-60)CCP	86 ± 2
a_5Ru(His-X)CCP	50 ± 5

See footnote to Table 4.1 for experimental conditions.

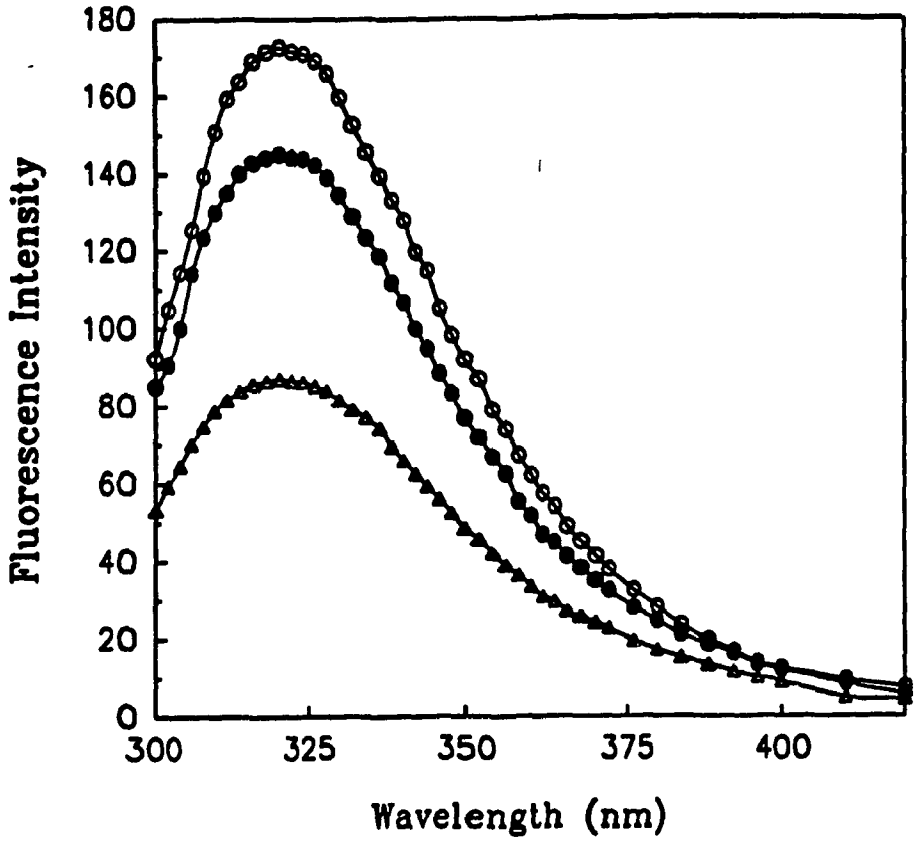

Figure 4.3: Fluorescence emission spectra obtained for 1 μM native CCP (open circles), a_5Ru(His-60)CCP (closed circles) and a_5Ru(His-X)CCP (triangles). The experimental conditions are the same as given in the caption to Figure 4.2.

complex on the protein surface.

Table 4.3 summarizes the fluorescence quenching of the a_5Ru(His)CCP derivatives by freely-diffusing quenchers. Cs^+ and I^- show no detectable quenching of fluorescence of either a_5Ru(His)CCP derivative, which indicates that the a_5Ru centres quench the fluorescence of the Trp residues accessible to these charged quenchers. In contrast, acrylamide quenches the fluorescence of a_5Ru(His-60)CCP as effectively as in native CCP (32%), but only 9% in a_5Ru(His-X)CCP. These findings suggest that binding of a_5Ru to His-X, but not to His-60 significantly quenches Trp residues accessible to acrylamide.

Calculated energy transfer efficiencies for singly-modified a_5Ru(His)CCP derivatives: Table 4.4 lists the overlap integrals (J) and the distance at which donor fluorescence is quenched by 50% (R_o), which were calculated for CCP, CCP-CN and compound I, using eqns 4 and 5. Data for the J and R_o values of a_5Ru(His)CCP are also shown. The individual Trp ---> heme fluorescence energy transfer efficiencies for CCP (Table 4.5) were calculated using eqn 3 and the data in Table 4.4. The total Trp ---> heme energy transfer efficiency for CCP was calculated to be 94.4% which compares favourably with the observed quantum yield of 5.2% (i.e., 94.8% energy transfer efficiency) for native CCP compared to NATA. Table 4.5 also lists the Trp ---> a_5Ru energy transfer efficiencies calculated for each possible singly-modified a_5Ru(His)CCP derivative (i.e., a_5Ru bound to one of the three surface His residues).

The estimated contribution of each Trp residue to the total fluorescence

Table 4.3

Relative fluorescence (%) intensities of the a_5Ru(His)CCP derivatives in the presence of freely-diffusing quenchers

0.73 M quencher	% fluorescence intensity	
	a_5Ru(His-60)CCP	a_5Ru(His-X)CCP
None	100 ± 2	100 ± 5
Cs^+	96 ± 3	100 ± 5
I^-	100 ± 3	100 ± 4
Acrylamide	67 ± 4	92 ± 3

See footnote to Table 4.1 for experimental conditions.

Table 4.4

Overlap integrals (J) and R_o's[a] calculated for Trp to heme fluorescence energy transfer in CCP, CCP-CN and compound I, as well as for Trp to a_5Ru fluorescence energy transfer in a_5Ru(His)CCP

Protein	Overlap Integral, J, (x 10^{14}) (cm^3 M^{-1})	R_o (Å) (using Q_a = 0.13)[d]	R_o (Å) (using Q_a = 0.20)[d]
CCP[b]	5.77	32	35
CCP-CN[b]	2.91	29	31
Compound I[b]	3.07	29	31
a_5Ru(His)CCP[c]	0.102	16.5	17.8

CCP-CN and compound I samples were prepared as outlined in Chapter 2
[a]J and R_o were calculated using eqns 4 and 5
[b]Trp ----> heme energy transfer
[c]Trp ----> a_5Ru energy transfer
[d]Q_a is the fluorescence quantum yield for Trp (see text).

of native CCP is given in Table 4.6. These values were calculated using the x-ray structure of CCP to provide distances from each Trp residue to the heme (Table 4.5), and a Trp ---> heme R_o value of 32 Å (Table 4.4). Further quenching of each Trp by energy transfer to a_5Ru in the three possible a_5Ru(His)CCP derivatives was also calculated, again using the x-ray structure of CCP to provide distances between the Trp residues and each His residue (Table 4.5). The data in Table 4.6 allow us to predict the fluorescence intensity of a_5Ru(His-6)CCP, a_5Ru(His-60)CCP and a_5Ru(His-96)CCP relative to CCP. The observed fluorescence intensity of a_5Ru(His-60)CCP at 324 nm, relative to CCP, was lower (84%) than the estimated relative quantum yields (94.4%) (Table 4.6). The observed fluorescence intensity of a_5Ru(His-X)CCP at 324 nm, relative to CCP, was 50% whereas the estimated relative quantum yields were 74 and 14% for a_5Ru(His-6)CCP and a_5Ru(His-96)CCP, respectively. Since extensive fluorescence quenching is expected if a_5Ru is attached to His-96, due to its close proximity to Trp-101 which is the major fluorophore in CCP, we assume that for a_5Ru(His-X)CCP, X = 6.

Fluorescence of other products from the CCP ruthenation reaction mixture: In agreement with the spectrophotometric a_5Ru determination (Table 2.2), bands 1 and 2 appear to contain no ruthenium since they exhibit a fluorescence intensity and an emission maximum at ~ 324 nm similar to native CCP. Due to its heterogeneous nature, band 3 was not analyzed. Peak 4c (see Figure 2.6) is more cationic than a_5Ru(His-60)CCP (peak 4a) but the fluorescence of this peak is similar to that of native CCP. This suggests that peak 4c does not contain a covalently-bound

Table 4.5

Efficiency of energy transfer from Trp to heme and

Trp to a_5Ru for CCP and a_5Ru(His)CCP derivatives[a]

[a]The a_5Ru centre was assumed to be attached to a surface His residue in each case. (Trp-51 and Trp-191 are excluded from the calculations since they are within 5 Å of the heme so the efficiency of energy transfer is unity, i.e. they do not contribute to the steady-state fluorescence of CCP. The remaining Trp residues are assumed to have equal fluorescence quantum yields (Q_a = 0.2).

[b]Trp residues from CCP x-ray crystal structure

[c]Closest distance from the heme Fe to the edge of the Trp residue concerned

[d]E is the efficiency of energy transfer (eqn 2) from Trp to heme in CCP and from Trp to a_5Ru in a_5Ru(His)CCP derivatives

[e]Closest distance from the His Nε2 atom to the edge of the Trp residue concerned

[f]Fluorescence quenching due to the covalent attachment of a_5Ru to the His residues indicated

[g]E_T is the summation of E for each Trp residue, giving an estimate of the total efficiency of fluorescence energy transfer in CCP.

Heme quenching (R_o = 32 Å) Native CCP			a_5Ru quenching (R_o = 17 Å)[f]					
			a_5Ru(His-60)CCP		a_5Ru(His-6)CCP		a_5Ru(His-96)CCP	
Trp residue[b]	Dist. to Heme (Å)[c]	E[d]	Dist. to His-60 (Å)[e]	E	Dist. to His-6 (Å)	E	Dist. to His-96 (Å)	E
57	15	0.990	10	0.960	6.3	0.997	22	0.176
126	17	0.978	26	0.072	15.2	0.679	12	0.890
223	15	0.990	29	0.039	37	0.009	40	0.006
211	16	0.985	33	0.018	38	0.008	38	0.008
101	26	0.776	32	0.018	21	0.220	8.5	0.985
Total energy transfer (E_T)[g]		0.944		0.221		0.383		0.413

Table 4.6

Estimated contribution (%) of each Trp residue to steady-state fluorescence of CCP and a_5Ru(His)CCP derivatives

Trp residue	Estimated contribution (%) to fluorescence[a]			
	Native CCP	a_5Ru(His-60)CCP	a_5Ru(His-6)CCP	a_5Ru(His-96)CCP
57	3.56	0.14	0.01	3.01
126	7.83	7.28	2.66	0.80
223	3.56	3.42	3.60	3.60
211	5.34	5.23	5.20	5.20
101	79.7	78.1	62.17	1.20
Total fluorescence (F_T)[b]	100.0	94.2	73.6	13.8
Observed fluorescence[c]	100 ± 2	86 ± 2	50 ± 5[d]	

[a]The fluorescence contribution of each Trp residue was calculated from the energy transfer efficiencies for Trp to heme and Trp to a_5Ru (Table 4.5)

[b]The total fluorescence (F_T) was calculated by adding the contribution from each Trp residue.

[c]Observed relative fluorescence intensities at 324 nm for CCP, a_5Ru(His-60)CCP and a_5Ru(His-X)CCP (Table 4.2)

[d]Location of the a_5Ru is on His-6 or His-96

quencher but is altered during the ruthenation procedure. Peak 5c (see Figure 2.7) is more cationic than a_5Ru(His-X)CCP (peak 5b) and it exhibits a shift in its emission maximum to 310 nm from 324 nm in native CCP as shown in Figure 4.4. Due to the small quantities of peak 5c obtained, no ruthenium determination or activity measurements were made.

Fluorescence of compound I: Titration of CCP with one equivalent of H_2O_2 gives 100% conversion to compound I as monitored by the Soret shift from 408 to 420 nm.[33,34] This species is formed within manual mixing time (3 s), and under the present experimental conditions it has a decay half-life of ~ 5 h.[33] Figure 4.5 shows the fluorescence spectrum of native CCP and the spectrum immediately following the addition of H_2O_2. In both spectra the fluorescence emission maximum is at 324 ± 2 nm; however, the fluorescence intensity of compound I at 324 nm is 9% greater than that of native CCP. This increase may be attributed to the shift in the Soret band maximum from 408 to 420 nm since the cyanide adduct of CCP, which has a Soret maximum at 422 nm,[34] is ~ 7 % more fluorescent than native CCP. Table 4.4 summarizes the calculated overlap integrals and R_o 's for Trp ---> heme energy transfer in CCP, CCP-CN and compound I. The overlap integrals for CCP-CN and compound I are similar in magnitude and are both smaller than that of native CCP which accounts for the observed fluorescence increase for CCP-CN and compound I, compared to native CCP.

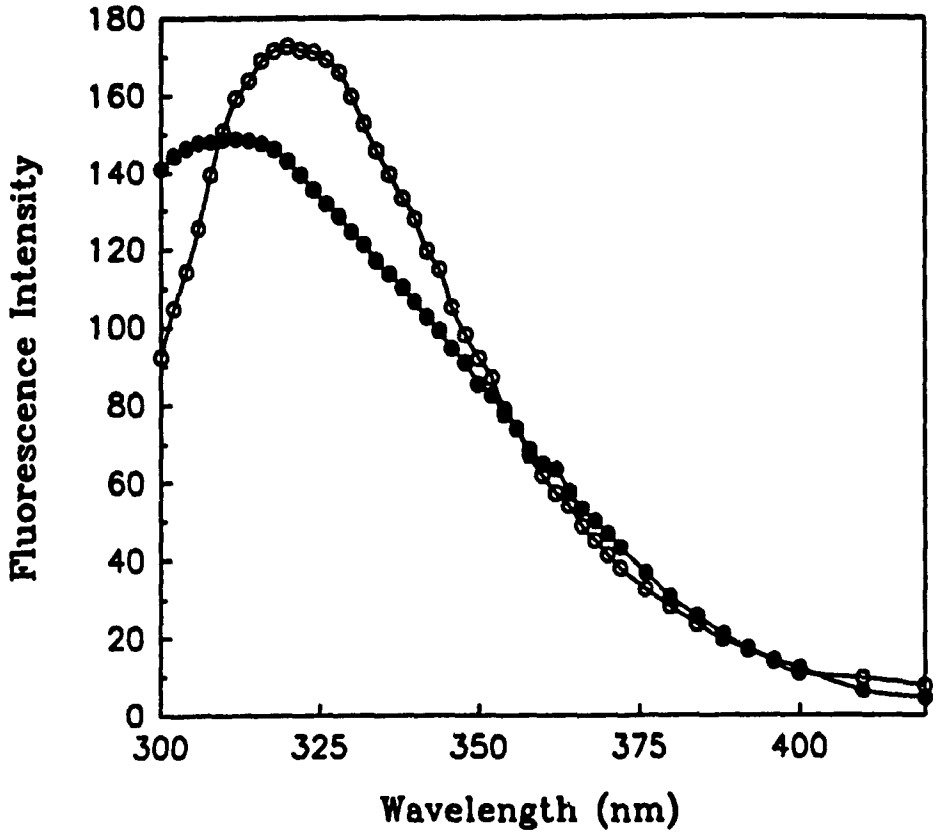

Figure 4.4: Fluorescence emission spectra obtained for 1 μM native CCP (open circles) and FPLC-purified peak 5c (closed circles). Experimental conditions are as given in the caption to Figure 4.2.

Fluorescence of unfolded native CCP & H_2O_2-oxidized CCP: In 8 M urea, the fluorescence intensity of CCP increases ~ 10-fold relative to the folded protein, indicating that quenching by the heme is significantly reduced (Figure 4.6). The emission maximum shifts to 350 ± 2 nm, consistent with unfolding of the protein and exposure of Trp residues to the aqueous solvent.[1c] Figure 4.7 shows that the unfolding transition occurs between 4 and 6 M urea and the fluorescence intensity levels off at 8 M urea suggesting that unfolding is complete. The time course of the unfolding process as monitored by the fluorescence increase at 350 nm indicates that CCP or compound I unfolding has a half-life of ~ 23 s (Figure 4.8). Changes in the Soret maximum are also consistent with exposure of the heme to solvent. For example, addition of compound I to 8 M urea gives rise to a Soret shift from 420 to 400 nm, and the decrease in absorbance at 424 nm has a half-life of ~ 30 s (Figure 4.8), similar to that for the fluorescence growth.

The fluorescence intensity of unfolded compound I is ~ 13% lower than unfolded CCP (Figure 4.9). Addition of one equivalent of ascorbate before unfolding yields a fluorescence intensity identical to that of unfolded CCP. Addition of a second equivalent of ascorbate has no effect on the observed fluorescence intensity, presumably because the radical has already been reduced by the first reducing equivalent. Figure 4.9 also shows that the unfolded protein exhibits a greater loss of fluorescence intensity if the enzyme is reacted with 10 molar equivalents of H_2O_2 prior to unfolding. Furthermore, the fluorescence intensity of H_2O_2-oxidized CCP continues to decrease over a 24 h period (Figure 4.10), although, the most rapid

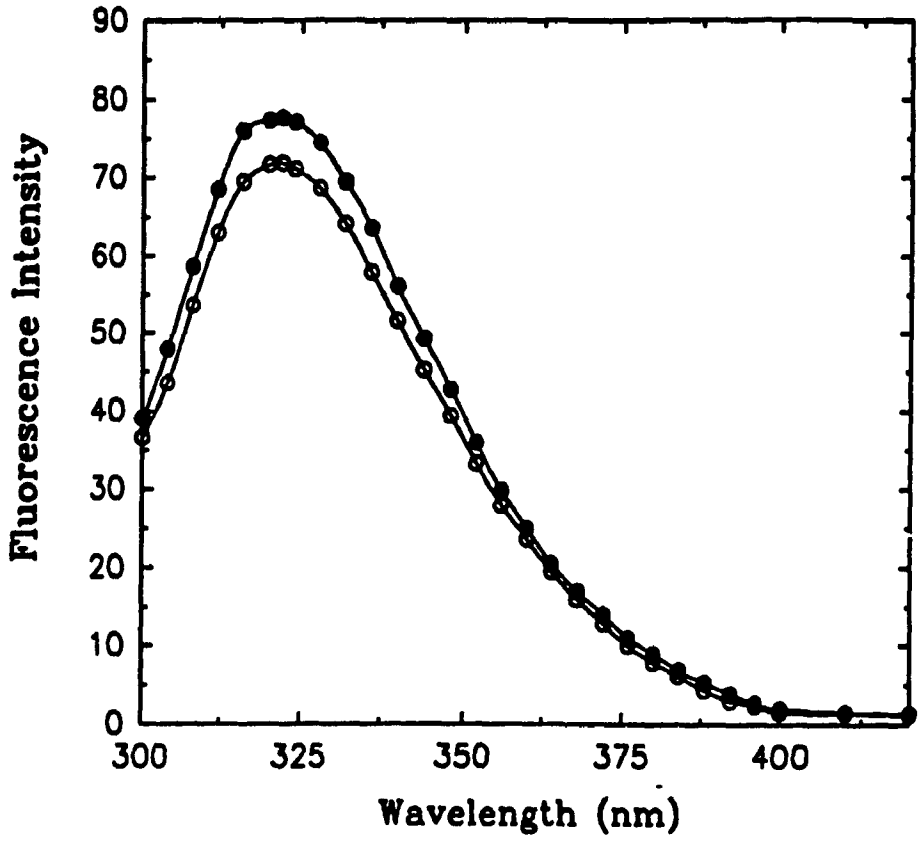

Figure 4.5: Fluorescence emission spectra obtained for 1 μM native CCP (open circles) and compound I of CCP (closed circle) when excited at 280 nm. Experimental conditions are as given in the caption to Figure 4.2 except that both the excitation and emission slit widths were 5 nm.

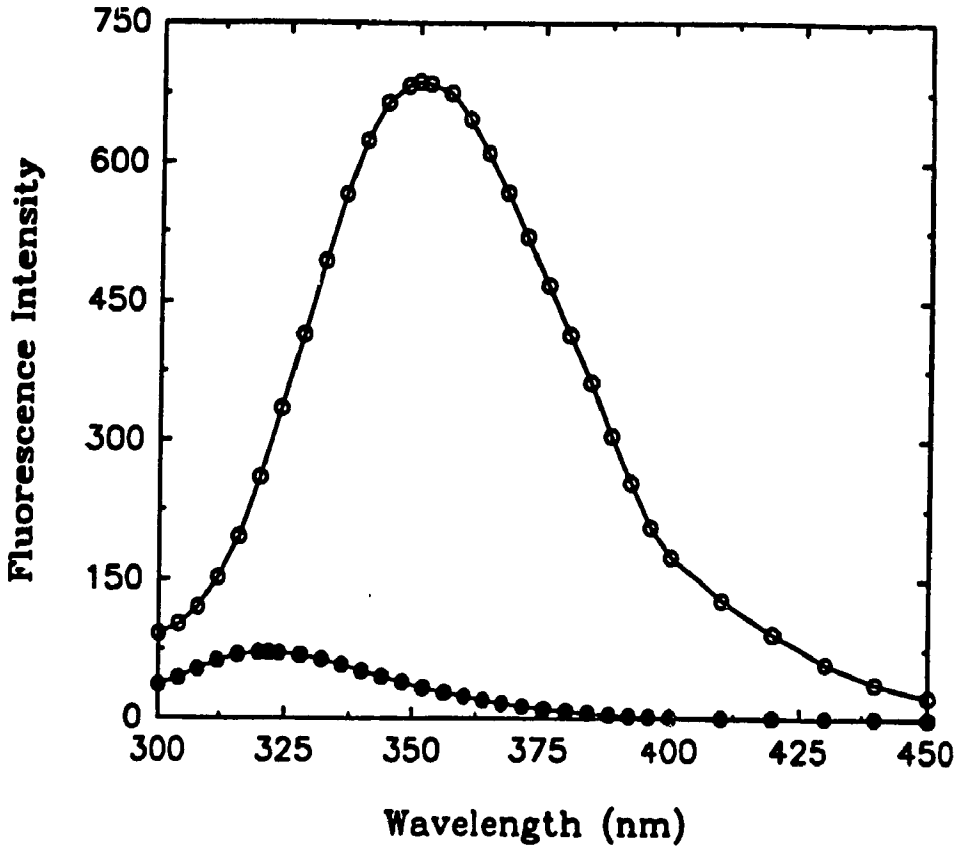

Figure 4.6: Fluorescence emission spectra at 350 nm obtained for 1 μM CCP (closed circles) and 1 μM unfolded CCP (open circles) in the presence of 8 M urea. Conditions are as given in the caption for Figure 4.5.

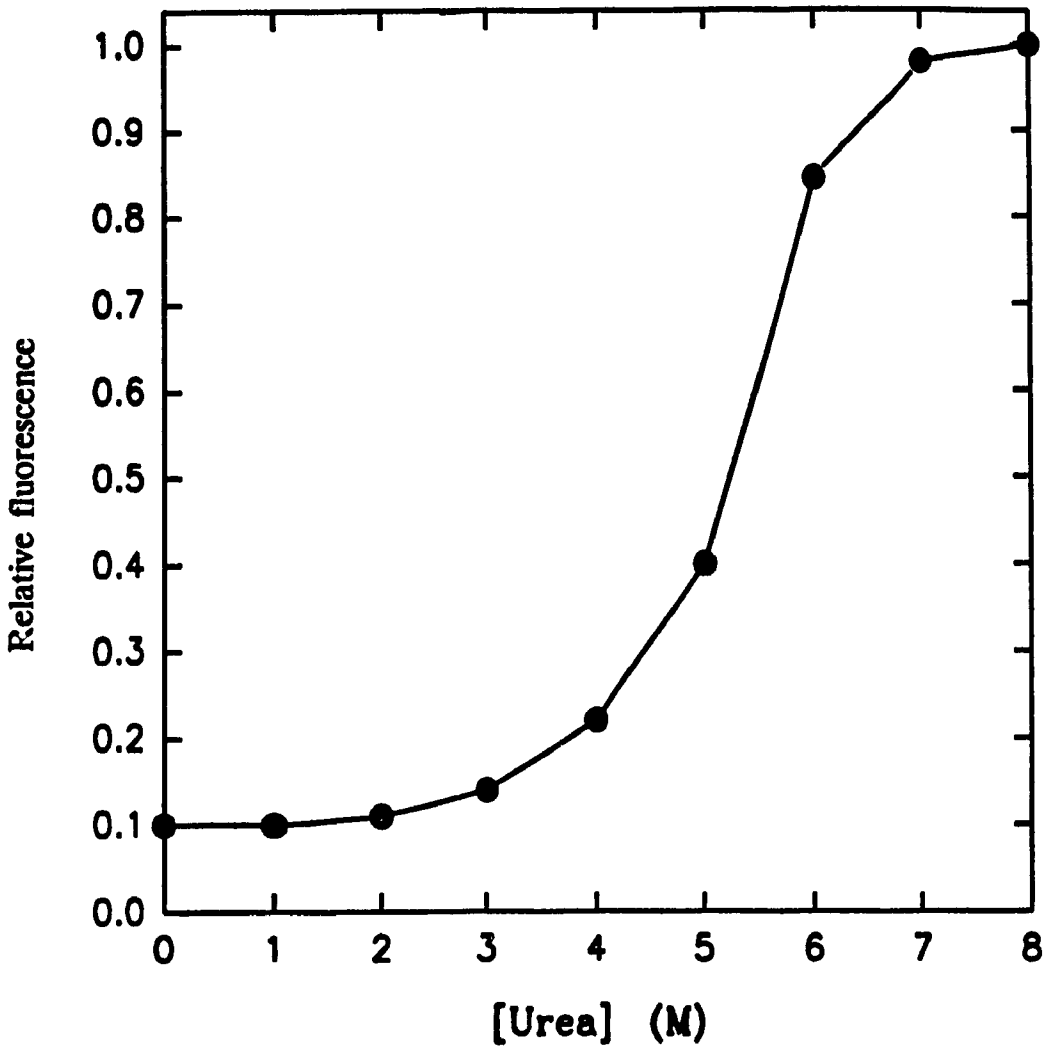

Figure 4.7: Relative fluorescence intensity of 1 μM CCP vs. urea concentration. Excitation and emission wavelengths were 280 and 350 nm, respectively. Conditions are as given in the caption for Figure 4.5.

decrease occurs within 15 s (Figure 4.11). Addition of a 5-fold molar excess H_2O_2 over CCP causes a fluorescence decrease similar to that observed for a 10-fold excess (Figure 4.11). A 3-fold excess H_2O_2 also causes a rapid (within 15 s of H_2O_2 addition) 25% decrease in fluorescence followed by a much smaller ~ 10% decrease over 24 h (Figure 4.11). These results are summarized in the appendix (Table 7.1).

Amino acid analysis of H_2O_2-treated CCP: Amino acid analyses were performed on CCP, compound I and H_2O_2-oxidized CCP (10-fold excess H_2O_2) by base hydrolysis (KOH) and by acid hydrolysis (methane sulphonic acid). Both methods yielded similar results, suggesting that 2-3 Tyr residues and 2 Trp residues are lost when CCP is treated with a 10-fold molar excess of H_2O_2. There appears to be no difference in the Trp and Tyr composition of CCP and compound I. These results are consistent with those reported previously.[24]

Enzymatic activity of H_2O_2-treated CCP: All activity measurements were made relative to native CCP stored at 4 °C throughout the experiment, which is assumed to retain 100% activity. Native CCP loses ~ 5-10% activity when left at 22 °C overnight, whereas compound I loses ~ 30% activity (Figure 4.12). For CCP oxidized with 3-, 5- and 10-fold molar excess H_2O_2, further decrease in activity is observed (Figure 4.12), suggesting that more catalytically important residues are being damaged. However, the loss in activity appears to occur on a slower timescale than the loss of fluorescence intensity (compare Figures 4.11 and 4.12). The data shown in Figures 4.11 and 4.12 are summarized in the appendix in Tables 7.1 and 7.2, respectively.

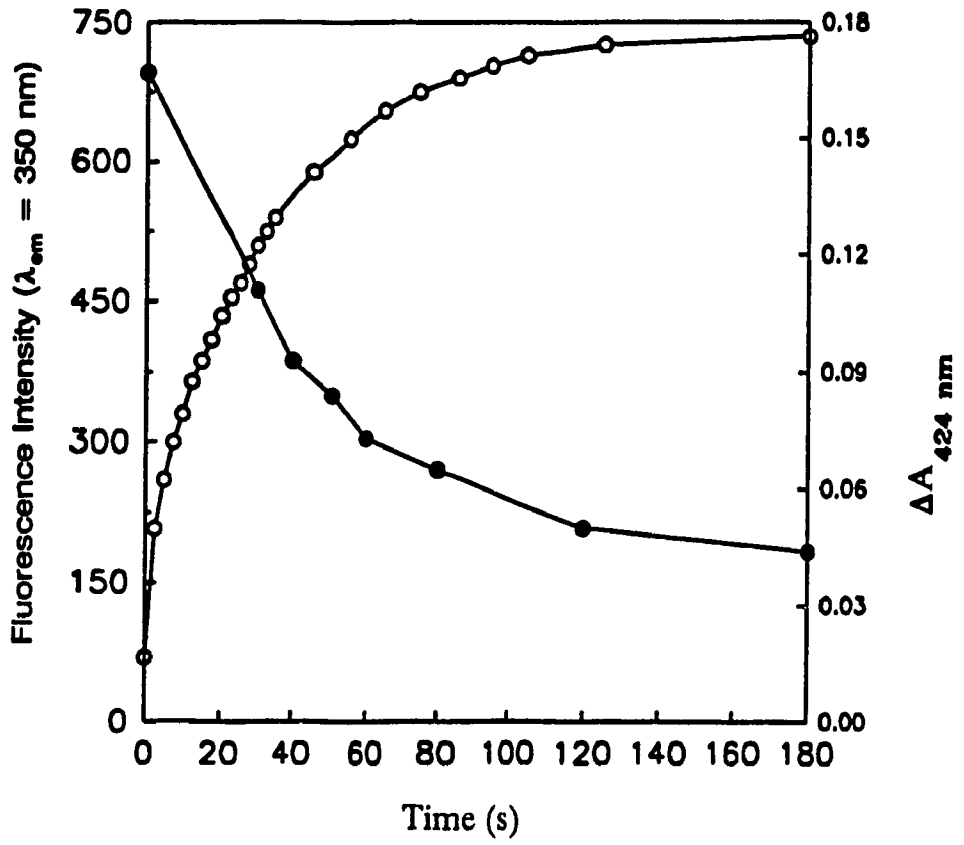

Figure 4.8: Increase in the fluorescence intensity at 350 nm of compound I vs. time (open circles) following addition of 1 μM protein to 8 M urea at 22 °C. The excitation wavelength was 280 nm and the excitation and emission slits were both 5 nm. Absorbance decrease at 424 nm vs. time (closed circles) following addition of 4 μM compound I to 8 M urea.

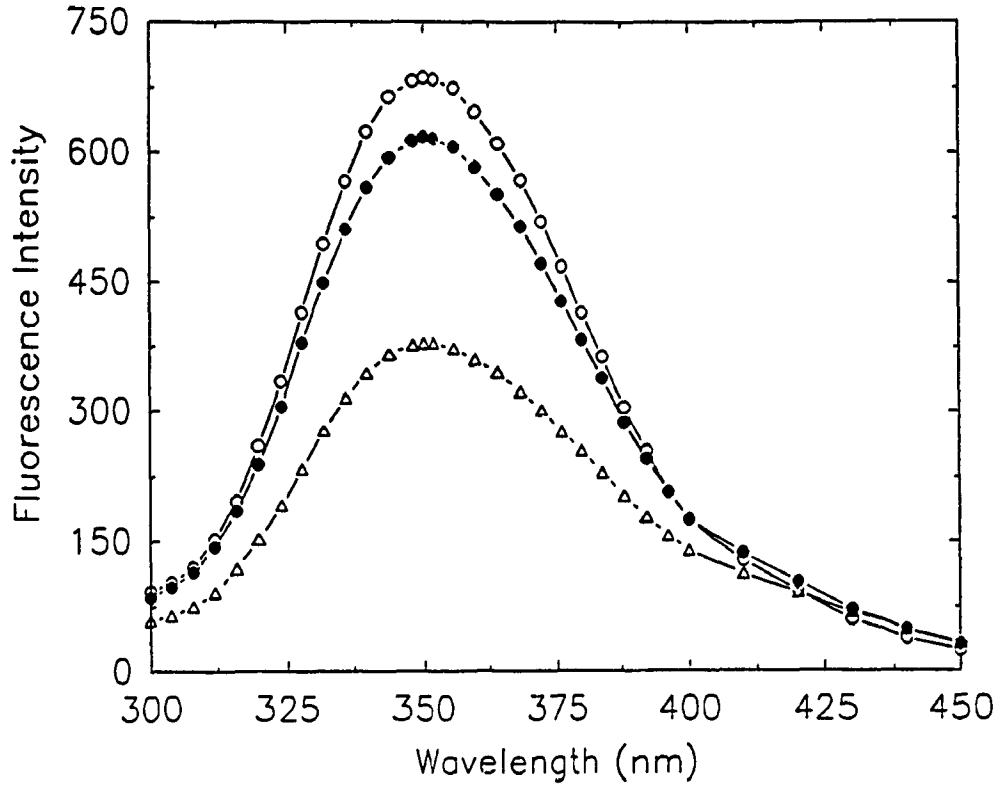

Figure 4.9: Fluorescence emission spectra obtained for 1 μM unfolded CCP in 8 M urea. The protein was reacted with a 0:1 (open circles), 1:1 (closed circles) and 10:1 (triangles) molar excess of H_2O_2 and unfolded in 8 M urea 15 s after addition of H_2O_2. Excitation was at 280 nm and the excitation and emission slit widths were both 5 nm. The scan rate was 114 nm/min. 22 °C.

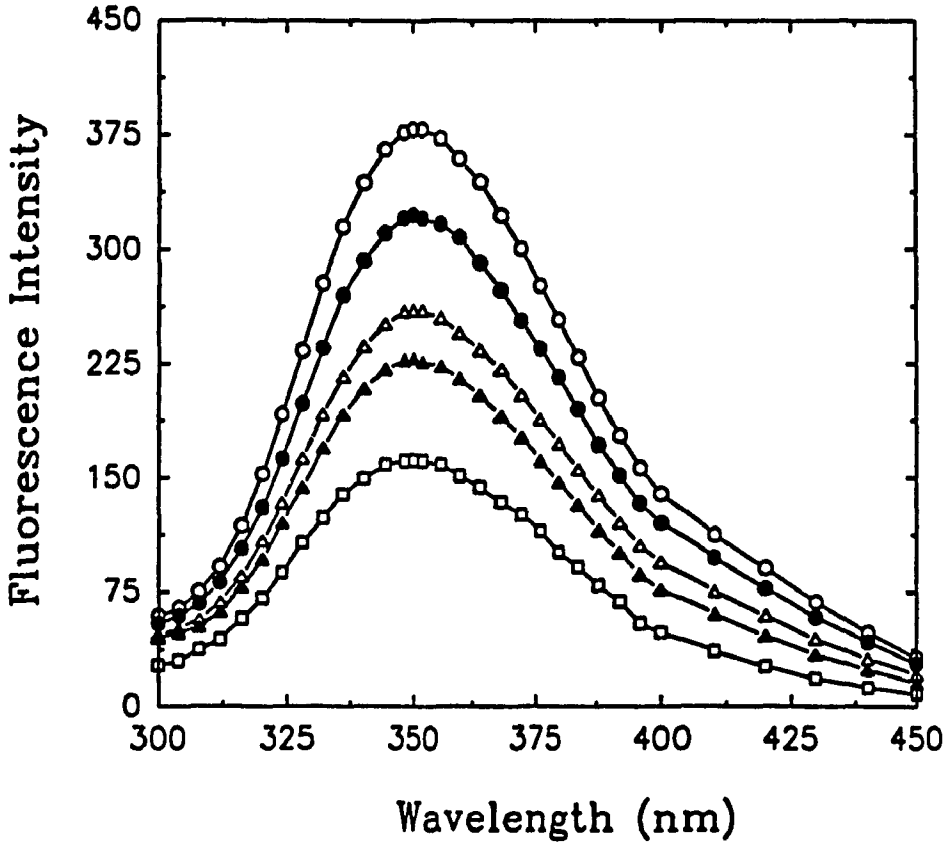

Figure 4.10: Time dependence of fluorescence spectra obtained for 1 μM unfolded CCP in 8 M urea. The protein was reacted with a 10-fold molar excess of H_2O_2 and unfolded in 8 M urea at the following times after addition of H_2O_2: 15 s (open circles), 5 min (closed circles), 10 min (open triangles), 20 min (closed triangles) and 24 h (open squares). Experimental conditions are the same as given in the caption for Figure 4.9.

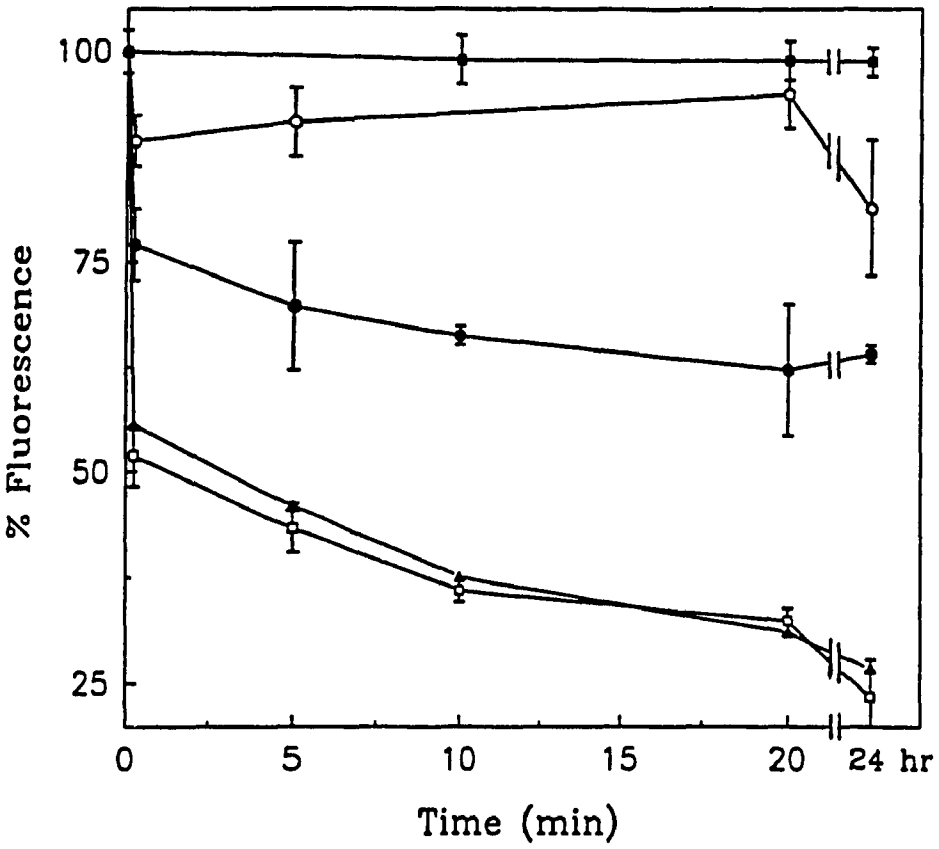

Figure 4.11: Time dependence of the percent fluorescence in 8 M urea of CCP (closed squares), compound I (open circles) and H_2O_2-oxidized CCP using 3:1 (closed circles), 5:1 (closed triangles) and 10:1 (open squares) molar ratios of H_2O_2/CCP. Fluorescence measurements were recorded at 15 s to 24 h after H_2O_2 addition. Excitation and emission wavelengths were 280 and 350 nm, respectively. Excitation and emission slits were 5 nm and a scan rate of 114 nm/min was used. Protein samples were stored at 22 °C.

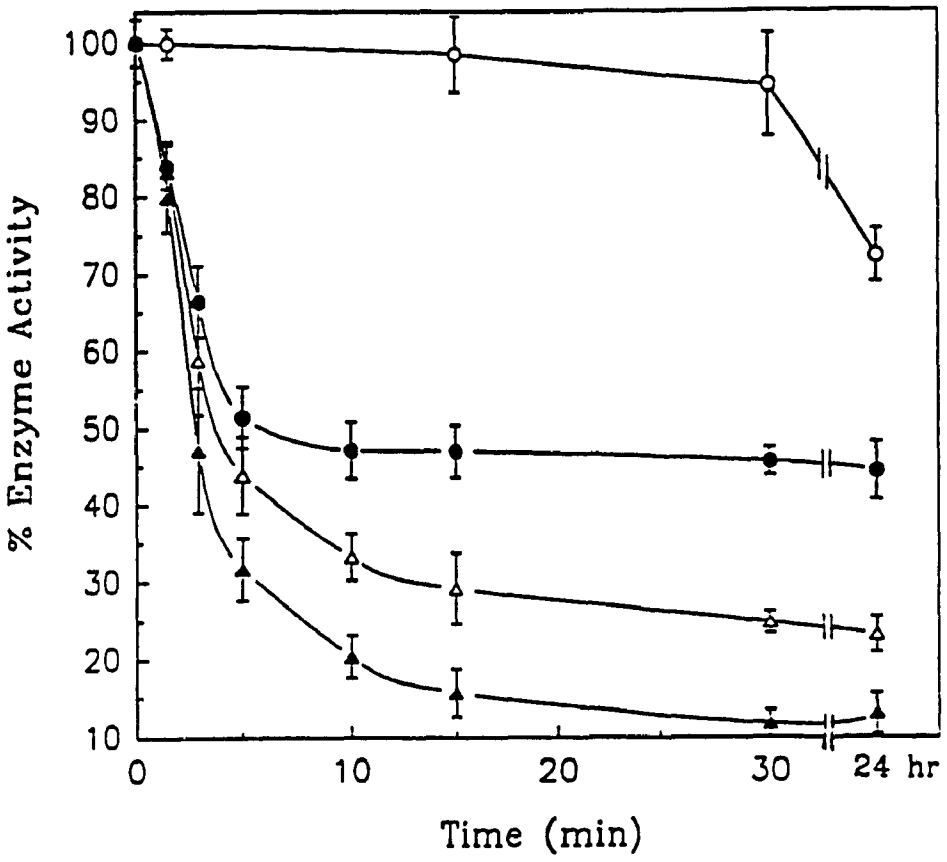

Figure 4.12: Time dependence of the percent enzymatic activity of the CCP samples in Figure 4.11. Activities were measured just prior to unfolding in 8 M urea. The symbols correspond to: 1:1 (open circles), 3:1 (closed circles), 5:1 (open triangles) and 10:1 (closed triangles) molar ratios of H_2O_2/CCP and the activity is relative to native CCP stored at 4 °C in the absence of H_2O_2). The procedure for activity measurements and the definition of activity are explained in Chapter 2.

4.4 Discussion

An emission maximum at 324 nm indicates that the fluorescent Trp residues in CCP are in a hydrophobic environment.[3] In instances where hydrophilic quenchers efficiently quench the fluorescence of exposed Trp residues in proteins, a blue shift in the emission is observed since the remaining fluorophores are in a more hydrophobic environment.[1e] The small degree of quenching by 0.73 M Cs^+ and I^- (Table 4.1), and the fact that the emission maximum remains at 324 nm in the presence of hydrophilic quenchers, indicates that the Trp are not accessible to hydrophilic quenchers, consistent with the blue-shifted emission maximum of CCP. In contrast, the same concentration of the neutral molecule acrylamide, quenches the fluorescence of native CCP by 32% (Table 4.1). The finding that acrylamide is more effective as a quenching agent is also consistent with the fluorescent Trp residues being buried in a hydrophobic environment, since acrylamide is able to penetrate the protein matrix.[8]

Trp ----> heme energy transfer is an efficient process in CCP which is not surprising since 6 of the 7 Trp residues are within 17 Å of the heme. Trp-101 is probably the major fluorophore because it is 26 Å from the heme. The calculated R_o of 32-35 Å for CCP is similar to that calculated for cytochrome c oxidase (35 Å).[9] The similarity between the calculated Trp ---> heme energy transfer efficiency (94.4%) which predicts a relative quantum yield of 5.6%, and the observed relative quantum yield (5.2%) for CCP, suggests that it was reasonable to assume an orientation factor (κ^2) of 0.67 in eqn 4.

Covalent binding to His-60 places the a_5Ru complex within 10 Å of Trp-57 (Table 4.5) which is well within the R_o of 17 Å calculated for Trp ---> a_5Ru fluorescence energy transfer (Table 4.4). This R_o is similar to those calculated for lysozyme and α-lytic protease. The 14% decrease in fluorescence yield on attachment of the Ru complex to His-60 (Table 4.3) suggests efficient energy transfer from at least one Trp, most likely Trp-57, to the Ru centre. However, Trp-101 is expected to be the major fluorophore in CCP (Table 4.4 and 4.5), and since this Trp residue is 32 Å from His-60, it is not expected to be quenched significantly in a_5Ru(His-60)CCP. The observed fluorescence intensity at 324 nm of 84% for a_5Ru(His-60)CCP compared to native CCP, is in reasonable agreement with the estimated relative fluorescence quantum yield of 94.2% (Table 4.6).

The estimated relative fluorescence quantum yields for the attachment of a_5Ru to His-6 or His-96, compared to CCP, are 73.6 and 13.8%, respectively. The observed fluorescence intensity at 324 nm for a_5Ru(His-X)CCP decreased ~ 50% compared to native CCP, which is 23.6% lower than the calculated relative quantum yield for a_5Ru(His-96)CCP, but 36.2% higher than that calculated for a_5Ru(His-6)CCP. A dramatic fluorescence decrease is expected for a_5Ru(His-96)CCP because the ruthenium centre is only ~ 7.8 Å from Trp-101 (Table 4.5), which should be the major contributor to the overall CCP fluorescence (Table 4.6). The distance from His-6 to Trp-101 is ~ 21 Å, so attachment of a_5Ru to His-6 should quench the fluorescence of Trp-101 much less than attachment to His-96 (Table 4.6).

The freely-diffusing quenchers, I^- and Cs^+, are inefficient quenchers of native

CCP fluorescence (Tables 4.1 and 4.3) indicating that the fluorescent Trp residues in CCP are in a hydrophobic region and inaccessible to ionic quenchers. Acrylamide is able to quench native CCP, a_5Ru(His-60)CCP and a_5Ru(His-X)CCP fluorescence presumably because it is nonpolar and can penetrate the protein matrix and access buried Trp residues, including Trp-101.

The fluorescence intensity of compound I is ~ 9% higher than that of native CCP. This may be attributed to the smaller spectral overlap integral, J, for compound I (Table 4.4) which occurs because the Soret band of CCP red-shifts by 12 nm upon compound I formation. The similar fluorescence increase observed on CCP-CN formation supports this conclusion, since the Soret band also red-shifts upon formation of the cyanide adduct.[34] The x-ray structures of compound I and CCP-CN show little change in the CCP structure compared to native CCP,[22] consistent with the fluorescence data presented here.

Addition of CCP or compound I to 8 M urea results in an exponential increase in fluorescence intensity at 350 nm, with a $t_{½}$ ~ 23 s (Figure 4.8). Since the absorption of compound I in 8 M urea resembles that of 5-coordinate ferric heme (λ_{max} = 400 nm), presumably the Fe^{4+}=O is rapidly reduced (i.e., in 1 min or less). The kinetics of Fe^{4+}=O reduction in 8 M urea is similar to the kinetics of protein unfolding (Figure 4.8) so we can assume that Fe^{4+}=O is solvent-exposed and reduced by an unknown exogenous or endogenous donor upon protein unfolding. We can also assume that the unfolded CCP does not react with any remaining H_2O_2 in the reaction medium.

Unfolded compound I exhibits a 13% fluorescence decrease compared to unfolded CCP, which strongly supports the assignment of a Trp as the radical site in compound I. Trp-191 is the most probable candidate due to its close proximity (5 Å) to the heme, since Trp-51 has been ruled out.[17,19] Addition of one reducing equivalent to compound I at pH 7 reduces the radical first.[35] Providing compound I with one reducing equivalent from ascorbate prior to unfolding did not reduce the Fe^{4+}=O centre, but on unfolding the fluorescence intensity was now equal to that of unfolded CCP. This suggests that the observed fluorescence loss is due to formation of the radical and not formation of ferric heme in 8 M urea. Addition of a second reducing equivalent to compound I reduces the ferryl iron and has no further effect on the fluorescence intensity of the unfolded protein.

Higher H_2O_2/CCP ratios causes a further decrease in the fluorescence intensity of unfolded CCP, presumably because more fluorescent residues act as endogenous donors to H_2O_2. The most dramatic fluorescence decrease occurs during the first 15 s after addition of 3 to 10-fold excess H_2O_2 (Figure 4.11). Figure 4.1 shows a cluster of aromatic residues around the heme which may act as initial endogenous donors during peroxide reduction. The fluorescence intensity decreases further when H_2O_2-oxidized CCP is allowed to stand for 24 h, indicative of the oxidation of more residues that contribute to fluorescence.

Amino acid analyses of CCP and compound I indicates that there is no change in the Trp and Tyr residue content of compound I compared to CCP. However, amino acid analysis of H_2O_2-oxidized CCP (10-fold excess H_2O_2) shows that,

compared to CCP and compound I, 2-3 Tyr and 2 Trp are destroyed due to the reduction of peroxide in the absence of exogenous donors. These results are consistent with amino acid analyses reported previously which have shown that when CCP at pH 7 is exposed to 10-fold excess H_2O_2, after 24 h ~ 3-4 Tyr and 2 Trp are destroyed.[24,25] Clearly, amino acid analysis does not indicate as much damage to fluorescent residues compared to steady-state fluorescence intensity measurements since ~ 75% of the fluorescence intensity is lost in samples exposed to 10-fold excess H_2O_2 (Figure 4.11, Table 7.1). The reasons for this discrepancy are not clear at the present time.

There is also a decrease in enzymatic activity of CCP upon exposure to excess H_2O_2, which is dependent on the number of equivalents of H_2O_2 added as well as the time delay between H_2O_2 addition and determination of enzymatic activity. However, activity loss appears to occur more slowly than the decrease in fluorescence intensity (Figure 4.11 vs. Figure 4.12); thus, it appears that if reducing equivalents are provided within a few minutes of H_2O_2 exposure, over 80% activity is retained. Addition of 5 or more molar equivalents of H_2O_2 did not cause any further fluorescence decrease (Figure 4.11). However, since the activity decreases further upon addition of up to 10 equivalents of H_2O_2, other catalytically important, non-fluorescent amino acid residues may be altered.

It is of particular interest that CCP retains > 10% activity 24 h after exposure to 10 equivalents of H_2O_2 (Figure 4.12). Since the Phe-191 CCP mutant has only 0.02% the activity of native CCP, Trp-191 may not be irreversibly altered on H_2O_2

oxidation of CCP. A stopped-flow study of H_2O_2 binding to H_2O_2-oxidized CCP would be of interest to see if the radical formed is the same as that for the Phe-191 mutant, which produces a transient porphyrin radical, rather than the Trp-191 radical formed in CCP.[20] Nonetheless, since only ~ 13% activity remains with respect to cyt c oxidation, considerable H_2O_2-induced damage to CCP must occur. From the observed fluorescence decrease, a number of aromatic residues must be altered. Figure 4.1 shows a large number of aromatic residues around the heme. There are 11 Tyr residues within 15 Å of the heme, and a pair of Trp residues (211 & 223) which may act as endogenous donors. It has been suggested that some of these aromatic residues may channel charge to and from the primary radical site (Trp-191),[22] and thereby act as endogenous donors to Trp-191. The reduction midpoint potentials (E_m) are known for Trp and Tyr neutral radicals:[37]

$$Trp^{\cdot} + H^+ + 1e^- \longrightarrow TrpH \qquad E_m \sim 1.05\ V$$

$$TyrO^{\cdot} + H^+ + 1e^- \longrightarrow TyrOH \qquad E_m \sim 0.94\ V$$

From these potentials, $Trp^{\cdot}$ radicals would be expected to oxidize Tyr residues and this has been reported.[36] Electron transfer between $Trp^{\cdot}$ and Tyr residues has been investigated in a number of proteins where pulse radiolysis was used to generate azide radicals which specifically oxidize Trp residues.[37] Rates of 10^2-10^4 s^{-1} were observed for intramolecular electron transfer from Tyr to $Trp^{\cdot}$ by monitoring the fate of Trp and Tyr radicals spectroscopically at 510 and 405 nm, respectively.[37]

CCP has three Tyr (187, 229 & 236) within 5 Å of Trp-191, the primary radical site. However, unfolded compound I shows a 13% decrease in fluorescence

intensity which is too large to be accounted for by the oxidation of a Tyr residue. Furthermore, unfolded H_2O_2-oxidized CCP shows up to 75% fluorescence loss suggesting that Trp as well as Tyr are being destroyed. This suggests that the E_m values in CCP are altered from the values obtained for free Trp and Tyr and may be due to their local environment in the enzyme. For example, E_m depends on pH so H-bonding may be important.

Clearly, unravelling the detailed mechanism by which CCP reduces H_2O_2 in the absence of exogenous electron donors will require much further investigation. Study of the fluorescence of unfolded CCP mutants, previously exposed to excess H_2O_2, may yield more information on the mechanism of electron transfer to H_2O_2 via the heme centre of CCP.

4.5 REFERENCES

1 Lakowicz, J. R. Principles of Fluorescence Spectroscopy, Plenum, New York. 1983. (a) p 341, (b) p 350, (c) p 356 (d) p 44, and (e) p 354.

2 Takio, K.; Yonetani, T. *Arch. Biochem. Biophys.* **1980**, 203, 605.

3 Burstein, E. A.; Vedenkina, N. S.; Ivkova, M. N. *Photochem. Photobiol.* **1973**, *18*, 263.

4 Willis, K. J.; Szabo, A. G.; Zuker, M.; Ridgeway, J. M.; Alpert, B. *Biochemistry* **1990**, *29*, 5270.

5 Finzel, B. C.; Poulos, T. L.; Kraut, J. *J. Biol. Chem.* **1984**, *259*, 13027.

6 Prince, R. C.; George, G. N. *Trends in Biochem. Sci.* **1990**, *15*, 170.

7 Calhoun, D. B.; Vanderkooi, J. M.; Englander, S. W. *Biochemistry* **1983**, *22*,

1533.

8 Eftink, M. R.; Ghiron, C. A. *Anal. Biochem.* **1981,** *114,* 199.

9 Hill, B. C.; Horowitz, P. M.; Robinson, N. C. *Biochemistry* **1986,** *25,* 2287.

10 Recchia, J.; Matthews, C. R.; Rhee, M.; Horrocks, W. D. *Biochim. Biophys. Acta.* **1982,** *702,* 105.

11 Poulos, T. L.; Finzel, B. C. *Pept. Protein rev.* **1984,** *4,* 115.

12 Dunford, H. B. *Adv. Inorg. Biochem.* **1982,** *4,* 41.

13 Sahlin, M.; Graslund, A.; Ehrenberg, A.; Sjöberg, B. M. *J. Biol. Chem.* **1982,** *257,* 366.

14 Nordlund, P.; Sjöberg, B. M.; Eklund, H. *Nature* **1990,** *345,* 593.

15 Dietz, R.; Nastainczyk, W.; Ruf, H. H. *Eur. J. Biochem.* **1988,** *171,* 313.

16 Debus, R. J.; Barry, B. A.; Babcock, G. T.; McIntosh, L. *Proc. Natl. Acad. Sci.* **1988,** *85,* 427.

17 Hori, H.; Yonetani, T. *J. Biol. Chem.* **1985,** *260,* 349.

18 Goodin, D. B.; Mauk, G. A.; Smith, M. *J. Biol. Chem.* **1987,** *262,* 7719.

19 Scholes, C. P.; Liu, Y.; Fishel, L. A.; Farnum, M. F.; Mauro, J. M.; Kraut, J. *Isr. J. Chem.* **1989,** *29,* 85.

20 Erman, J. E.; Vitello, L. B.; Mauro, J. M.; Kraut, J. *Biochemistry* **1989,** *28,* 7992.

21 Goodin, D. B.; Mauk, G. A.; Smith, M. *Proc. Natl. Acad. Sci. U. S. A.* **1986,** *83,* 1295.

22 Edwards, S.; Xuong, N. H.; Hamlin, R. C.; Kraut, J. *Biochemistry* **1987,** *26,*

1503.

23 Sivaraja, M.; Goodin, D. B.; Smith, M.; Hoffman, B. M. *Science* **1989,** *245,* 738.

24 Coulson, A. F. W.; Yonetani, T. *Biochem. Biophys. Res. Commun.* **1972,** *49* 391.

25 Erman, J. E.; Yonetani, T. *Biochim. Biophys. Acta.* **1973,** *393,* 343.

26 Coulson, A. F. W.; Yonetani, T. *Eur. J. Biochem.* **1972,** *26,* 125.

27 Balny, C.; Anni, H.; Yonetani, T. *Fed. Eur. Biochem. Soc.* **1987,** *221,* 349.

28 Teale, F. W. J.; Weber, G. *Biochem. J.* **1957,** *65,* 476.

29 Chen, R. F. *Anal. Lett.* **1967,** *1,* 35.

30 Lakowicz, J. R.; Maliwal, B. P.; Cherek, H.; Balter, A. *Biochemistry,* **1983,** *22,* 1741.

31 Stryer, L. *Ann. Rev. Biochem.* **1978,** *47,* 819.

32 Campbell, I. D.; Dwek, R. A. *Biological Spectroscopy* Benjamin Cummings, Menlo Park. 1984, pp 113.

33 Erman, J. E.; Yonetani, T. *Biochim. Biophys. Acta.* **1975,** *393,* 350.

34 Erman, J. E. *Biochemistry* **1974,** *13,* 39.

35 Coulson, A. F. W.; Erman, J. E.; Yonetani, T. *J. Biol. Chem.* **1971,** *246,* 917.

36 DeFilippis, M. R.; Murthy, C. P.; Faraggi, M.; Klapper, M. H. *Biochemistry* **1989,** *28,* 4847.

37 Butler, J.; Land, E. J.; Prutz, W. A.; Swallow, A. J. *Biochim. Biophys. Acta* **1982,** *705,* 150.

5.0 SUMMARY

Chapter 2

Modification of CCP with the histidine-specific reagent $a_5Ru^{2+}H_2O$, produces a complex mixture of species which cannot be separated by anion-exchange chromatography. However, at least six species can be separated by cation-exchange chromatography at ambient pressure. Resolution of the bands is better by FPLC and rechromatography of peaks 4a and 5b under isocratic conditions yields two peaks (4a' and 5b') which can not be further resolved. These peaks are of interest because spectrophotometric ruthenium determination indicates that these species contain one covalently-attached a_5Ru centre per heme. A pH-induced spectral shift, due to the a_5Ru-His complex, occurs in peaks 4a' and 5b' but not in native CCP. DEPC, another histidine-specific reagent, reacts with three surface His-residues in CCP at pH 7, but is only able to react with two surface His-residues in a_5Ru-modified derivatives (peaks 4a' and 5b'). This suggests that one His residue is already coordinated to a a_5Ru centre. The high resolution x-ray crystal structure of peak 4a' shows that the a_5Ru is attached specifically to residue His-60, the expected site of modification. The crystal structure of peak 5b' has not been determined but reactivity with DEPC suggests that the a_5Ru is attached to one of the remaining surface His residues (6 or 96); this is supported by fluorescence (Chapter 4).

Chapter 3

Electron transfer rates between the a_5Ru^{2+} and the Fe^{4+}=O heme were

studied in the two singly-modified a_5Ru(His)CCP derivatives using 5-deazariboflavin to rapidly reduce the a_5Ru centre in situ. The reactive flavin semiquinone decays with a rate constant of ~ 10^9 M^{-1} s^{-1} in the presence of either a_5Ru(His-60)CCP or a_5Ru(His-X)CCP compared to a rate constant of ~ 10^6 M^{-1} s^{-1} in the presence of native CCP. This shows that reduction of the surface-bound a_5Ru is highly selective and extremely rapid. The reduction of Fe^{4+} was monitored spectroscopically and intermolecular and intramolecular electron transfer processes were observed to occur on overlapping timescales. Intermolecular electron transfer rates of 1.2 x 10^6 and 0.64 x 10^6 M^{-1} s^{-1} were obtained for a_5Ru(His-60)CCP and a_5Ru(His-X)CCP, respectively. The intermolecular rates of electron transfer are dependent on ionic strength and complexation with cyt c. Intramolecular electron transfer rates of 3.2 and 1.6 s^{-1} were measured for a_5Ru(His-60)CCP and a_5Ru(His-X)CCP, respectively.

Chapter 4

Due to quenching by the heme the quantum yield for steady-state Trp fluorescence of CCP is ~ 5 % that of free NATA, and an R_o value for Trp ---> heme energy transfer was calculated to be 32-35 Å. The emission maximum at 324 nm is indicative of buried Trp residues, consistent with the inability of freely-diffusing ionic quenchers (Cs^+ and I^-) to efficiently quench the fluorescence of CCP. Acrylamide, a nonpolar quencher, partially penetrates the protein matrix and decreases the observed CCP fluorescence intensity by ~ 32%. Attachment of a_5Ru to surface His residues results in 14-50% quenching of Trp fluorescence, and a R_o

value for Trp ---> a_5Ru energy transfer was calculated to be 17-18 Å. Unfolding of CCP in 8 M urea substantially relieves heme quenching and increases the observed fluorescence intensity ~ 10-fold. The fluorescence of unfolded compound I is ~ 13% lower than CCP, presumably because the primary radical site in CCP is a Trp residue (probably Trp-191). Treating CCP with up to 10-fold excess H_2O_2 causes a dramatic decrease in fluorescence of unfolded CCP and a corresponding decrease in enzymatic activity. CCP treated with a 10-fold molar excess of H_2O_2 and allowed to stand for 24 h, still retains ~ 13% activity, suggesting that the primary radical site is not irreversibly damaged since the Phe-191 mutant retains only 0.02% activity of native CCP.

6.0 SUGGESTIONS FOR FURTHER STUDY

Prepare ZnP-substituted a_5Ru(His)CCP derivatives to investigate the importance of the reorganization energy for reduction of $Fe^{4+}=O$

Determine the temperature dependence of intramolecular electron transfer in a_5Ru(His-60)CCP and a_5Ru(His-X)CCP to investigate the importance of the reorganization energy for reduction of $Fe^{4+}=O$

Use site-directed mutagenesis to introduce surface His residues that are situated closer to the heme, and preferably closer to what is thought to be the electron transfer pathway between cyt c and CCP. Modification with a_5Ru may yield derivatives with better electron transfer pathways than seen for the His-60 and His-X derivatives

These other a_5Ru(His)CCP derivatives will also be useful in attempts to understand the fluorescence quenching caused by the attached ruthenium centre and may lead to a more accurate determination of R_o for energy transfer to a_5Ru

Investigate H_2O_2-induced damage in mutants of CCP by fluorescence, particularly the Phe-191 mutant which does not possess the Trp residue thought to be the primary radical site in CCP

Carry out time-resolved fluorescence on CCP, compound I and H_2O_2-oxidized CCP to try to identify individual Trp residues and the effect of H_2O_2 on them

7.0 APPENDIX

Table 7.1

Summarized data for the time dependence of % fluorescence of CCP, compound I and H_2O_2-oxidized CCP in 8 M urea shown in Figure 4.11

Time (min)	0:1	1:1	3:1	5:1	10:1
0.25	100 ± 2.5	89.4 ± 3.0	77.1 ± 5.1	55.6 ± 1.4	51.9 ± 3.6
5		91.6 ± 4.1	69.7 ± 7.6	46.0 ± 2.9	43.4 ± 2.9
10			66.3 ± 1	37.6 ± 3.7	36.0 ± 1.4
20	101 ± 3.1		62.2 ±	31.1 ± 3.2	32.4 ± 1.5
24 (h)	98.8 ± 1.7	87.1 ± 5.1	64.1 ± 1.(	5.8 ± 4.1	23.5 ± 4.4

Table 7.2

Summarized data for the time dependence of % enzymatic activity of CCP, compound I and H_2O_2-oxidized CCP in 8 M urea shown in Figure 4.11

Time (min)	0:1	1:1	3:1	5:1	10:1
1.5		99.9 ± 1.9	83.9 ± 2.9	83.2 ± 4.0	79.9 ± 4.5
3		95.1 ± 4.9	66.4 ± 4.6	58.8 ± 7.1	47.1 ± 8.1
5		101.6 ± 8.0	51.4 ± 4.0	43.9 ± 5.0	31.7 ± 4.0
10		102.2 ± 0.3	47.2 ± 3.7	33.3 ± 3.0	20.4 ± 2.8
15	97.8 ± 4.8	98.5 ± 2.9	47.1 ± 3.4	29.2 ± 0.5	15.7 ± 3.1
30	100 ± 2.3	94.5 ± 6.6	45.7 ± 3.2	24.8 ± 1.4	14.1 ± 2.4
24 (h)	92.2 ± 5.0	72.5 ± 3.9	33.4 ± 5.4	17.7 ± 3.2	13.0 ± 2.6